Modeling the effects of irrigation management on soil salinity and crop transpiration at the field level,

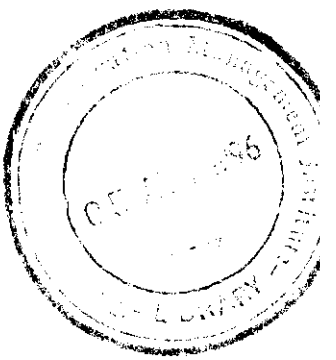

by

S.M.P. Smets

Wageningen Agricultural University
Department of Water Resources
Wageningen, The Netherlands

June 1996
International Irrigation Management Institute
Lahore, Pakistan

TABLE OF CONTENTS

LIST OF ANNEXES

LIST OF FIGURES

LIST OF TABLES

FOREWORD

Traditionally, salinity in Pakistan has been associated with the rise in water tables brought about by the advent of large-scale irrigation. However, in the late seventies, the Soil Survey of Pakistan (SSP) provided evidence that salinization was much more complex. They distinguished between primary salinization, caused by weathering of parent material, and secondary salinization, induced by either capillary rise from high water tables or by use of low quality groundwater. SSP further warned about the risk of sodicity, which appeared to be a bigger problem than salinity per se. This was substantiated by a survey undertaken by WAPDA from 1977-1979, which indicated that of 16.72 million ha of irrigated land, 4.22 million ha was affected by salinity, which is about 25%. The same survey showed that of these affected lands only about one quarter (28%) was qualified as saline, while the remainder was found to be (saline-) alkaline. Recent research studies show that the rapid development of tubewells, especially in the Punjab, and subsequent use of groundwater, which is of much lower quality than canal water, are likely to accelerate sodification.

Since 1989, the International Irrigation Management Institute (IIMI) has carried out research on problems of salinity associated with irrigated agriculture in Pakistan. The aim of the research is to provide tools and methodologies to policy makers and irrigation managers to evaluate the economic and environmental impact of irrigation management interventions. This requires us to understand the causes and development of salinity and attempt developing a predictive capability to assess the salinization as a function of the irrigation environment. A first step in that direction was made about four years ago when IIMI used the model SOWATSAL (developed by Hanks) to determine the impact of irrigation management on salinization. The effort was continued recently in collaboration with the Department of Water Resources of Wageningen Agricultural University, using the agro-hydrological model SWAP93. A first output of this collaboration was presented in a NATO conference in 1994 in which the authors asserted that a combination of dynamic simulation models with carefully selected field experiments were necessary to suggest changes in irrigation management for better salinity control.

The present report presents the results of a careful field calibration and validation in four fields in the Fordwah-Eastern Sadiqia area. Then, the model was used to assess the impact of "fixed" parameters (e.g. soil hydraulic properties) and dynamic management variables (e.g. irrigation water quality, quantity) on soil salinity. The importance of this study is not only that it allows us to assess to which degree the different management variables are really contributing to salinization, but also that a predictive tool is now available that can be part of a policy or management tool to verify *a priori* the economic and environmental impact of irrigation management interventions. At the moment, IIMI is testing the potential of geo-chemical modelling in order to get a better handle on sodification.

The author of the study, Susanna Smets, was associated with IIMI for a period of 7 months working on her MSc thesis for Wageningen Agricultural University. The paper is one of several outputs that have been recently produced by IIMI on salinity in Pakistan.

Marcel Kuper

SUMMARY

Since 1989, IIMI-Pakistan has conducted multi-disciplinary research on inter-related aspects of irrigation, salinity and agricultural production, with the aim to devise irrigation management interventions that support a sustainable management of irrigated agriculture. Research efforts are currently focussed on the Chishtian sub-division in south-east Punjab, where a multi-disciplinary team is working on the various research components at different levels of the irrigation system. To fullfill the increasing crop water requirements of the Chishtian sub-division, not only surface water, but also an increasing amount of groundwater, is used for irrigation purposes. Since the groundwater contains a high amount of sodium, concerns have been expressed about the increasing use of tubewell water, which will lead to soil salinization and sodification, and eventually will result in decreased agricultural production. Therefore, it is important to study the effects of irrigation management on the development of soil salinity and sodicity and on crop production.

This study is part of the abovementioned research framework and relates to the field level. The objectives of this study are: 1) to obtain a better understanding of the transport processes of water and salts in the unsaturated zone in relation to the physical environment, and 2) to evaluate the effects of a different irrigation management (quantity, quality, frequency) on soil salinity and crop transpiration.

To realize these objectives the agro-hydrological model SWAP93 is used, as it describes the water and salt balance of an irrigated field. For four fields in the Chishtian sub-division - representing different soil types and different irrigation environments - SWAP93 is calibrated and validated under prevailing conditions.

The main problem during the calibration process was the overestimation of the leaching of salts by the model. The underestimation of the soil salinity can be explained by the underlying assumptions of the model. SWAP93 does not include any chemical processes (exchange processes, dissolution/precipitation), which can be a cause for the differences between measured and simulated salinity data. The physical reason for the underestimation of the soil salinity can be found in the assumption that the infiltration of water is homogeneous at the field scale. In reality, the permeability over the field and the distribution of water over the field is heterogeneous, resulting in a lower average leaching of salts over the field. This phenomenon is modeled by using the concept of preferential flow at the field scale. In this concept, the soil is divided into an immobile and mobile fraction, and the exchange of salts takes place between those two fractions. Although the calibration of the salt balance is improved, several disadvantages are related to the use of preferential flow at the field scale. Another way to address the non-uniform water distribution is to split the field into different parts with different amounts of irrigation water, and to take an average of the salt balances of the different parts. At the writing of this report, this option is being tested and the preliminary results are positive.

A sensitivity study is carried out for one of the four fields, to obtain a better understanding of the sensitivity of several environmental parameters upon the behaviour of the system (e.g. soil hydraulic parameters, preferential flow parameters, agronomical parameters, and meteorological parameters). The Van Genuchten-Mualem (VGM) parameters influence the calibration results to a large extent, but at the same time they vary considerably within a textural class (for two fields the VGM-parameters are determined via multi-step pressure outflow experiments). Therefore, the VGM-parameters should be derived from literature instead of doing costly and time-consuming laboratory experiments.

For the four calibrated fields, several simulations are performed to evaluate the impact of different irrigation management scenarios, by using Vadose Zone Response Numbers as performance indicators. The short-term (i.e. two growing seasons) effects on the water and salt balance of an irrigated field are evaluated for different irrigation water quantities (underirrigation and overirrigation), irrigation water qualities (canal water and tubewell water), irrigation frequencies (high and low frequency) and initial salinity levels (high and low level). For the long term (i.e. ten years), three scenarios are performed for all of the four soil types, i.e. reference scenario, underirrigation scenario and tubewell water scenario. For one of the four fields, a more detailed scenario analysis is carried out in order to obtain a better understanding of the marginal effects of varying the quantity and quality of the irrigation water. In addition, the effect of a shallow groundwater table is tested for different irrigation management scenarios.

The quantity of irrigation water can be concluded as the most important factor regarding the crop transpiration. However, the frequency of irrigation has a large impact on the crop transpiration as well, especially for sandy soils. The quality of the irrigation water affects the crop transpiration only slightly, since cotton and wheat are salt tolerant crops and the salt concentration in the mobile fraction is hardly limiting the root water uptake. Concerning the soil salinity, the quantity of the irrigation water determines the build up of salts to a large extent. Even when a field is irrigated with tubewell water, the salinization can be controlled by applying an irrigation water quantity, which is sufficient to leach the excess of salts out the soil profile. However, the high sodium content of the tubewell water negatively affects the soil structure and thereby the crop transpiration. Not only the quantity of irrigation water determines the salinization, but also the frequency of irrigation affects the leaching of salts. A smaller irrigation interval has a positive effect on the crop transpiration, but at the same time the soil salinity is increased, as the leaching of salts is less efficient. The more sandy soils have a higher conductivity and a lower retention capacity than the loamy soils, which results in a more efficient leaching of salts in the sandy soils, and at the same time a less efficient crop transpiration. Thus, heavier soils are more sensitive to salinization than lighter soils.

The insights obtained during this field level study can be used at a larger scale. This means that SWAP93 has to be extrapolated from the field level to e.g. the watercourse level. Although SWAP93 offers the possibility to model the water and salt balance of a field in a very detailed way, the model can also be used to describe the water and salt balance of a larger area in a more simple way. Obviously, the accuracy of the predictive capability is decreased when using SWAP93 at a larger scale, but the model can still be used to predict trends in soil salinity and crop transpiration.

CHAPTER 1 INTRODUCTION

1.1 Institutional background and problem statement

Low levels of agricultural productivity in Pakistan have long been associated with a low performance of the management of the Indus Basin River Irrigation System, resulting in inequitable and highly variable canal water supplies along with environmental problems such as salinity, sodicity and waterlogging (Bhutta and Van der Velde, 1992; Kijne and Kuper, 1995; World Bank, 1994). Since large investments in irrigation and drainage infrastructure have not met expectations in adressing issues of agricultural productivity and environmental problems, the Federal Government of Pakistan and donors took another course that would combine research and development approaches and that adresses physical as well as institutional issues. This stresses the importance of institutes such as the International Irrigation Management Institute (IIMI), who are asked to put forward practical suggestions for solving complex problems.

Since 1989, IIMI-Pakistan has conducted multi-disciplinary research on inter-related aspects of irrigation, salinity and agricultural production with an aim to devise irrigation management interventions that support a sustainable management of irrigated agriculture. Research efforts are currently focussed on the Chishtian Sub-division in south-east Punjab, where a multi-disciplinary team is working on the various research components at different levels of the irrigation system: field level, farm level, tertiary level, secondary and main canal level[1].

The Chishtian Sub-division (about 67,000 ha) receives it's surface irrigation water through the Fordwah Branch Canal (see Annex A). This canal water is very suitable for irrigation purposes since the sodium concentration is very low (EC = 0.19 dS/m). Besides, irrigation with canal water contributes to the soil fertility, since the concentration of trace elements in the canal water is relatively high. Traditionally, the surface water supplies have been augmented by groundwater, tapped through open wells in the area. However, the groundwater has a naturally high sodium concentration, since the aquifers consist of marine sediments. As high sodium contents damage the crop and the soil structure, the groundwater is less suitable for irrigation. However, since the early sixties the open wells have been substituted by, and increasingly replaced with, private tubewells (nowadays approximately 12 per 100 ha). While the development of groundwater exploitation has contributed to a rapid increase in cropping intensities, concerns have been expressed about the use of the sodium rich groundwater, which will lead to soil salinization and sodification, and eventually will result in decreased agricultural production. Therefore, it is important to study the effects of irrigation management (a combination of surface and groundwater) on the development of soil salinity and sodicity and on crop production.

---

[1] Recently, IIMI-Pakistan has made a commitment to integrate the different research studies, in order to develop a methodology to evaluate the economic and environmental impact of changes in irrigation management (IIMI, 1996).

This study is part of the research framework concerning the whole Chishtian Sub-division and relates to the field level. Field level studies of salinity have hardly been undertaken and the marginal impact of various irrigation management variables is not known. Sophisticated models are now available, that can help identify the marginal effects of different irrigation management variables on the evolution of salinity (Kijne and Kuper, 1995). The field is chosen as a sub-system, since at this scale irrigation water - whether canal water or tubewell water - is transformed into crop transpiration and soil salinity, while the environmental parameters (soil type, drainage conditions, etc.) and the management variables (irrigation water quality, irrigation water application, etc.) are more or less uniform[2].

1.2 Objectives of the study

The objectives of this field-level study are:

1) To obtain a better understanding of the transport processes of water and salts in the vadose zone in relation to the physical environment;

2) To evaluate the short-term effects of a different quantity, quality and frequency of irrigation water applications on soil salinity and crop transpiration (one agricultural year); and

3) To evaluate the long-term effects of different irrigation management practices on soil salinity and crop transpiration (10 years).

1.3 Approach of the study

To realize the abovementioned objectives, the agro-hydrological model SWAP93 is used, since it incorporates all the components that are necessary to simulate the water and salt balances of an irrigated field. In order to use SWAP93 in a proper way, the model should first be calibrated and validated for the prevailing conditions.

In May 1994, IIMI-Pakistan started a detailed monitoring of four sample fields in the Chishtian Sub-division (IIMI, 1995). SWAP93 has been calibrated for these four fields, for the prevailing conditions during two growing seasons: the cotton season (Kharif '94) and the wheat season (Rabi'94/'95). A validation of the model for these four fields has been done for the Kharif'95 season.

To obtain a better understanding of the transport processes of water and salts in relation to their physical environment, a sensitivity study of the environmental parameters was carried

---

[2] In the integrated approach to analyse the large scale irrigation system of the Chishtian Sub-division, the basic unit of analysis is the watercourse. The insights obtained in this field level study will be used for the analysis at the watercourse level (extrapolation from field to watercourse unit).

out. This sensitivity study was done for the prevailing conditions of the calibration period for one of the four sample fields (Field 4). In order to study the marginal effects of different environmental parameters, several performance indicators have been used, the so called Vadose Zone Response Numbers (Bastiaansen, 1993).

The effects of irrigation management variables on soil salinity and crop transpiration (on the short and on the long-term) is evaluated for all of the four soil types, for 'average' conditions. This means that the field specific data of the calibrated fields are replaced by more general data, e.g. climatic data instead of meteorological data of one specific year, an average crop calendar instead of field specific sowing and harvesting data, etc.

To study the short-term effects on soil salinity and crop transpiraion, several simulations were carried out, changing the management variables, e.g. the quantity, quality and frequency of the irrigation water applications. For the long-term study, several irrigation management scenarios were developed, based on the results of the sensitivity study of the management variables.

1.4 Structure of the report

In the next paragraph (Paragraph 1.5), the irrigation system of the Chishtian Sub-division is briefly described and the problems related to irrigation and salinity are illustrated. Additionally, some general information about the four sample fields is given. In Chapter 2, the principles of the model SWAP93 are described and the underlying assumptions and limitations of the model are discussed. Chapter 3 deals with the calibration and validation of SWAP93 for the four sample fields; the calibration procedure is discussed and the results are evaluated. In Chapter 4, the sensitivity of the environmental parameters is described and related to the calibration process. Chapter 5 deals with the short-term analysis of the different management variables for the different soil types, while Chapter 6 describes the effects of a different irrigation management on salinity and crop transpiration for the long-term. In the last chapter (Chapter 7), conclusions are drawn and recommendations for future research are made.

1.5 Description of the research area

1.5.1 Location of the research area

The Chishtian Sub-division, located in the south-east Punjab, is part of the Fordwah/Eastern Sadiqia area and receives its surface water via the Fordwah Branch Canal (see Figure 1.1). The Chishtian Sub-divsion comprises about 470 watercourses and in eight sample watercourses (four on Azim Distributary and four on Fordwah Distributary) research is carried out on the field and farm level.

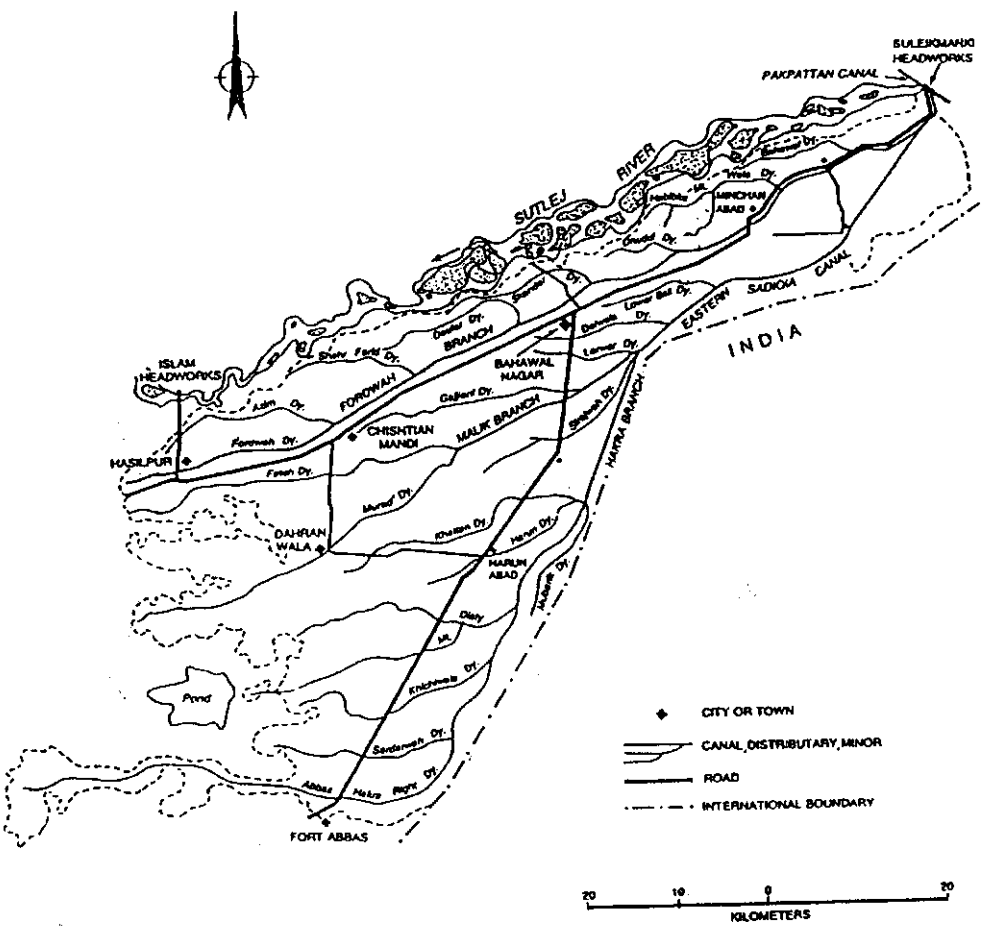

Figure 1.1 *Fordwah/Eastern Sadiqia location map.*

Four sample fields

The four sample fields used in this field-level study are located in two of the eight sample watercourses, two in Fordwah 62-R and two in Azim 111-L. (see Annex A). In Table 1.1 the field code and the area under cultivation is given for the concerned growing seasons (m^2).

Table 1.1 *Basic data for four sample fields.*

watercourse	field code	Kharif'94	Rabi'94/'95	Kharif'95
Fordwah 62-R	1: 351/15/17	3280	3180	1440
Fordwah 62-R	2: 351/10/21	3800	3500	3590
Azim 111-L	3: 173/15/22	4050	4270	4770
Azim 111-L	4: 173/11/07	4290	4100	4250

1.5.2 Climate and cropping pattern.

The Chistian sub-division has an arid climate with annual evaporation (2400 mm) far exceeding anual rainfall (260 mm). Figure 1.2 shows the average monthly rainfall and reference evapotranspiration, calculated by the model CROPWAT (Smith, 1992)[3].

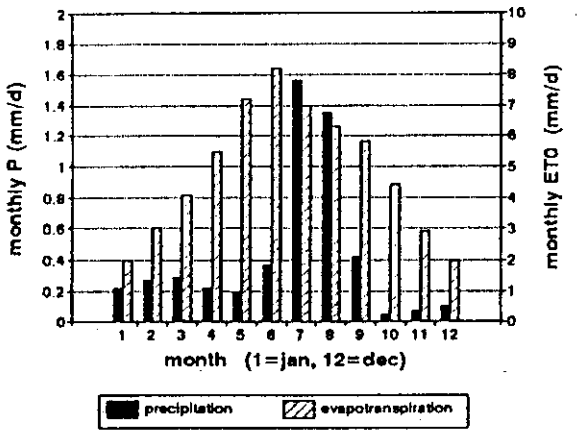

Figure 1.2 *Monthly precipitation and evaporation (mm).*

The agricultural year can be divided into two seasons: Kharif-season (summer), from June till December, and Rabi-season (winter), from January till May. The monsoon period comprises July and August, and rainfall can amount upto 85 mm per month. The Chishtian Sub-division is located in the cotton-wheat agro-ecological zone of the Punjab. The dominant crop in Kharif is cotton (45 % of the cultivated area), while in Rabi it is wheat (60-70 %). Tradionally, rice is an important crop in the area, while the livestock necessitates the cultivation of fodder crops. The cropping intenstity is presently at 130 % (IIMI, 1995). The very high cropping intensity in the Punjab (>125%) is an obvious indicator for the significance of the conjunctive use of canal supplies and pumped groundwater. The canal commands were designed in the late 19th century with the expectation of annual cropping intensities ranging from only 50% to 75% (Kijne and Kuper, 1995). However, this particular irrigation was constructed about 1930.

1.5.3 Irrigation system and tubewells

The Chishtian Sub-division is located in the tail of Fordwah Branch Canal, which takes it water from Fordwah Main Canal, starting from Suleimanki Headworks on the Sutlej River (see Figure 1.1). Anually an amount of 420 million m^3 (or 620 mm) is diverted to the Chishtian Sub-division. The irrigation system in the Chishtian sub-division is an odd mixture of perennial and non-perennial distributary canals[4] (IIMI, 1995). Two sample fields located in the perennial watercourse Fordwah-62 (taking off from Fordwah distributary) and the other two fields are located in the non-perennial watercourse Azim-111 (taking off from Azim distributary).

The watercourse is the smallest unit of an irrigation system and it links the farmers to the Irrigation Department by means of the warabandi system ('wara' means turn and 'bandi'

---

3 The data are climatic averages for 1960-1990 (Bahawalpur meteo-station). These climatic data are used for the irrigation mangement simulations (Chapters 5 and 6).

4 Non-perennial distributaries receive water from April 15th to October 15th. Perennial ones receive water all year round, except for the month of January, when canals are closed for anual maintenance.

means fixation). The warabandi is the sequence in which farmers receive the right of access to canal water, supplied to the watercourse. In the warabandi, which generally has a duration of 7 days, each farmer receives the entire watercourse discharge during a fixed period of time of the week (Rinaudo, 1994).

In reality, the canal water supply according to the warabandi system is often inadequate, inequitable, unreliable and does not meet the crop water requirements during the year. Farmers have reacted to these perceived deficiencies of the canal water supply by installing private tubewells and pumping groundwater, thus augmenting their irrigation water supplies (Strosser and Kuper, 1992). The contribution of groundwater to the total irrigation supply is considerable, which is illustrated in Table 1.2.

Table 1.2 *Irrigation application for sample watercourses in 1991/1992.*

watercourse	surface water (EC=0.19 dS/m)		groundwater			total
	mm	%	mm	%	EC (dS/m)	mm
Azim-63	320	35	592	65	0.90	912
Azim-111	80	7	1145	93	1.21	1225
Fordwah-62	885	82	190	18	1.09	1075
Fordwah-130	695	58	503	42	1.24	1198
Fateh-184	815	89	101	11	3.49	916

Table 1.2 emphasizes the fact that the degree of access to canal water determines the share of groundwater in the total irrigation application, with the Azim watercourses using relatively more groundwater than the Fordwah watercourses. The relatively small share of groundwater in the irrigation application in Fateh-184 is related to the low quality of the groundwater.

Four sample fields

The four sample fields of this study have been selected on the basis of two criteria: access to canal water and the farmer's ownership of a tubewell, as illustrated in Table 1.3.

Table 1.3 *Irrigation environment of four sample fields.*

field	access to canal water	owner of tubewell	% canal water
1	yes	yes	75
2	yes	no	67
3	no	no	0
4	no	yes	0

This was the situation at the time the sample fields were selected. However, in January'95, Farmer 2 installed a tubewell, thereby changing the irrigation environment of his farm. Farmer 4 has been the owner of a tubewell since '93, but at the beginning of Kharif'94 an arrangement was made between farmers 3 and 4, giving Farmer 3 the right to 50% of the pumped groundwater of the tubewell of Farmer 4, while sharing the electricity bill. In Table

1.3 the percentage of canal water for the total irrigation application for Kharif'94, Rabi'94'/'95 and Kharif'95 is given for each sample field.

1.5.4 Soils and salinity.

The soils in the area are a mixture of alluvial and eolian depositions. Silty alluvia, containing a substantial amount of fine sands, and sandy deposits of eolian origin have mixed into thick uniform deposits of silt to fine sandy textures (IIMI, 1995).

Four sample fields
Textural analysis was done for the four sample fields and the textural classes are listed in Table 1.4 (IIMI, 1995).

Field 1 is classified as a Jhang soil serie (SSP, personal communication), and consists of a loamy sand top soil, underlain by a sandy subsoil. Field 2 is less sandy and is classified as a Rasulpur soil serie, with a sandy loam top soil, underlain by a loamy sand subsoil. Field 3 is the sample field with the heaviest soil and consists of a loamy top soil, underlain by a sandy loam subsoil. Field 3 is classified as a Sultanpur soil serie. Field 4 has a somewhat higher silt content and a lower clay content than Field 3 and is classified as a Harunabad soil serie. The soil consists of a (silty) loam topsoil, underlain by a loamy sand subsoil.

Table 1.4 *Textural classes for four sample fields.*

field	15 cm	30 cm	60 cm	90 cm	120 cm	150 cm	200 cm
1	SL	LS	SL	LS	LS	S	S
2	L	SL	SL	L	SL	LS	LS
3	L	L	SiCL	L	LS	LS	LS
4	L	L	SiL	SiL	SL	LS	LS

S : sand LS : loamy sand SL : sandy loam
L : loam SiL : silt loam SiCl : silty clay loam

The four sample fields have different soil types, together representing the most common soil types in the Chishtian Sub-division (namely from a loamy sand to a silty clay loam). Therefore, the obtained results from these four sample fields may be extrapolated to the whole Chishtian Sub-division.

Soil Salinity
The present soil salinity in the Chishtian sub-division is not exactly known. The last visual salinity survey was done in 1977. In 1977, the main part of the Chishtian Sub-division was not severly effected by salts. However, the increased use of groundwater of marginal quality has lead to a salinization of especially those watercourses that receive less canal water and where relativly more groundwater of marginal quality is recycled (see Table 1.5). It can be seen that the SAR is considerably higher with increasing use of sodium rich groundwater. This implies that not only salinity but also - and maybe even to a larger extent - sodicity threatens sustainable irrigated agriculture in the Punjab.

Table 1.5 *Access to canal water and groundwater quality versus EC and SAR values.*

watercourse	total	% surface water	groundwater quality (dS/m)	EC (dS/m) June 1992	SAR (dS/m) June 1992
Azim-63	912	35	0.90	1.3	4.7
Azim-111	1225	7	1.21	2.3	11.1
Fordwah-62	1075	82	1.09	1.5	6.7
Fordwah-130	1198	58	1.24	1.4	6.8
Fateh-184	916	89	3.49	2.2	9.1

CHAPTER 2 THE MODEL SWAP93

2.1 Introduction

During the last decade a number of complex simulation models describing the dynamics of the soil-water-plant-atmosphere system have been developed. These simulation models have become indispensible tools to study soil physical and chemical processes in the unsaturated and saturated zone (Feddes et al., 1988). Once these computer models have been tested with field experiments and parameters have been derived, numerical experiments may be performed to study the marginal effects of the different parameters, which determine the behaviour of the system. Besides, different scenarios may be performed to predict the behaviour of the system and to indicate the trends that occur under certain conditions. In this way, the tedious and time consuming field experiments are replaced by numerical experiments that allow for a fast evaluation of irrigation and drainage systems for a number of different meteorological years (Kabat et al., 1992).

Feddes et al. (1978) developed the one dimensional SWATR (Soil Water Actual Transpiration Rate) model to describe transient water flow in a heterogenous soil-root system, which is under the influence of groundwater. A new version SWATRE (SWATR Extended) was developed by Belmans et al. (1983), who applied a different numerical solution scheme[5] and extended the possibilities of using different types of boundary conditions at the bottom of the soil system. Feddes et al. (1984) combined the SWATRE and the crop production model CROPR (Feddes et al., 1978) into SWACROP. This model was further developed by Wesseling et al. (1990). Van Dam (1991) incorporated solute transport in the SWATRE model. The SWATRE 1991 version is revised and extended by the Working Group SWAP (1994). The SWAP 1993 version includes for example hysteresis according to the concept of Kool and Parker (1987), the possibility for simulating preferential flow (Van Dam et al., 1990), adsorption and decomposition processes as described by Boesten and Van der Linden (1991), etc. At present, adjustments are still being made. In this study the SWAP 1993 version is used to simulate water and solute movement through the soil profile; crop production is not taken into account.

2.2 Water transport

2.2.1 Soil water balance

The one dimensional water balance of the soil profile can be described with the following equation:

---

5 The numerical solution scheme that is used in SWATRE is an implicit finite-difference scheme, which applies an explicit linearization (see Haverkamp et al., 1977).

$$\frac{\Delta W}{\Delta t} = P + I - E - T - q_d - q_b \qquad (2.1)$$

ΔW : change in soil moisture storage (cm)
Δt : time period (d)
P : precipitation (cm/d)
I : irrigation (cm/d)
E : soil evaporation (cm/d)
T : plant transpiration (cm/d)
q_d : lateral drainage (cm/d)
q_b : net bottom flux (percolation minus capillary rise) (cm/d)

A schematic cross section of the soil profile and the concerning water balance components is given in Figure 2.1.

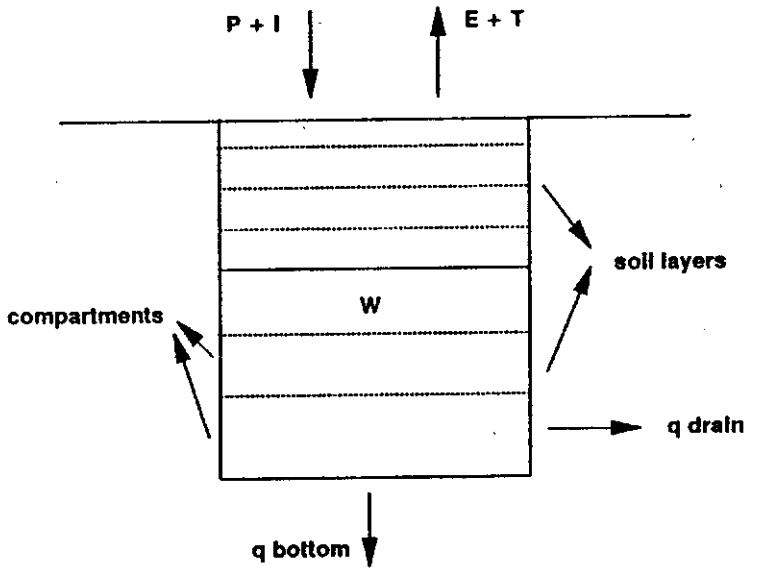

Figure 2.1 *Schematic cross section of the soil profile with water balance components.*

2.2.2 Soil water flow in the unsaturated soil.

In SWAP93, the soil water flow is calculated by combining Darcy's law and the principles of mass conservation, which leads to the Richards equation. Darcy's law can be described as follows:

$$q = - K(h) \left(\frac{\partial h}{\partial z} + 1 \right) \qquad (2.2)$$

q : soil water flux, positive upwards (cm/d)
h : pressure head (cm)
K(h) : unsaturated hydraulic conductivity (cm/d)
z : height, positive upwards, origin at the soil surface (cm)

The mass conservation principle for the soil-root system can be expressed as:

$$\frac{\partial \theta}{\partial t} = - \frac{\partial q}{\partial z} - S(h) \qquad (2.3)$$

θ : soil moisture content (cm^3/cm^3)
t : time period (d)
S(h) : root water uptake, represented by sink term (1/d)

Combining Equations 2.2 and 2.3 yields the Richards equation:

$$\frac{\partial \theta}{\partial t} = \frac{\partial \theta}{\partial h} \frac{\partial h}{\partial t} = C(h) \frac{\partial h}{\partial t} = \frac{\partial}{\partial z} [\, K(h) \, (\frac{\partial h}{\partial z} + 1 \,)] - S(h) \qquad (2.4)$$

C(h) : differential moisture capacity (1/cm)

Equation 2.4 is the basic flow equation of SWAP93 in a homogeneous soil-water-root system. This equation has the advantage of being applicable for saturated and partially saturated flow. The use of pressure head h, instead of moisture content θ as the dependent variable, has the advantage of being applicable in layered soils, where h remains continuous at the boundaries between different soil layers.

The soil profile can be split up into maximally five soil layers, having different physical properties, while the total soil profile is divided into numerical compartments (maximum 40) (see Figure 2.1). The height of the compartments has to be varied according to the expected soil moisture gradients that occur in the profile. For example, the size of the compartments in the top soil should be small (ca. 5 cm), since the soil moisture gradients will be large. The maximum compartment size for the unsaturated zone is advised not to exceed 25 cm. Although the abovementioned concepts are simple, the numerical solution of Equation 2.4 is not easy due to the non-linear relationship between θ, h and K. For the present numerical solution scheme, see Celia et al. (1990).

2.2.3 Soil hydraulic functions

To solve Equation 2.4, the soil hydraulic functions (describing the relations between the soil moisture content, the pressure head and the unsaturated hydraulic conductivity) should be known. The Mualem-Van Genuchten model is an analytical model, which describes the soil hydraulic functions with a limited number of parameters. In SWAP, the h(θ) and K(θ) relations are determined by the Van Genuchten-Mualem parameters (VGM-parameters).

The soil moisture content is expressed as a function of the pressure head h with the empirical equation:

$$\theta = \theta_r + \frac{\theta_s - \theta_r}{(1 + (\alpha |h|)^n)^m} \tag{2.5}$$

where:

$$m = 1 - \frac{1}{n} \tag{2.6}$$

The unsaturated hydraulic conductivity as a function of the pressure head is written as:

$$K(h) = K_s \frac{((1 + |\alpha h|^n)^m - |\alpha h|^{n-1})^2}{(1 + |\alpha h|^n)^{m(\lambda+2)}} \tag{2.7}$$

θ_s : saturated soil moisture content (cm^3/cm^3)
θ_r : residual soil moisture content (cm^3/cm^3)
K_s : saturated hydraulic conductivity (cm/d)
α : empirical shape parameter (1/cm)
λ, n : empirical shape parameters (-)

The parameter α, which is the reciprocal of the air entry value, roughly corresponds to the inverse of h at the inflection point of the retention curve ($\partial\theta/\partial h$ is maximal), n is the gradient $\partial\theta/\partial h$ and is a measure of the width of the pore size distribution. The parameter λ is a pore connectivity factor that expresses the correlation between pores and flow path tortuosity (Wösten and Van Genuchten, 1988). The soil hydraulic functions determine the flow of water in the soil and, therefore, the VGM-parameters play an important role in the calibration process (see Chapter 3).

The values of VGM-parameters for different soil types have been determined by various researchers. In Annex B, three tables are listed with VGM-parameter sets as derived by Rawls et al. (1982), Carsel and Parrish (1988) and Wösten et al. (1987). In Table 2.1 the VGM-parameters determined by the abovementioned authors are given for a coarse, medium and fine textured soil.

Table 2.1 *Standard values of VGM-parameters for three major soil types.*

soil type	sand %	silt %	clay %	author	θ_r[6] -	θ_s -	K_s cm/d	α 1/cm	λ[7] -	n -
coarse: sand	> 90	< 10	< 10	Wösten	-	0.35	100	0.022	0.8	2.19
				Rawls	0.02	0.42	504	0.138	-	1.59
				Carsel	0.05	0.43	713	0.145	-	2.68
medium: silt	< 8	> 88	< 10	Wösten	-	0.43	57.4	0.021	-2.1	1.22
				Rawls	0.02	0.49	31.7	0.048	-	1.21
				Carsel	0.03	0.46	6.0	0.016	-	1.37
fine: clay	< 45	< 40	> 50	Wösten	-	0.58	38.0	0.112	-13.0	1.06
				Rawls	0.09	0.39	1.4	0.027	-	1.13
				Carsel	0.07	0.38	4.8	0.008	-	1.09

It can be concluded that the differences in the VGM-parameters are considerable, which can be caused by the different methodologies that were used. Within a textural class, the saturated moisture content and the saturated hydraulic conductivity can vary enormously, thereby influencing the values of the shape parameters α, λ and n. The value of the shape factor α shows large differences among the different authors, thereby almost covering the whole range of values for α. The value of the shape factor n is quite similar for the different authors. In Chapter 3 and Chapter 4, the ranges of the VGM-parameters in relation to soil physical characteristics are discussed, as part of the calibration process and sensitivity study.

2.2.4 Preferential flow

Most simulation models for the unsaturated zone consider the soil to be isotropic and homogeneous. However, transport of water is often heterogeneous with part of the infiltrating water travelling faster than the average wetting front (Feddes et al., 1988). This phenomenon is generally called preferential flow and has a large effect on the leaching of nutrients, salts and pesticides to the saturated zone. In some soils, preferential flow occurs through large pores in an unsaturated soil matrix, a process known as bypass flow or shortcircuiting (Hoogmoed and Bouma, 1980). In other soils, different flow rates vary more gradually, while matrix and preferential pathways cannot be distinguished easily. Preferential flow can be caused by different mechanisms, one of them being the occurence of noncapillary sized

---

6 Wösten and Van Genuchten fixed the residual water content at zero, while determining the other VGM-parameters.

7 Rawls et al. (1982) and Carsel and Parrish (1988) fixed λ at 0.5 while determining the other VGM-parameters (based on Mualem's (1976) finding that λ can be set at 0.5).

macropores (Feddes et al., 1988). This can be caused by shrinking and cracking of a clay soil, by plant roots or by tillage operations. In non-structured soils, such as sandy soils, preferential flow paths occur due to wetting front instability. This is caused by either a change in soil texture i.e. a soil layer of low conductivity overlying a layer of high conductivity, or by water repellency due to organic substances coating mineral soil particles.

Flow in water repellent soils can be simulated by two concepts: the dual porosity concept and the mobile-immobile concept (see Ritsema and Dekker, 1994 and Van Genuchten and Wagenet, 1989). The mobile-immobile concept has been used in SWAP93 and Van Dam (1990) employed this concept to simulate soil water flow and bromide transport for water repellent sandy field soils.

In SWAP93, the mobile-immobile model is determined by the following parameters (for each soil layer):

F_{mobile} : volume fraction of preferential paths (-)
$\theta_{immobile}$: constant soil moisture content in immobile part of the soil profile (cm^3/cm^3)

In water repellent soils, the mobile fraction is a function of the moisture content of the soil and F_{mobile} has to be entered for two different pF values (and is linearly interpolated between those values).

In SWAP93, the transport of water and the root water uptake only takes place in the mobile fraction, and therefore the moisture content in the immobile fraction has a constant value. The interaction between the mobile and immobile phase is only related to the transport of solutes and is described by the following equation:

$$q_{mobile-immobile} = K_{mobile} * (c_{mobile} - c_{immobile}) \qquad (2.8)$$

$q_{mobile \rightarrow immobile}$: solute flux between mobile and immobile part ($g/cm^3/d$)
K_{mobile} : exchange rate between mobile and immobile part (d^{-1})
c_{mobile} : solute concentration of soil water in mobile parts (g/cm^3)
$c_{immobile}$: solute concentration of soil water in immobile parts (g/cm^3)

The exchange rate K_{mobile} is determined by the diffusion coefficient in the soil and by the distance between mobile and immobile parts in the soil profile.

Van Dam (1996) gives more detailed information about the incorporation of the preferential flow concept in SWAP93.

2.2.5 Root water uptake

The sink term S in Equations 2.3 and 2.4 represents the uptake of water by the roots, which is equal to the actual transpiration of the plant. A complete physical description of soil water extraction by roots is very complex.

Therefore, Feddes et al. (1978) described the root water uptake semi-empirically by:

$$S(h) = \alpha(h)\, S_{max} \qquad (2.9)$$

$\alpha(h)$: prescribed plant specific function of soil water pressure head (-)
S_{max} : maximum possible water extraction by roots (1/d)

Under non-optimal conditions (too dry or too wet), S_{max} is reduced by means of the pressure head dependent α-function, which is shown in Figure 2.2. Water uptake below $|h_1|$ (oxygen defiency) and above $|h_4|$ (wilting point) is set equal to zero. Between $|h_2|$ and $|h_3|$ (reduction point) water uptake is maximal. The value of $|h_3|$ varies with the drying capacity of the atmosphere and thus with the potential transpiration rate.

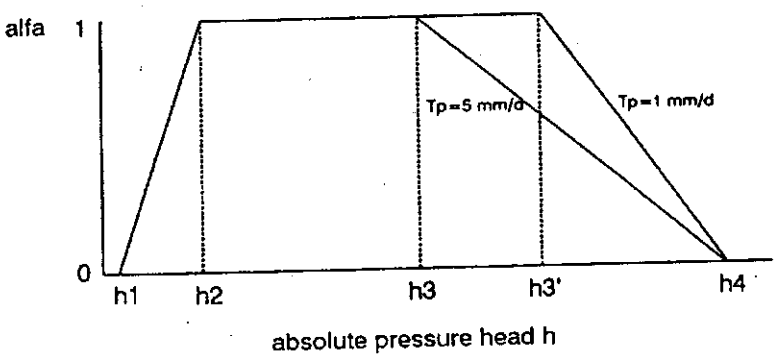

Figure 2.2 *Dimensionless sink term function $\alpha(h)$.*

SWAP offers different options to describe S_{max}, e.g. according to Feddes et al. (1988) and to Prasad (1988) (see Figure 2.3).

Feddes et al. (1988) assumed a uniform distribution of S_{max} with depth according to:

$$S_{max} = \frac{T_{pot}}{|z_r|} \qquad (2.10)$$

T_{pot} : potential transpiration rate (cm/d)
z_r : rooting depth (cm)

The model presented by Prasad assumes that under optimal conditions, roots extract water from the moist top layers, leaving the deeper layers relatively untouched.

S_{max} is a function of the depth z (cm) and can be expressed as:

$$S_{max}(z) = \frac{2T_{pot}}{|z_r|}\left(1 - \frac{|z|}{|z_r|}\right) \qquad (2.11)$$

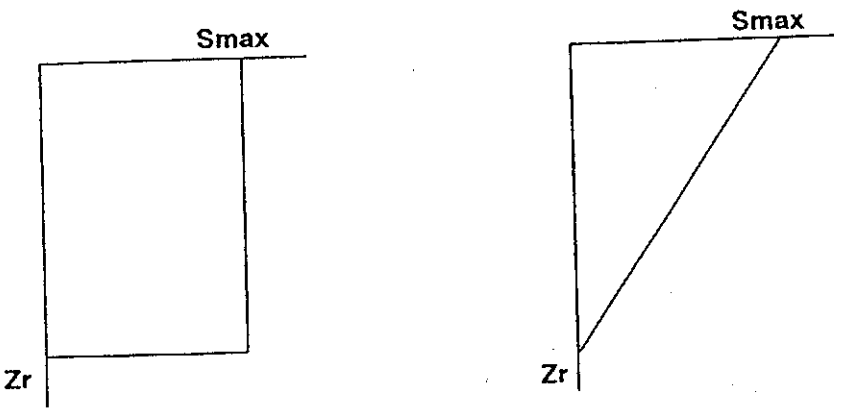

Figure 2.3 *Root water uptake functions according to Feddes (left) and Prasad (right).*

2.2.6. Upper boundary conditions

The upper boundary conditions of the soil-water-plant-atmosphere system are determined by the incoming and outgoing fluxes, respectively irrigation and effective precipitation, and evapotranspiration. The maximum possible flux through the soil and crop surface is calculated from the potential evapotranspiration rate (ET_{pot}). SWAP provides different options to calculate ET_{pot} (on a daily basis):

- potential evapotranspiration is entered as potential evaporation (E_{pot}) and potential transpiration (T_{pot})
- potential evapotranspiration is entered as a reference evaporation (ET_0) to be multiplied by crop factors (k_c) (e.g. Penmann, Makkink, pan evaporation)
- potential evapotranspiration is calculated with the Priestley and Taylor equation (Belmans et al., 1983)
- potential evapotranspiration is calculated with the Monteith-Rijtema equation (Belmans et al., 1983)

If potential evaporation is not directly entered as potential soil evaporation and potential plant transpiration, ET_{pot} is divided over E_{pot} and T_{pot} taking into account the leaf area index (LAI):

$$E_{pot} = e^{-0.6\ LAI}\ ET_{pot} \tag{2.12}$$

where:

$$LAI = \alpha\ sc + \beta\ sc^2 + \gamma\ sc^3 \tag{2.13}$$

sc : soil cover (cm^2/cm^2)
α,β,γ : empirical regression coefficients

The actual soil evaporation depends on the conditions prevailing in the soil profile. SWAP offers two reduction models: the Black model (Black, 1947) and the Boesten model (Boesten and Stroosnijder, 1986).

Black's model calculates the cumulative soil evaporation during a drying cycle as:

$$\sum E_{act} = \alpha \sqrt{t} \qquad (2.14)$$

α : soil dependent parameter characterizing soil evaporation (cm $d^{-1/2}$)
t : time after preceeding rainfall or irrigation event (d)

The actual soil evaporation according to Boesten depends on the sum of E_{pot} since the last rainfall event:

$$\sum E_{act} = \beta \sqrt{\sum E_{pot}} \qquad (2.15)$$

β : soil dependent parameter characterizing soil evaporation ($cm^{1/2}$)

The soil dependent parameters can be measured by carrying out micro-lysimeter experiments.

If necessary, SWAP takes into account the evaporation of a ponding layer, resulting from irrigation or rainfall. A ponding layer occurs when the infiltration rate of the soil is less than the irrigation or rainfall rate (no runoff).

2.2.7 Lower and lateral boundary conditions.

In SWAP93 the assumption is made that, in the unsaturated zone, the water flows vertically. In the saturated zone, the water may flow vertically to deeper soil layers, but also laterally to drains and ditches. The lateral flow can be described by different drainage formulas, e.g. Hooghoudt and Ernst, depending on the actual soil profile.

At the bottom boundary of the schematic soil profile SWAP93 offers different options:

- water table depth is given as input and the model calculates the upward or downward bottom flux.
- the bottom flux is given as input and the model calculates the groundwater table depth.
- the flux as a function of the groundwater table depth can be prescribed at the bottom of the profile.
- in case of an impermeable layer, a zero flux can be entered.
- if the soil profile remains unsaturated, the pressure head at the bottom of the profile can be prescibed and the model will calculate the bottom flux.
- free drainage at the bottom of the profile; the flux equals the hydraulic conductivity at the bottom of the profile (unit gradient).

2.3 Solute transport

2.3.1 Salt balance

In SWAP93 solutes are considered as being conservative, which means that exchange processes and chemical reactions do not take place. In case of conservative solutes, the salt

balance for a one dimensional soil-water-plant-atmosphere system can be described with the following equation (see Figure 2.1):

$$\frac{\Delta S}{\Delta t} = P_s + I_s - q_{d,s} - q_{b,s} - R_s \qquad (2.16)$$

ΔS : change in salt storage (g/cm^2)
Δt : time period (d)
P_s : salts in precipitation (g/cm^2/d)
I_s : salts in irrigation (g/cm^2/d)
$q_{d,s}$: salts in lateral drainage flux (g/cm^2/d)
$q_{b,s}$: salts in net bottom flux (percolation minus capilairy rise) (g/cm^2/d)
R_s : salts taken up by the roots (g/cm^2/d)

The salt concentration is expressed as 'mass/volume'. Instead of 'g/cm^3', often the electrical conductivity (dS/m) of the soil water is used to express the salt concentration, as it is proportional to the salt concentration itself.

2.3.2 Solute transport in the unsaturated zone.

The rate at which solutes move through the soil is determined by several transport mechanisms. The mechanisms often act simultaneously on the solute and may include such processes as convection, dispersion and diffusion, adsorption and decomposition (Feddes, 1995). Although adsorption and decomposition are incorporated in the latest version of SWAP, only convection, dispersion and diffusion of solutes are considered in this study.

The dominant process causing the motion of solutes in the soil is convection: the solute is being carried along by the moving liquid phase. In addition, the solutes may move as a result of mechanical dispersion and molecular diffusion, together called hydrodynamic dispersion. Mechanical dispersion is caused by the differences in size and shape of the pores, while molecular diffusion results from variation in solute concentration within the liquid phase. Both processes tend to smooth any sharp boundary of a concentration front and their significance depends on the average pore water velocity in the soil.

In case of transient one-dimensional vertical flow in the soil-root system, the solute transport of conservative solutes can be discribed by the conversion-dispersion equation:

$$\frac{\partial(\theta\ c)}{\partial t} = -\frac{\partial q_s}{\partial z} - S_r \qquad (2.17)$$

where:

$$q_s = - \theta D(V,\theta) \frac{\partial c}{\partial z} + q c \qquad (2.18)$$

and:

$$D(V,\theta) = D_h(V) + D_e(\theta) \qquad (2.19)$$

θ : soil moisture content (cm^3/cm^3)
c : solute concentration (g/cm^3)
q_s : totale solute flux ($g/cm^2/d$)
S_r : sink term for solute loss due to salt uptake by plant ($g/cm^3/d$)
q : water flux (cm/d)
V : average pore water flow velocity ($V=q/\theta$) (cm/d)
D_h : mechanical dispersion coefficient (cm^2/d)
D_e : molecular diffusion coefficient (cm^2/d)
D : hydrodynamic dispersion coefficient (cm^2/d)

For detailed information about the numerical solution scheme, see Boesten and Van der Linden (1991).

2.3.3 Root water uptake under saline conditions

The three most important effects of salinization are an increased osmotic head of the soil water, toxic effect on plant physiology and change of soil physical properties, especially due to sodification. Only the first effect is incorporated in SWAP93.

Van Genuchten (1987) assumed that plant response to pressure head h and osmotic head π could be modelled by the same mechanism. Combining water and salinity stress to determine the reduction of root water uptake can be achieved in several ways. The approach used in SWAP93 is to add h and π and use the total head h_{total} to derive α according to Figure 2.3. The osmotic head π of a saline soil can be related to the electrical conductivity of the soil water solution (EC_{sw}) and is described as follows:

$$\pi = A + B\, EC_{sw} \qquad (2.20)$$

π : osmotic head (cm)
EC_{sw} : electrical conductivity of the soil water (dS/m)
A,B : empirical coefficients

As the effect on root water uptake varies between crops, a crop specific coefficient C should be used to account for the osmotic potential:

$$h_{total} = h + C \pi \qquad (2.21)$$

The coefficient B is generally set at -360 cm/dS/m (USSL, 1954), while A and C are dependent on the salt tolerance of the crop. That means on the threshold level at which yield reduction will occur, and the slope of the salinity-yield reduction curve for the specific crop (Maas and Hoffman, 1977) (see Annex C for determination of A and C). The effect of the osmotic potential on the flow of soil water is not included in the model.

2.4 Assumptions and restrictions of the model.

SWAP is a deterministic model based on the abovementioned physical laws. A suitable scale for deterministic agrohydrological models is the field scale as farmers cultivate and irrigate each field differently (Van Dam, 1993). On this scale, factors such as water application, crop type, soil type drainage condition etc. are assumed to be more or less uniform and can be simulated with a one-dimensional model.

SWAP calculates the actual transpiration, which is related to the reduction in the potential transpiration due to water and salinity stress only. All other conditions are assumed to be optimal. That means that there are sufficient nutrients for the plant to take up, there are no pests and diseases, and cultural practices (e.g. seed bed preparation, ploughing, etc.) are optimal. To come to the *actual* reduction in transpiration, all these management practices of the farmer should also be taken into account.

SWAP93 calculates the actual transpiration of the crop, and does not calculate directly the crop yield. The reduction in potential transpiration calculated by SWAP93 is assumed to be proportional to the reduction in crop yield due to water and salinity stress. Crop growth has until recently been calculated by the CROPR routine as described by Van Wijk and Feddes (1989). With this routine, the SWAP93 version is able to calculate potato growth only. For other crops, the crop routine has to be adapted. At the restructuring of the model it was decided to use the WOFOST model (Van Diepen et al., 1988) for calculation of crop development and transpiration. At the moment, the interactions between SWAP93 and WOFOST are still being tested and this version is not yet reliable. In the near future, it will be possible to calculate crop growth with SWAP93.

Another restriction of the model is that only salinization can be simulated and sodification cannot be adressed. SWAP does not make a distinction between the different cations and anions in the soil solution, but considers only the total amount of soluble salts. SWAP does not take into account the chemical processes that occur in the soil, e.g. precipitation and dissolution processes, and cation exchange processes to the clay complex. In the future, the model might be extended to predict SAR values, but this is still very tentative. Sodification might be more directly evaluated by measuring hydraulic conductivity of sodic soils in the field or by adopting relations from literature.

In Chapter 7 the application of SWAP93 in relation to this study is evaluated and its limitations are reviewed.

CHAPTER 3 CALIBRATION AND VALIDATION OF SWAP93 FOR FOUR SAMPLE FIELDS

3.1 Calibration and validation procedure

3.1.1 Calibration procedure

To calibrate the SWAP model, simulation results have to be compared with measured data, that are collected for four sample fields in the Chishtian Sub-division. For calibration of the model, measured pressure heads, soil moisture content and salt concentration (EC_e) are used, as these data are independent of the model input. The way the input data were adjusted to match the simulation results with the measured data is discussed below.

The model input can be divided into three categories: (1) input data at the bottom of the system describing the transition of the unsaturated to the saturated zone; (2) input data at the transition of the soil and plant to the atmosphere (top of the system) and (3) input data describing the soil system itself, namely the soil hydraulic parameters and the presence of preferential flow paths (Kelleners, 1993).

ad 1)
Since a drainage system is absent in the Chishtian Subdivision, the bottom of the system is determined by the groundwater table depth. The network of piezometers around the four sample fields is rather dense and groundwater table depths are determined very accurately. Therefore, bottom boundary conditions - whether a groundwater table or free drainage - were not changed during the calibration proces.

ad 2)
Input data at the top of the system consists of agronomical, meterological and irrigation data. As the agronomical and meteorological data are either measured in a rather accurate way, or derived from literature, they were kept constant during the calibration process (e.g. reference evaporation, crop factors, sink terms, Boesten parameter).

The accuracy of the irrigation data is less because of fluctuating discharges in the watercourses. Since the outlets are calibrated, the discharge is precisely known for a certain water level. However, the waterlevel is fluctuating during the day, so the daily measured discharge does not necessarily correspond with the actual discharge at the time the farmer was irrigating his field. Therefore, the irrigation depths were varied during the calibration process. Since one of the problems during calibration was the excessive leaching of salts, the irrigation depths were reduced to 60% of the original depths. However, this reduction in irrigation depths did not yield satisfactory calibration results, as simulated pressure heads did not correspond with measured values anymore. Thus, in the final calibrated models, the irrigation depths were fixed at their original values.

ad 3)
The determination of the VGM-parameters forms the main part of the calibration process, as they describe the characteristics of the soil system itself. The VGM-parameters influence the calibration results the most (pressure heads and moisture content).

A good methodology for determining a field specific retention curve is to plot measured moisture contents versus simultaneously measured pressure heads, and fit these data with the retention curve, described by Van Genuchten. Unfortunately, moisture content was only measured twice, which is not sufficient to fit a retention curve.

A second method for determining the VGM-parameters for a specific field is to take undisturbed soil samples and conduct pressure outflow measurements (e.g. multi step outflow method). For Field 3 and Field 4, the International Waterlogging And Salinity Research Institute (IWASRI) carried out these experiments to determine the field specific VGM-parameters and their limits (IWASRI, 1995). The results are shown in Table 3.1.

Table 3.1 *Limits for VGM-parameters for Field 3 and Field 4 at different depths.*

field	depth (cm)	θ_r (-)	θ_s (-)	K_s (cm/d)	α (1/cm)	λ (-)	n (-)
3	30	0-0.06	0.33-0.38	6.4-115	0.007-0.012	-0.47-3.45	1.24-2.13
	60	0-0.02	0.36-0.45	3.2-16.1	0.005-0.140	-2.0-10.0	1.20-3.00
	90	0-0.03	0.44-0.48	0.5-2.0	0.006-0.180	6.0-12.0	1.25-1.35
4	30	0	0.43-0.46	3.5-7.3	0.004-0.005	1.29-5.10	1.38-1.48
	60	0	0.39-0.42	1.8-2.8	0.006-0.011	4.70-5.00	1.27-1.39
	90	0	0.49-0.50	8.6-12.0	0.003-0.010	2.65-7.24	1.42-2.65

In general, it is difficult to correlate parameters determined in the laboratory with parameters that are valid for the prevailing field conditions. Asher (1993) and Kelleners (1993) found that the VGM-parameters determined in the laboratory did not yield satisfactory calibration results, when directly used in the SWAP model. Considering the VGM-parameters listed in Table 3.1, it can be said that the limits at each depth are very wide. Moreover, for fields 3 and 4, the upper soil layer in the model extended to one meter depth, so the determined limits for the VGM-parameters of the upper soil layer are even wider. This means that it is very difficult to derive a set of VGM-parameters from the laboratory data, that can be used to start the calibration process with. The averaged VGM-parameter set did not yield satisfactory calibration results, and the findings of the above mentioned authors are confirmed. Therefore, it is not adviced to determine the VGM-parameters in the laboratory, as this methodology is costly and time consuming. The results cannot directly be used in SWAP, since it is difficult to extrapolate the laboratory results directly to field conditions.

The least time consuming methodology for determining the VGM-parameters of a soil is to derive the parameters from literature. Based on texture, in combination with organic matter content, bulk density and medium sand diameter, a good indication of the VGM-parameters can be derived from the tables developed by Wösten et al. (1987), Carsel and Parrish (1988)

and Rawls (1982) (see Annex B). However, also these tables show large ranges for the VGM-parameters of the different textural classes.

The determination of the final soil hydraulic parameters was done by 'trial and error', mainly guided by Wösten et al. (1987) and also by Rawls et al. (1982), Carsel an Parrish (1988) and other reports on SWAP-modelling (Asher, 1993; Akbar, 1995; Bastiaansen, 1993; Kelleners, 1993). This 'trial and error' process resulted eventually in the most suitable VGM-parameters for the soil layers of the four sample fields. In Table 3.2 the calibrated VGM-parameters, as well as the VGM-parameters from the Wösten series, are listed for the different textural classes, which are representing the soil layers of the four sample fields (see paragraph 1.5.4).

Table 3.2 *VGM-parameters for different textural classes (**calibrated** and Wösten series).*

soil layer	texture	θ_s	K_s	α	λ	n
		calibrated / Wösten et al. (1987)				
upper	LS/O3/B1 field 1	**0.33**/0.34/0.37	**45**/45/33	**0.028**/0.027/0.021	**0.0**/-0.3/0.6	**2.1**/1.5/1.7
	SL/O8/B3 field 2	**0.33**/0.42/0.45	**20**/26/18	**0.050**/0.025/0.015	**-0.5**/-0.6/-0.2	**1.8**/1.3/1.4
	L/O10/B8 field 3	**0.39**/0.44/0.40	**16**/26/23	**0.030**/0.023/0.031	**-1.0**/-2.2/-3.6	**1.6**/1.2/1.2
	(Si)L/O9/B4 field 4	**0.38**/0.41/0.42	**12**/24/55	**0.016**/0.028/0.016	**-1.0**/-1.6/0.2	**1.6**/1.3/1.6
lower	S/O1 field 1	**0.35**/0.35	**150**/100	**0.026**/0.022	**1.0**/0.8	**2.6**/2.2
	LS/O2 field 2,3,4	**0.35**/0.38	**90**/64	**0.028**/0.018	**1.0**/0.9	**2.6**/1.9

From Table 3.2, it can be concluded that the VGM-parameter values derived by Wösten et al. (1987) can be used as a good starting point for calibration. Combined with the parameter sets of Rawls et al. (1982) and Carsel and Parrish (1988), good calibration results can be obtained.

As stated before, one of the problems during calibration was the excessive leaching of salts from the soil profile. First, an attempt was made to decrease the leaching of salts by reducing the irrigation depths. Since this did not yield satisfactory results, the concept of preferential flow was used to avoid excessive leaching form the model

As explained in paragraph 2.2.4, preferential flow paths can occur in water repellent sandy soils and clayey soils with swelling and shrinkage cracks. However, the concept of preferential flow can not only be used at the scale of the soil profile itself, but also at the field scale (the soil profile in SWAP is assumed to be representative for the total field). This means that preferential flow is not only regarded as the heterogeneous movement of water through the profile (vertical axes), but also as the heterogeneous infiltration of water over the field (horizontal axes).

The concept of preferential flow at soil profile and field scale is illustrated in figure 3.1.

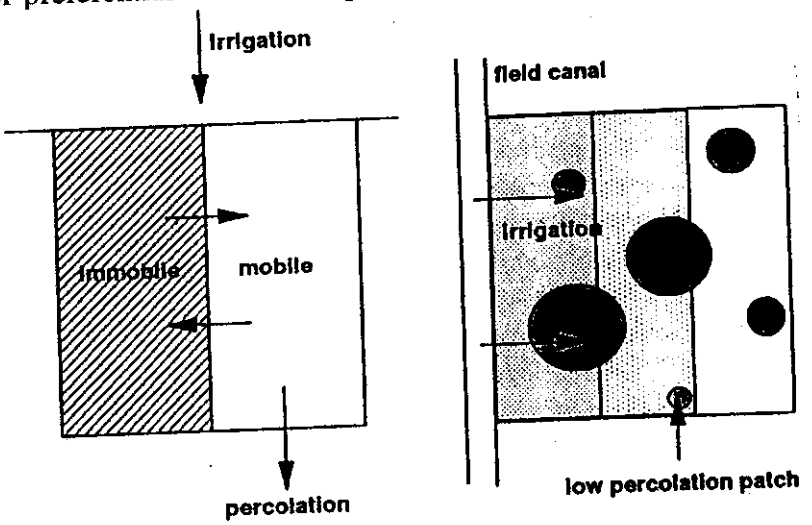

Figure 3.1 *Preferential flow at soil profile (left) and field scale (right).*

Thus, the concept of preferential flow at the field scale is used in this study to account for the large heterogeneity of infiltration, which is explained by the following phenomena:

- The heterogeneity in permeability within the field will cause an unequal infiltration of water. In case of basin irrigation, more water will infiltrate in the parts of the field with a higher conductivity, than in parts of the field with a low conductivity.
- Farmers' non-uniform water distribution over the field will contribute to a heterogeneous infiltration. Even though farmers try to prevent this nonuniform water distribution as much as possible, more water will infiltrate close to the field channel (nakka), than at the end of the field.

The heterogeneity in soil characterestics (texture, EC_e, SAR) within the sample fields is very high, so the concept of preferential flow at the field scale can be physically justified (see Annex D). Also, sodification, which causes clay dispersion and crust setting, will increase the heterogeneity in conductivity and thereby the heterogeneity of infiltration rates within the field (low permeability patches).

In conclusion, the use of preferential flow at the field scale will lead to an unequal infiltration. The average percolation for the whole field will be higher than the percolation in case the preferential flow concept is not used. However, less salts are leached out of the profile, because a part of the salts is fixed in the immobile fraction of the soil. The immobile fraction of the soil represents the least permeable parts of the field, where less water salts are leached. Salts can only be removed from the immobile fraction by diffusing to the mobile fraction. As explained in paragraph 2.2.4, the exchange of salts between the mobile and immobile fraction is determined by the exchange coefficient K_{mobile}. Since there is hardly any horizontal flow in the unsaturated zone, the exchange between the mobile (high permeability patch) and immobile (low permeability patch) will be none and consequently K_{mobile} is set at zero for the calibration and validation period. During the calibration process, F_{mobile} and $\theta_{immobile}$ were altered arbitrarily in order to match the simulated salt and moisture content profiles with the measured profiles.

3.1.2 Validation procedure

During the above described calibration process, a set of input parameters is altered and eventually fixed at certain values. This set of parameters determines the behaviour of the system and the calibrated model is supposed to generate the processes which occured in the past and will occur in the future. This ability is limited to a certain extent, and is determined by the range of behaviour in the system during the calibration period. To check whether the set of fixed parameters not only represents the behaviour of the system within the calibration period, but also within a larger range of extremes, the calibrated model has to be verified for a second set of input data; the so-called validation of the model. If the model reflects the behaviour of the system during both the validation and calibration period, it can be assumed that the model describes the processes that occur in reality in an adequate way.

Unfortunately, the model could be validated for the water balance only. Pressure heads at different depths and a moisture content profile at the end of the validation period are available to verify the model. At the writing of this report, the soil samples, which are taken at the end of the validation period, are still in the laboratory for determination of EC_e, so no check on the salt balance is possible yet.

3.2 Input data

3.2.1 Calibration and validation period

Four sample fields were monitored during three growing seasons: Kharif'94, Rabi'94/'95 and Kharif'95. For this period, an extensive data set was collected for these four fields, including soil data, agronomical data, meteorological data, irrigation data, salinity data, etc.

The calibration period comprises 12 months and is defined from 6-7-94 to 5-7-95, that means from calibration day number 1 to calibration day number 365. The first day of the calibration period is set at 6-7-94, as the EC_e is determined for that day. These EC_e data are used to calculate the initial salt concentrations in the soil profile. Unfortunately, the actual moisture content was not measured at that date, so the initial moisture content is determined by simulating a one-year prior to the calibration period ($\Delta W=0$). During the calibration period, two EC_e measurements were done, namely at the end of Kharif'94 (23-11-94 = day nr 141) and at the beginning of Kharif'95 (28-6-95 = day nr 358 and 5-7-95 = day nr 365). During the calibration period, only one measurement of the actual moisture content was done; namely, at the same day as the second EC_e measurement (day 358 and 365).

Tensiometers were installed at the beginning of Rabi'94/'95, so accurate calibration starts in December'94, as pressure heads are an important calibration parameter. This means that a more precise calibration is done for the wheat season only.

The validation period starts at 6-7-95 (= validation day nr 1), immediately after the calibration period. On this day, the actual moisture content and EC_e were measured and can directly be used as the initial condition for the validation period. The validation period ends at the beginning of Rabi'95/96 (end of December'95). At that time, the soil samples are

taken to determine the actual moisture content and the EC_e (day nr 174, 178, 169, 171). Thus, the validation of the model is done for the cotton season.

In Table 3.3, the different growing seasons during the calibration and validation period are given for the four fields.

Table 3.3 *Growing seasons during calibration and validation period.*

		Field 1	Field 2	Field 3	Field 4
Kharif'94	sowing cotton	28-5-94 (-)	20-5-94 (-)	25-5-94 (-)	16-6-94 (-)
	last picking cotton	19-12-94 (day 167)	10-12-94 (day 158)	13-12-94 (day 161)	4-1-95 (day 183)
Rabi'94/'95	sowing wheat	30-12-94 (day 178)	24-12-94 (day 172)	19-12-94 (day 167)	20-1-95 (day 199)
	harvesting wheat	30-4-95 (day 299)	11-5-95 (day 310)	27-4-94 (day 296)	20-5-95 (day 319)
Kharif'95	sowing cotton	3-6-95 (day 333)	5-6-95 (day 335)	2-6-95 (day 332)	9-6-95 (day 339)
	last picking cotton	17-11-95 (day 135)	24-1-96 (-)	19-12-95 (day 167)	16-12-95 (day 164)
Rabi'95/'96	sowing wheat	18-11-95 (-)	fallow (-)	22-12-95 (-)	17-12-95 (-)

3.2.2 Soil data

In Table 3.4, a short description of the soil layers and their VGM-parameters is given for the four sample fields. The soil layers in SWAP correspond with the layers that can be distinghuished according to the textural analysis done for the four fields (see paragraph 1.5.4).

Table 3.4 *VGM-parameters four sample fields.*

VGM-parameters				θ_r (-)	θ_s (-)	K_s (cm/d)	α (1/cm)	λ (-)	n (-)
field	layer	depth (cm)	number of compartments						
1	1	0-140	19	0.0	0.33	45.0	0.028	0.0	2.1
	2	140-315	9	0.0	0.35	150.0	0.026	1.0	2.6
2	1	0-125	18	0.0	0.33	20.0	0.05	-0.5	1.8
	2	125-290	9	0.0	0.35	90.0	0.028	1.0	2.6
3	1	0-105	16	0.0	0.39	16.0	0.030	-1.0	1.6
	2	105-210	7	0.0	0.35	90.0	0.028	1.0	2.6
4	1	0-195	16	0.0	0.38	12.0	0.016	-1.0	1.6
	2	105-210	7	0.0	0.35	90.0	0.028	1.0	2.6

In Table 3.5, the final preferential flow parameters are given. For the four fields, the mobile fraction is approximately the same. The moisture content in the immobile fraction is higher for fields 3 and 4 than for fields 1 and 2. This corresponds with a higher retention capacity of loamy soils compared with the retention of sandy soils. The exchange coefficient K_{mobile} is set at zero.

Table 3.5 *Parameters describing preferential flow.*

	layer 1		layer 2	
	F_{mobile}	$\theta_{immobile}$	F_{mobile}	$\theta_{immobile}$
field 1	0.55	0.10	0.55	0.10
field 2	0.55	0.10	0.55	0.10
field 3	0.60	0.12	0.60	0.12
field 4	0.60	0.20	0.65	0.15

Since the detailed calibration on VGM-parameters and preferential flow parameters is very time consuming, a 'simplified' calibration was done for the four fields in order to use these 'simplified' models for more routine studies. In this 'simplified' calibration, the concept of preferential flow is not used and VGM-parameters are directly derived from the Wösten series. The results are given in Annex E.

3.2.3 Evapotranspiration and agronomy data

One of the upper boundary conditions for the system is the potential crop transpiration and the soil evaporation, together called the potential evapotranspiration (ET_{pot}). First, the reference evapotranspiration (ET_0) is calculated by the agrohydrological model CROPWAT

(Smith, 1992). This reference evapotranspiration is based on the modified Penmann approach. The input data for this calculation are derived from the meteorological station in Bahawalpur[8] (e.g. wind speed, humidity, air temperature, etc.). Multiplying the reference evapotranspiration with corresponding crop factors (Doorenbos and Pruitt, 1977), results in the potential evapotranspiration. The crop factors differ for cotton and wheat and the development stages of each crop. In Table 3.6, the crop factors that are used in the calibrated models are listed. The duration of the different development stages is adapted according to the length of the growing season and the crop development of the specific sample fields.

Table 3.6 *Crop factors for different development stages.*

development stage	cotton		wheat	
	period (days)	crop factor	period (days)	crop factor
initial	20-30	0.45	15-20	0.35
crop development	40-50	0.75	25-30	0.75
mid-season	50-60	1.15	50-65	1.10
late-season	40-55	0.85	30-40	0.65
harvest/picking	10-20	0.68	-	0.25

The crop factors, as defined by Doorenbos and Pruitt (1977), include both crop transpiration and soil evaporation. The division over crop transpiration and soil evaporation is based on the amount of soil cover, or the leaf area index. As the soil cover is estimated for the four fields, and the relationship between soil cover and leaf area index is not exactly known for these fields, the following division of the evapotranspiration into soil evaporation and crop transpiration is used (Feddes, 1995):

$$T_{pot} = sc * k_c * ET_0 = sc * ET_{pot} \quad (3.1)$$

and:

$$E_{pot} = (1 - sc) * k_c * ET_0 = (1 - sc) * ET_{pot} \quad (3.2)$$

ET_0 : reference evapotranspiration (cm/d)
ET_{pot} : potential evapotranspiration (cm/d)
T_{pot} : potential transpiration (cm/d)
E_{pot} : potential evaporation (cm/d)
sc : soil cover (-)
k_c : crop factor (-)

8 As the daily hours of sunshine are not measured in Bahawalpur, the values from the meteorological station in Bahawalnagar are used for the calculations with CROPWAT.

Since the estimation of the soil cover of a field is quite rough, the division of ET_{pot} over E_{pot} and T_{pot} is not very precise. However, it still gives a good indication about which part of the potential evapotranspiration can be transpired by the crop itself.

For the fallow period, the crop factor is more or less a calibration parameter. However, tensiometers have not been read during the fallow period and, therefore, calibration of the crop factor for the fallow period is not possible. Crop factors for bare soil can vary between 0 and 1.1 according to Doorenbos and Pruitt (1977) and is arbitrarily set at 0.5. The value of the crop factor for the fallow period does not influence the results to a great extent, as the fallow period is relatively short because the wheat-cotton cycle covers the whole agricultural year.

For the reduction in potential soil evaporation to actual soil evaporation, the Boesten model is used. The Boesten parameter β for medium textured soils is 0.63 $cm^{1/2}$.

The actual crop transpiration depends on the conditions for root water uptake in the soil profile. Therefore, the root development has to be known. It is assumed that the roots grow at a constant rate from germination to physiological maturity of the crop (Borg and Grimes, 1986). This is assumed to be in the middle of the mid-season stage (Doorenbos and Kassam, 1979). After this maximum is reached, the rooting depth remains constant until harvesting. The maximum rooting depth for cotton is assumed to be 1.60 m and for wheat 1.10 m. The root distribution is assumed to be according to the Prasad distribution, as root density in irrigated fields is generally higher in the upper soil layers.

Besides the root development and distribution, the values of the pressure heads at which root water uptake becomes limited have to be entered (see paragraph 2.2.5). Because there is a lack of literature about the limiting pressure heads for cotton, they are assumed to be the same as for wheat (derived from Taylor and Ashcroft, 1972). This assumption is also made by Van Dam (1993) and by IWASRI (1996, personal communication). The soil water potential for the reduction of root water uptake (h_{total}) consists of both the matric head (h_m) and osmotic head (h_{osm}) (see paragraph 2.3.3). Based on the salt tolerance data by Maas et al. (1990) the 'average' plant specific regression coefficients for cotton and wheat are determined, and are listed in Table 3.7 (see Annex C).

Table 3.7 *Parameters determining water uptake cotton and wheat.*

crop	h_1 (cm)	h_2 (cm)	h_3 (cm)	h_3' (cm)	h_4 (cm)
cotton	-0.1	-1.0	-500	-900	-16000
wheat	-0.1	-1.0	-500	-900	-16000

crop	A (cm)	B (cm m/dS)	C (-)
cotton	3920	-360	1.50
wheat	5122	-360	1.17
average (SWAP input)	4521	-360	1.335

3.2.4 Irrigation and rainfall

Irrigation applications and rainfall events form another upper boundary condition of the system. In Figure 3.2, the irrigation applications, whether canal or tubewell water, and the rainfall events are shown for the calibration period of the four sample fields (Annex F shows the irrigation and rainfall for the validation period of the four fields).

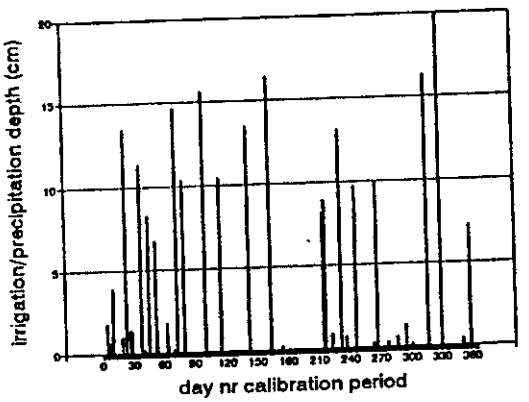

Figure 3.2a *Irrigation and rainfall calibration period field 1.*

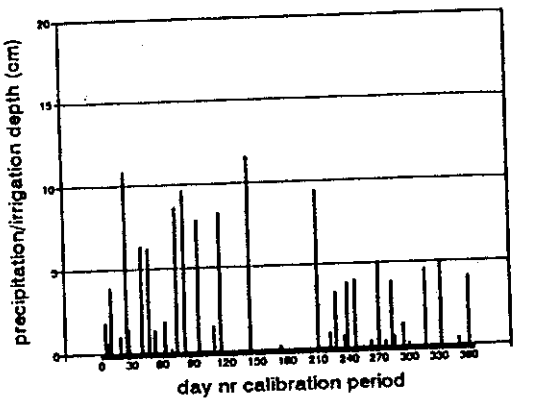

Figure 3.2b *Irrigation and rainfall calibration period field 2.*

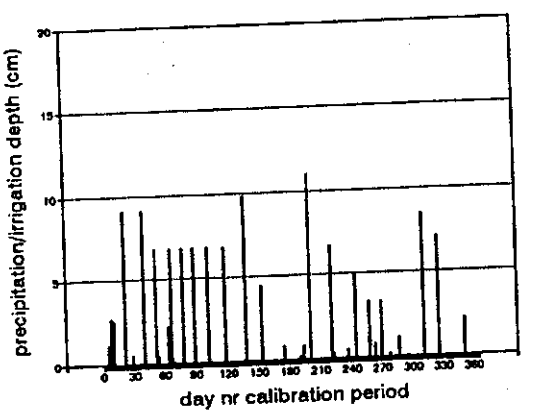

Figure 3.2c *Irrigation and rainfall calibration period field 3.*

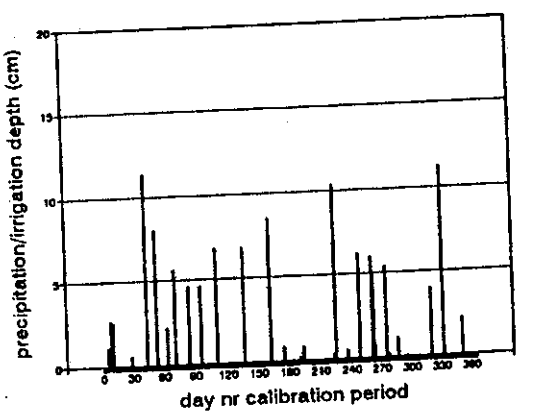

Figure 3.2d *Irrigation and rainfall calibration period field 4.*

The quantity of the irrigation applications is calculated in the following way. Regarding the canal water applications, the water level at the head of the watercourse is measured almost every day and is converted into a discharge (calibrated outlet). Seepage losses from the head of the watercourse (mogha) to the field (nakka) are based on the distance between mogha and nakka and on previously determined seepage rates (Barral, 1994 and Pintus, 1995). The time period that the farmer irrigates the sample field is registered, so the final irrigation depth is calculated by dividing the volume of water applied to a certain field by the cultivated area of the field. In case of tubewell water application, the same procedure is followed, concerning seepage losses (distance from tubewell to nakka). The discharges of the tubewells were previously determined (accuracy is about 5 %), and are dependent on e.g. the type of pump, the diameter of the pipe, the angle of outflow, etc. Precipitation is recorded in each watercourse by means of a rain gauge.

3.2.5 Groundwater table

The bottom boundary of the system is determined by the depth of the groundwater table. Fields 1 and 2 are located in Fordwah 62-R, where the water tables fluctuate around 2.0 to 3.0 m below the ground surface level. Figure 3.3 shows the water table depth during the calibration period for Fields 1 and 2 (see Annex F for water table depths during the validation period).

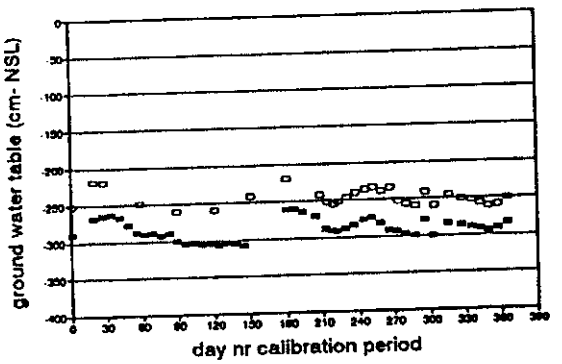

These data are based on piezometer readings in the surrounding area. Fields 3 and 4 are located in Azim 111-L, where the water table is very deep, around 6.0 m below the ground surface level. For Fields 1 and 2, a daily groundwater table is given as the bottom boundary condition of the system. Therefore, the soil profile is extended to about 3.0 m depth. Since water tables are very deep for field 3 and 4, free drainage is applied at the bottom of the system (2.0 m depth).

Figure 3.3 *Groundwater table depth calibration period Field 1 and Field 2.*

3.2.6 Salinity data

The salt balance is largely influenced by the amounts of salts in the irrigation water. The electrical conductivity (EC) of the canal water is 0.19 dS/m, while the EC of the tubewell water used for irrigation of the four fields varies between 0.6 and 1.3 dS/m. The EC of the rainfall is assumed to be 0 dS/m. In case of capillary rise, the amount of salts in the groundwater will influence the salt balance. However, the EC of the groundwater is not important for the calibration, as Fields 1 and 2 are overirrigated, so capillary rise hardly occurs (besides the soils of Fields 1 and 2 are sandy).

The initial salt storage in the soil profile is another important component of the salt balance and influences the transports of salts in the soil. The EC_e of the soil was measured for the four fields by taking soil samples at 10 locations at different depths. This was done at the beginning of the calibration period, representing the initial condition concerning the salt balance (see Table 3.8).

Table 3.8 *Initial EC_e values (dS/m) calibration period for four fields.*

	15 cm	30 cm	60 cm	90 cm	120 cm	150 cm	200 cm
Field 1	1.95	1.53	1.95	2.15	1.67	1.39	1.31
Field 2	1.91	1.97	1.54	1.21	0.79	0.87	0.71
Field 3	1.39	1.21	1.29	1.34	1.41	1.17	1.16
Field 4	2.21	2.40	2.89	3.88	2.71	1.83	1.64

The measured EC_e has to be converted in the EC of the soil water (EC_{sw}) by the following equation:

$$EC_{sw} = EC_e * \frac{\theta_s}{\theta_a} \tag{3.3}$$

The actual moisture content (θ_a) consists of two parts; namely, the moisture content in the immobile fraction and the moisture content in the mobile fraction. The moisture content in the immobile fraction is entered, while the moisture content in the mobile fraction is calculated by SWAP, simulating one year prior to the calibration period. The EC_{sw} represents the average salt concentration weighted to the moisture content in the mobile as well as the immobile fraction. It is assumed that, initially, the salt concentration in the mobile fraction equals the salt concentration in the immobile fraction and consequently equals the initial EC_{sw}.

3.3 Calibration and validation of SWAP93

3.3.1 Results and discussion of calibration process for water balance

In this section, the simulation results are compared with the measurements, namely with the pressure heads and the moisture contents. Pressure heads are measured in the field by means of tensiometers, which are installed at 15, 30, 45, 60, 90, 120, 150 and 200 cm depth. The tensiometers are located in the sample fields, approximately two meters off the border of the field. Some general remarks can be made about the accuracy of the tensiometers. In the traject 0 to -500 cm pressure head values are relatively accurate, below -500 cm, when the soil becomes rather dry, accurate measurements are not possible anymore. Secondly, the tensiometers register the average behaviour of the soil matrix and not the behaviour in the preferential paths of the soil. Thirdly, the tensiometers have a certain reaction time to the changing moisture content in the surrounding soil. Taking into account the above remarks, the calibration is acceptable when the range and behaviour of the pressure heads is reasonably simulated by the model, as a more accurate calibration for field conditions is almost impossible. The acceptable range varies from approximately 100 cm in the traject of 0 to -500 cm, to 300 cm below pressure heads of -500 cm. In the graphs that compare measured data with simulation results, the measured pressure heads are represented by filled squares, while the simulation results are represented by a continuous line.

At the end of the calibration period, the moisture contents at 15, 30, 45, 60, 90, 120, 150 and 200 cm depth are determined. This is done by augering 10 holes in each sample field and taking soil samples at the abovementioned depths. For each soil sample, the moisture content is determined by weighing the samples, before and after drying at 100 C (oven drying). The depth interval is approximately 15 cm, since the auger can hardly be maneuvered with a depth accuracy better than 7.5 cm (Bastiaansen, 1993). In the graphs representing the moisture profiles, a margin of 7.5 cm is assumed. The acceptable margin of the moisture content itself equals the standard deviation of the measured moisture contents of the ten soil samples at each depth. In the graphs of the moisture content profiles, the standard deviation is indicated by the length of the rectangles. This scatter in the moisture content is caused by the heterogeneity of the moisture content in the field and by errors made during the determination of the moisture content in the laboratory. The heterogeneity of moisture

content in the field is, in turn, caused by the heterogeneity of the soil physical characteristics and by the non-uniform distribution of irrigation water over the field. When the simulated moisture content (represented by a continuous line) matches with the measured values (represented by rectangles), the calibration process can be stopped.

To obtain the best calibration results, it is necessary to calibrate both on the pressure heads and on the moisture content, as the retention curve is determined by the relation between these two variables.

Field 1

In Annex G.1, the measured and simulated pressure heads at all depths are given. Figure 3.4 illustrates the measured and simulated pressure heads at 45 and 90 cm depth, representing the behaviour of the soil in the root zone.

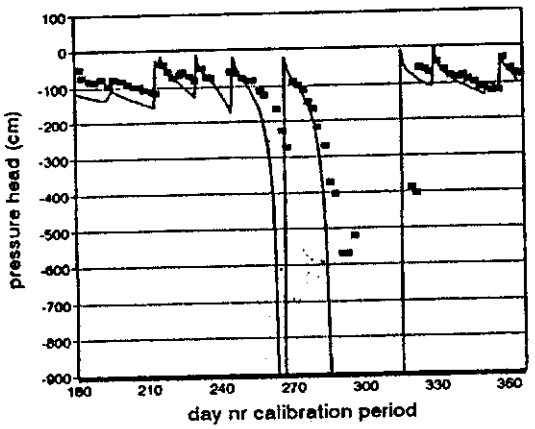

Figure 3.4a *Pressure heads at 45 cm for calibration of Field 1.*

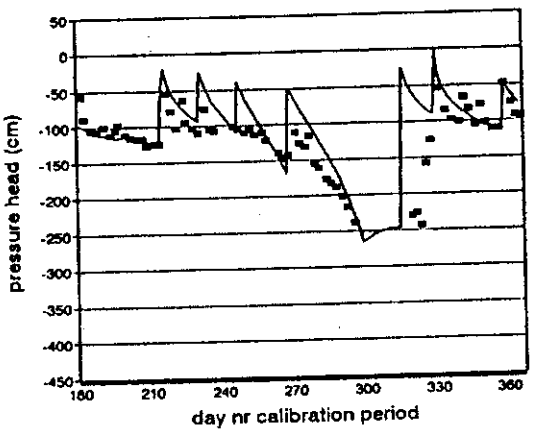

Figure 3.4b *Pressure heads at 90 cm for calibration of Field 1.*

The conclusion can be made that the model simulates the measured pressure heads in the total soil profile quite well. The most striking aspect is that the simulated pressure heads show more pronounced peaks at the time an irrigation event is applied. This can be explained by the use of the preferential concept, since the water is added to the mobile part only;therefore, the saturation of the soil is more pronounced. Besides, at the time that the peaks occur, the field is flooded, so no measurements are taken to avoid structure loss of the soil. Another discrepancy between measured and simulated pressure heads is the more pronounced decline in pressure head after an irrigation application. This can also be explained by the use of preferential flow paths, causing a quicker drainage of the soil.

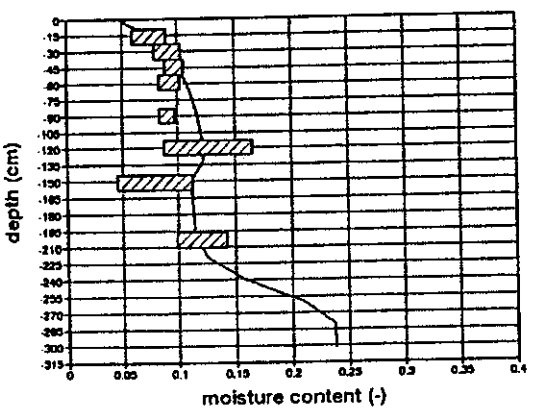

Figure 3.5 *Moisture content at day 365 for calibration of Field 1.*

Figure 3.5 illustrates the moisture content profile at day 365. In general, the simulated moisture content matches quite well with the measured data. Only between 90 and 120 cm, the moisture content is overestimated by the model. This corresponds with discrepancies between simulated and measured pressure

heads at 90 and 120 cm. In the SWAP model, the soil is artificially divided into two soil layers, while this division is more gradual in the field. This can be a cause of the difference between simulated and measured values at around 110 cm depth.

In Annex G.1 the components of the water balance of Field 1 are given for the total calibration period.

Field 2

In Annex G.2, the measured and simulated pressure heads at all depths are given for sample Field 2. In Figure 3.6, the pressure heads are given at the 45 and 90 cm depths.

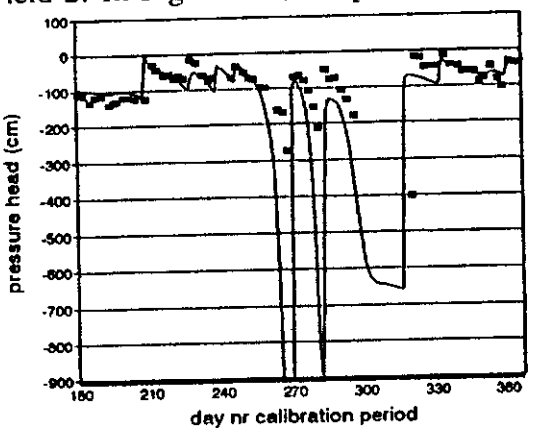

Figure 3.6a *Pressure head at 45 cm for calibration of Field 2.*

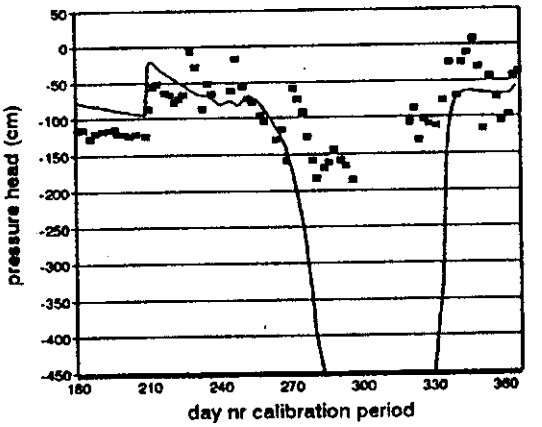

Figure 3.6b *Pressure heads at 90 cm for calibration of Field 2.*

Another conclusion is that, at the end of the wheat season (after day 265), the simulated pressure heads correspond less well with the measured pressure heads, especially not at deeper depths. This can be explained by having a more profound look at the location of the tensiometers. They are located at the border of the field and the soil is almost bare round about the tensiometers. Thus, hardly any water is taken up by surrounding roots, which is the reason that the measured pressure heads stay very high during the growing season. The simulated pressure heads decline the most at the end of the season, since the roots are totally developed and crop factors are the highest (highest ET_p).

The moisture content at day 365 is illustrated in Figure 3.7 and matches very well with the measured data. In this figure, the effect of water uptake by roots is not that important, since day 365 is at the beginning of the cotton season, when roots are still shallow and cotton covers the soil marginally.

In Annex G.2, the water balance components of Field 2 are given for the total calibration period.

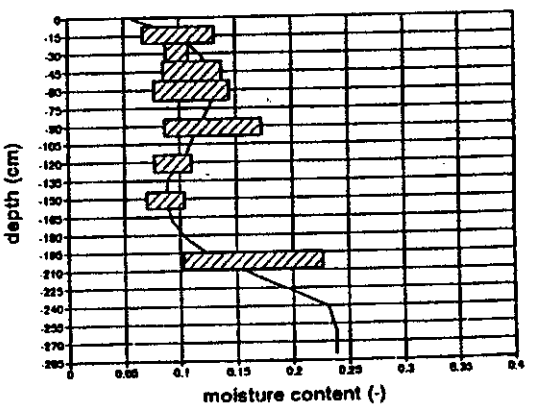

Figure 3.7 *Moisture content at day 365 for calibration of field 2.*

Field 3

Sample Field 3 was the most difficult field to calibrate, since the soil texture is very heterogeneous, both in the horizontal as well as in the vertical direction. At 60 cm depth, a silty clay layer of about 25 cm depth is present, which influences the transport of water to a large extent. However, the soil profile is divided into two layers (see paragraph 3.2.1), in order to keep the calibration process simple and to avoid numerical problems. The silty clay layer also influences the rooting depth, as roots can hardly penetrate the dense layer. The rooting depth of cotton and wheat is set at 60 cm, which yielded better results compared to 'normal' rooting depths (wheat: 110 cm; cotton: 160 cm).

In Annex G.3, the measured and simulated pressure heads at all depths are given for Field 3. In Figure 3.8, the simulated and measured pressure heads are shown at the 30 and 60 cm depths to represent the processes in the rooting zone.

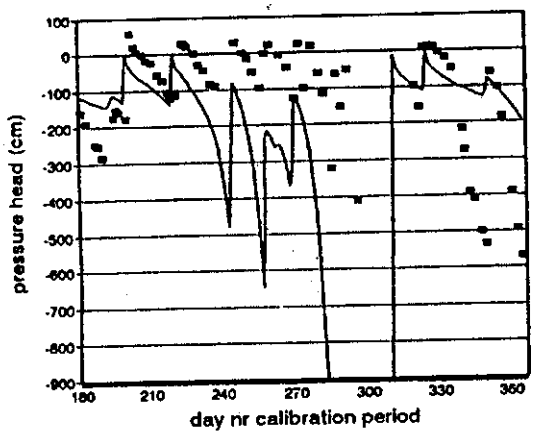

Figure 3.8a *Pressure heads at 30 cm for calibration of Field 3.*

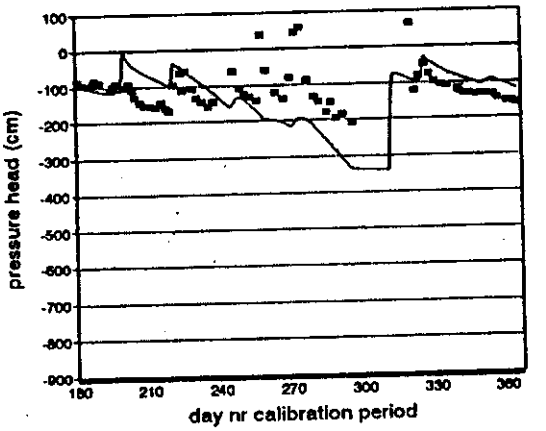

Figure 3.8b *Pressure heads at 60 cm for calibration of Field 3.*

For sample Field 3, the simulated pressure heads deviate from the measured data. In the beginning of the growing seasons (wheat: day 175-200; cotton: day 310-365), at shallow depths, the measured pressure heads show a sharp decline after an irrigation application, while the simulated pressure heads drop much less. This can be caused by extraction of water by roots of grasses and weeds around the tensiometers, while this is not simulated by the model, since only roots of cotton and wheat are considered. Thus, the extraction calculated by the model is very low, as roots are shallow and crop factors are low in the beginning of the growing season. To account for these differences in pressure heads, the Boesten parameter can be increased. This will cause a sharper decline of pressure heads as well, since more water is evaporated from the soil. However, to match the simulated pressure heads with the measured ones, the Boesten parameter has to be set at an unrealistically high value ($\beta >$ 1) and therefore β is kept at its original value (0.63). At the end of the growing season (wheat: day 250-290), simulated pressure heads drop, because of high transpiration of the crop, while measured values stay at a higher level. Again, this can be explained by the absence of a deep rooting crop at the location of the tensiometers.

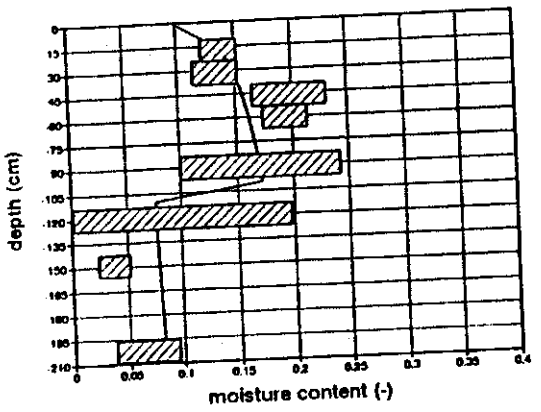

Figure 3.9 *Moisture content at day 358 for calibration of Field 3.*

The moisture content profile at day 358 is shown in Figure 3.9. In this figure, the influence of the silty clay layer can be seen very clearly, as the moisture content is higher at 60 cm depth due to a higher retention. The fact that this layer is not separately accounted for in the model is a considerable cause of the discrepancies between simulated and measured data.

In Annex G.3, the water balance components of Field 3 are given for the total calibration period.

Field 4

In Annex G.4, the measured and simulated pressure heads at all depths are given for sample field 4. In Figure 3.10, the simulated and measured pressure heads are shown at the 45 and 90 cm depths. In figure 3.11, the moisture content at day 358 is illustrated.

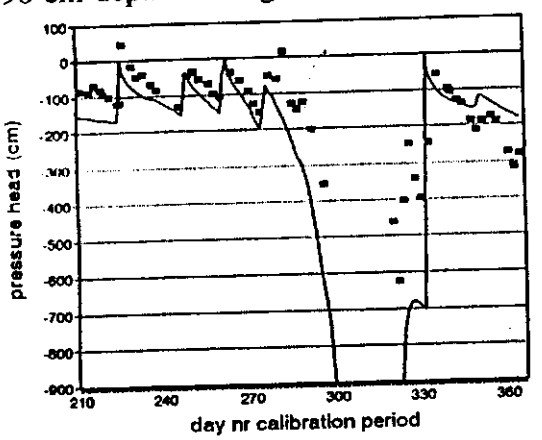

Figure 3.10a *Pressure heads at 45 cm for calibration of Field 4.*

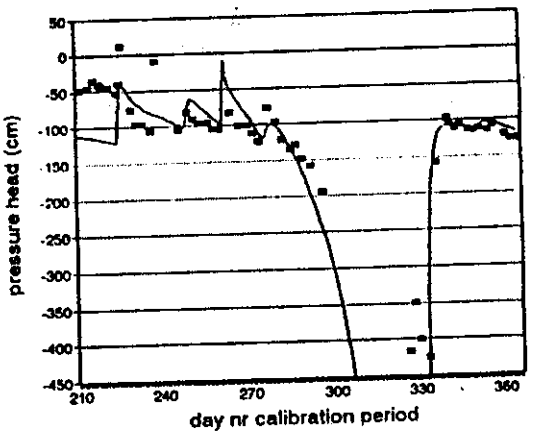

Figure 3.10b *Pressure heads at 90 cm for calibration of Field 4.*

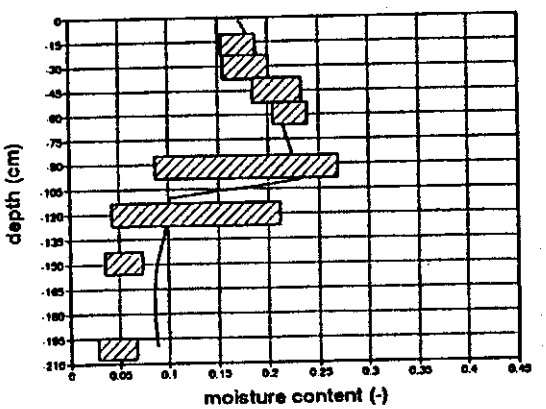

Figure 3.11 *Moisture content at day 358 for calibration of Field 4.*

The calibrated model simulates the processes in the unsaturated zone quite well. Soil hydraulic functions are properly chosen and simulated moisture content matches very well with measured moisture content. The extraction by roots actually takes place in the field, as measured and simulated pressure heads both drop at the end of the wheat season.

In Annex G.4 the water balance components of Field 4 for the total calibration period are given.

3.3.2 Results and discussion of calibration process for salt balance.

In this section the measured soil salinity is compared with the simulation results. The ideal situation would be to measure the soil salinity in situ. Since this is seldom feasible, the use of the electrical conductivity of the saturation extract has been recommended for evaluating soil salinity (Biggar, 1996). To determine the soil salinity for this study, ten holes were augered in each sample field and soil samples were taken at the 15, 30, 60, 90, 120, 150 and 200 cm depths. In the laboratory, the samples were saturated and the electrical conductivity of the water saturated paste (saturation extract) was determined (EC_e). In Figure 3.12, it is shown how soluble and relatively insoluble salts respond to increasing the water content for obtaining the soil extract. For soluble salts (e.g. NaCl, $CaCl_2$, Na_2SO_4, etc.), the total amount of salts will be independent of the water content. However, the concentration of soluble salts will decrease with increasing water content according to the simple dilution process. For relatively insoluble salts, e.g. $CaCO_3$, $CaMg(CO_3)_2$, $CaSO_4$, etc., these compounds will follow the solubility product principle. The concentration of these salts will remain constant as the amount of water increases. However, the amount of salts brought into solution with increasing water content is proportional to the water content (assuming excess solid phase present). An additional problem in determining the EC_e is that the ratio of ions may change as a result of exchange processes and ion complex formation.

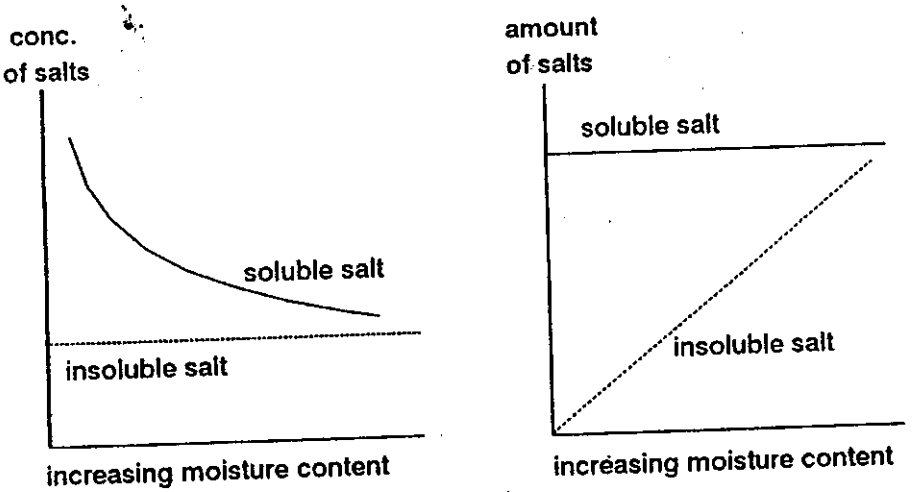

Figure 3.12 *The effect of increasing moisture content on the ionic composition of the extract.*

Thus, the disadvantages of evaluating the soil salinity by means of EC_e measurements are (Biggar, 1996):

- Insoluble salts dissolve at higher water contents that might otherwise not be present in the soil solution. A corresponding shift in exchangeable salts and soluble ions will occur as the soil solution is diluted or concentrated (dilution effect).
- Complex ion effects are ignored.

The abovementioned disadvantages can cause a discrepancy between the simulated soil salinity and the measured soil salinity. Another cause can be the heterogeneity of the salinity within the field, as salinity in the research area has a patchy character. In the graphs representing the salt storage of the soil profile, a rectangle instead of a point is given for each EC_e measurement, while the simulated EC_e is represented by a continuous line. The

rectangle represents the depth interval (7.5 cm) and the standard deviation of the ten EC_e measurements at every depth. The simulated salt balance is acceptable when the simulated EC_e values fall within the measured rectangles, then the calibration process can be stopped.

As the transport of salts in strongly related to the transport of water in the soil, calibration of the water balance is the first step in the total calibration process. The transport of salts itself can be influenced by changing the dispersion and diffusion length, but the effects on the salt balance are marginal. As explained in section 3.1.1, the concept of preferential flow is needed to obtain better results regarding the salt balance. Since K_{mobile} is set at zero, the initial salt content of the profile influences the calibration result to a large extent. Because the saturated and initial actual moisture content are not measured, the initial salt content of the profile is not precisely known. The initial salt content is determined by the measured EC_e, F_{mobile}, $\theta_{immobile}$ and the calculated actual moisture in the mobile part of the soil. From this, it can be concluded that uncertain initial conditions hamper the calibration process and can be a possible source for the discrepancies between measured and simulated EC_e values. The initial EC_e profiles for the four sample fields are given in Table 3.8 and Annex G.

Another factor, which makes the calibration of the salt balance more difficult, is the fact that SWAP calculates the electrical conductivity of the actual moisture content. For converting EC_{sw} to EC_e, the saturated and actual moisture content should be known, which is not the case in this study[9]. To reduce the effects of different (saturated or actual) moisture contents, calibration is done by comparing EC_e values instead of EC_{sw} values. Keeping in mind the above remarks, the results of the salt balance calibration will be briefly discussed.

Field 1

Figure 3.13 illustrates the salt content profiles at day 141 and 365 for calibration of field 1.

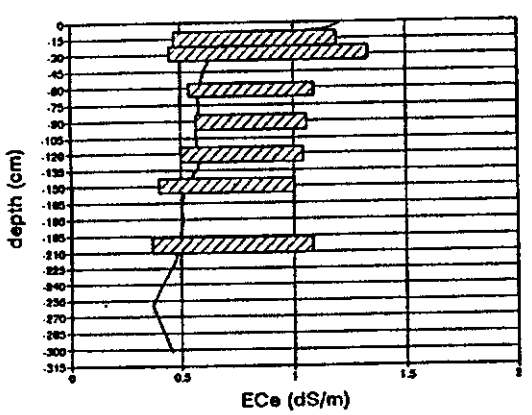

Figure 3.13a *EC_e profile at day 141 for calibration of Field 1.*

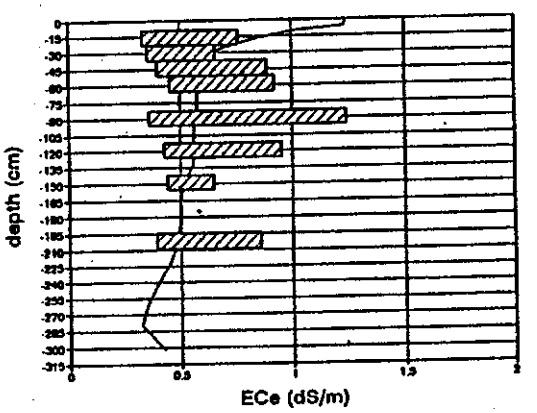

Figure 3.13b *EC_e profile at day 365 for calibration of Field 1.*

The model underestimates the measured EC_e values, although they are still within the

9 Only at day 365/358 both the actual moisture content and the EC_e are measured. Thus, for an accurate calibration of the salt balance, field observations should include soil moisture and salinity profiles at the same moment and the same location. Saturated moisture content should be determined as well.

prescribed range. In the upper soil layers, the simulated EC_e values are too high, which is caused by a very low moisture content in the mobile fraction. The total salt content is mainly determined by the salt content in the immobile fraction, which is still at the same level as initially (K_{mobile}= 0). This illustrates the influence of the initial conditions on the salt balance over the year. At 90 cm depth, the EC_e values are underestimated the most (day 365), which corresponds with an overestimation of the moisture content at that depth (see Figure 3.5). This illustrates the influence of the actual moisture content on the simulated EC_e.

In Annex G.1, the components of the salt balance of Field 1 are given for the total calibration period.

Field 2

Figure 3.14 illustrates the salt storage profiles for calibration of sample Field 2. The simulated EC_e values again underestimate the measured values, although an overestimation occurs at day 365 (90-120 cm). This cannot be explained by a deviating moisture content, as can be seen in Figure 3.7. Possibly, it can be explained by the irrigation event at day 360, that influences the EC_e profile in the form of an excessive 'salinity wave'.

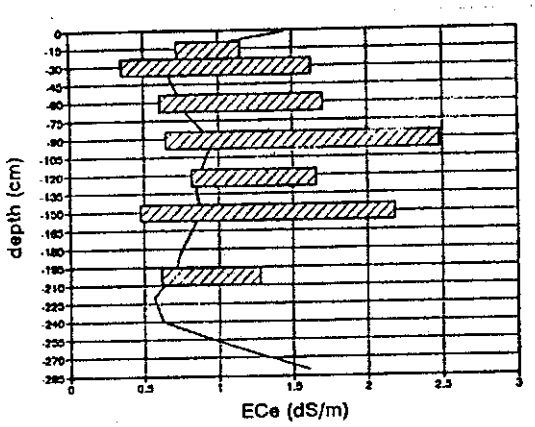

Figure 3.14a *EC_e profile at day 141 for calibration of Field 2.*

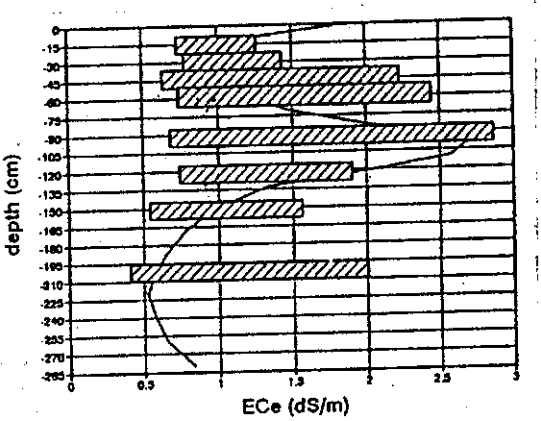

Figure 3.14b *EC_e profile at day 365 for calibration of Field 2.*

In Annex G.2, the salt balance components of Field 2 are given for the total calibration period.

Field 3

In Figure 3.15, the simulated and measured EC_e values for calibration of Field 3 are given. The model underestimates the EC_e in the first soil layer. The before mentioned reasons for this underestimation hold as well for sample Field 3.

In Annex G.3, the components of the salt balance of Field 2 are given for the total calibration period.

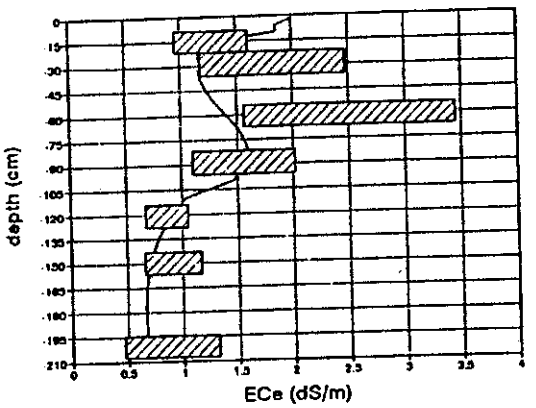

Figure 3.15a *EC_e profile at day 141 for calibration of Field 3.*

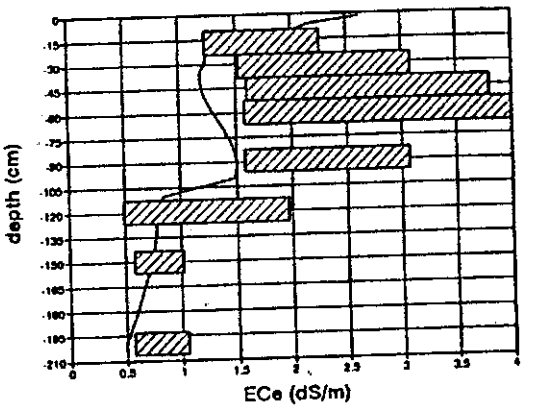

Figure 3.15b *EC_e profile at day 358 for calibration of Field 3.*

Field 4.

In Fgure 3.16, the simulated and measured EC_e values for calibration of Feld 4 are given. At day 141, the model simulates the measured salt content quite well. The overestimation at day 141 can be caused by the irrigation event at day 136.

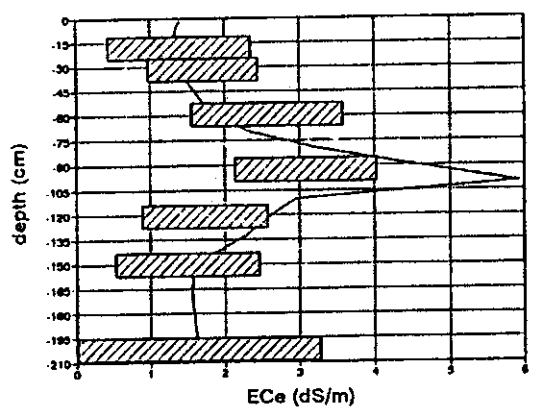

Figure 3.16a *EC_e profile at day 141 for calibration of Field 4.*

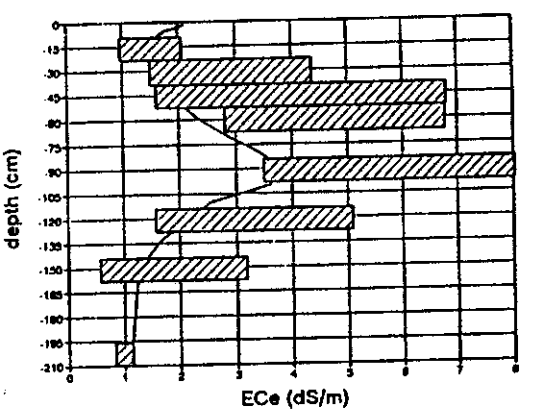

Figure 3.16b *EC_e profile at day 358 for calibration of Field 4.*

In Annex G.4, the salt balance components of Field 4 are given for the total calibration period.

Concerning the calibration process of *all* the sample fields, it can be concluded that the salt storage of the soil profile is underestimated by SWAP and too many salts are leached out of the profile. Some possible causes of the discrepancies are already mentioned in the beginning of this section (e.g. error in the EC_e determination, discrepancy due to heterogeneity etc.). However, these causes cannot totally explain the differences that occur. Based on the overall calibration process of the salt balance, doubts may be expressed by the concept that salts are assumed to be conservative. It may not be justified to neglect the chemical processes (exchange processes and precipitation processes) taking place in the soil. These processes may significantly affect the salt balance. However, the influence of inaccuracies of the water balance on the salt balance may not be ignored. A decrease in irrigation, or an increase in the potential evapotranspiration, influences the percolation and desalinization to a large extent.

3.3.3 Results and discussion of validation process for water balance

Field 1

In Annex G.1, the measured and simulated pressure heads are given for the validation period. Figure 3.17a illustrates the simulated and measured pressure heads at 60 cm depth. The simulated pressure heads correspond quite well with the measured values. The simulated pressure heads show much sharper peaks than the measured pressure heads, due to the use of the preferential flow concept.

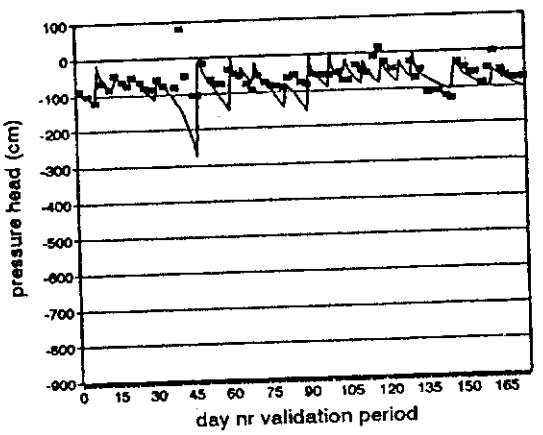

Figure 3.17a *Pressure heads at 60 cm for validation of Field 1.*

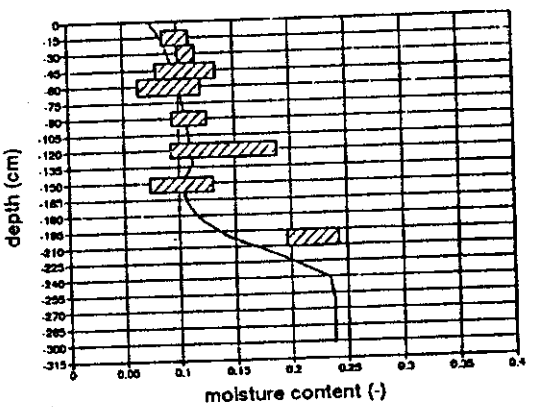

Figure 3.17b *Moisture content at day 174 for validation of Field 1.*

Figure 3.17b shows the moisture content profile at day 174. The measured and simulated moisture content compare very well. Thus, it can be concluded that the fixed set of parameters of Field 1 describes the behaviour of the system very well.

Annex G.1 gives the water balance components of Field 1 for the total validation period.

Field 2

In Annex G.2, the measured and simulated pressure heads are given for the validation period for Field 2. Figure 3.18a illustrates the simulated and measured pressure heads at 60 cm depth.

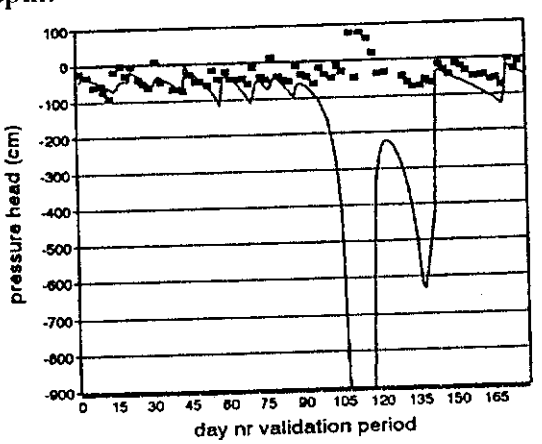

Figure 3.18a *Pressure heads at 60 cm for validation of Field 2.*

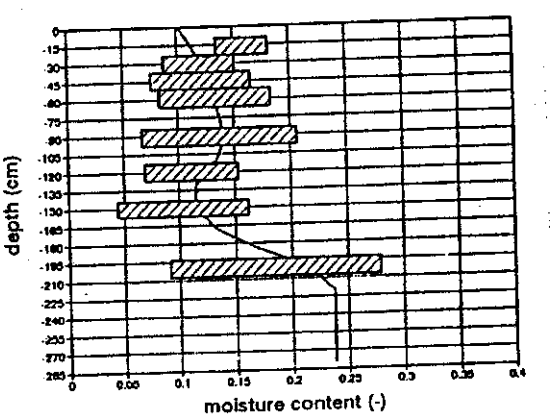

Figure 3.18b *Moisture content at day 178 for validation of Field 2.*

At the end of the growing season, especially at deeper depths, the same phenomenon occurs

as during the calibration period. Because the tensiometers are not located among the crop, pressure heads do not drop during the growing season.

Figure 3.18b shows the measured and simulated moisture content profile. As the simulated values match very well with the measurements, it can be concluded that the fixed set of parameters for Field 2 reflects the behaviour of the system quite well.

Annex G.2 shows the water balance components of Field 2 for the total validation period.

Field 3

In Annex G.3 the measured and simulated pressure heads are given for Field 3 during the validation period. Figure 3.19a illustrates the simulated and measured pressure heads at 60 cm depth. The simulated pressure heads compare quite well with the measured values, although the model simulates sharper peaks and lower pressure head at the end of the growing season. The lower pressure heads at the end of the growing season result in a lower moisture content than the measured moisture content (see Figure 3.19b). This means that the discrepancy between measured and simulated pressure heads cannot only be explained by the lack of roots around the tensiometers. Since the soil samples are spread all over the field, they represent the average moisture content of the field and not the situation in the unsaturated zone near the tensiometers.

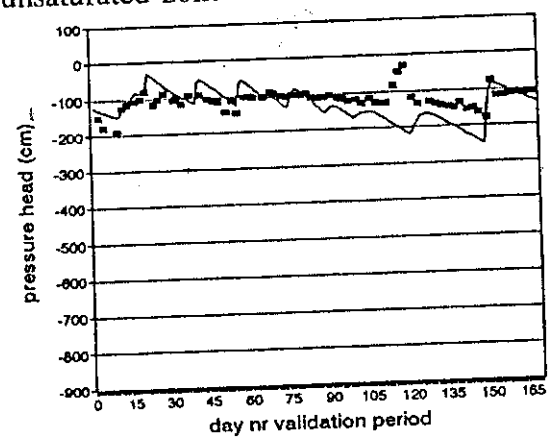

Figure 3.19a *Pressure heads at 60 cm for validation of Field 3.*

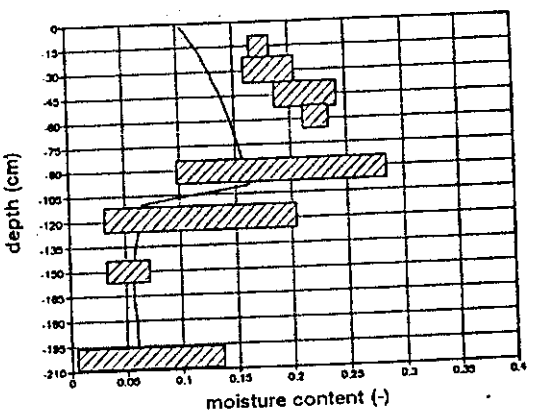

Figure 3.19b *Moisture content at day 169 for validation of Field 3.*

Annex G.3 shows the water balance components of Field 3 for the total validation period.

Field 4

In Annex G.4, the measured and simulated pressure heads are given for Field 4 during the validation period. Figure 3.20a illustrates the simulated and measured pressure heads at 60 cm depth. The simulated pressure heads correspond quite well with the measured values. However, after day 143, at which the rauni irrigation for wheat is given, the simulated and measured pressure heads show a large discrepancy. This can be explained by a too low simulated irrigation event, compared with the event, which was actually given to the crop, as the duration of this irrigation application was not registered in the field, but estimated afterwards. Another reason might be too high of a crop factor for the fallow period, since this fallow crop factor could not be determined during the calibration process. The moisture content profile shows the same trend: the simulated moisture content is smaller than

measured in the field (see Figure 3.20b). Although there are differences between measured and simulated values, it can be concluded that the calibrated model reflects the processes in the unsaturated zone in a reasonable way.

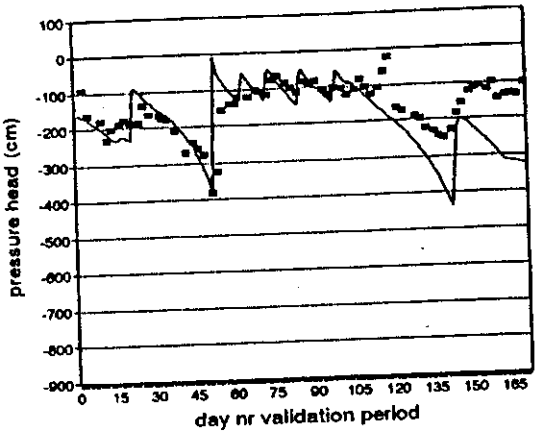

Figure 3.20a *Pressure heads at 60 cm for validation of Field 4.*

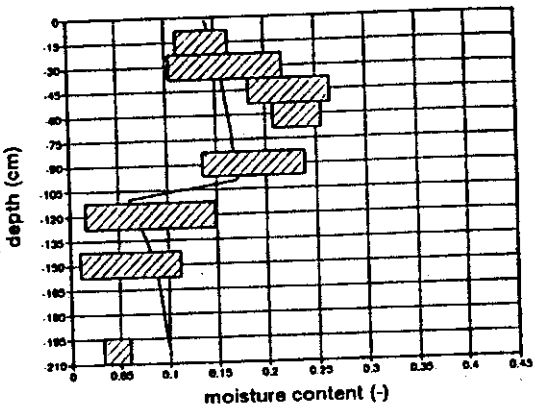

Figure 3.20b *Moisture content at day 171 for validation of Field 4.*

Annex G.4 shows the water balance components of Field 4 for the total validation period.

CHAPTER 4 SENSITIVITY ANALYSIS OF ENVIRONMENTAL PARAMETERS

4.1 Introduction

A study was conducted to determine the sensitivity of different input parameters on the behaviour of the system. Two different categories of input data can be distinguished: the so-called environmental parameters and the management variables. The environmental parameters are related to the physical environment of the system (e.g. soil parameters, agronomical parameters, meteorological parameters and hydrological parameters). These parameters determine whether the farmer is operating under favourable or unfavourable physical conditions. The management variables concern the irrigation management of the system (e.g the quality, quantity and frequency of the irrigation applications). These variables are managed by the farmer himself, although socio-economic factors often restrict the farmer's irrigation management. In this chapter, the sensitivity of the environmental parameters is discussed, while Chapter 5 deals with the effects of management variables on soil salinity and crop yield.

The first objective of this sensitivity study is to identify the most sensitive input parameters. If possible, these parameters should be measured in the field or the laboratory, as the objective of doing measurements is to establish the physical laws of the system. Thus, by carrying out a sensitivity study, it can be concluded which data should be collected with a high accuracy and recommendations can be made about a more suitable data collection program in the future. For the calibration process itself, it is not that important whether the sensitive or less sensitive parameters are calibrated. A general directive is to change the parameters within their measuring inaccuracy. Unfortunately, this inaccuracy is often not exactly known. In practice, the number of calibration parameters is kept as small as possibe. Therefore, the sensitive parameters, with relatively high inaccuracy, are used for calibration as well.

The second objective of this sensitivity study is to determine which environmental parameters a farmer should focus on when aiming to manage his environment in the best way. Therefore, the effects of the environmental parameters on the water and salt balances of the system have to be studied.

In this sensitivity analysis, the calibrated model of Field 4 is taken as the reference situation. Since this field is overirrigated, the sensitivity of some input parameters is also determined for a second reference situation, in which the irrigation applications of the first reference situation are divided by two. In this way, a sensitivity analysis is carried out for an over- and underirrigated field, and the results will be different.

Table 4.1 gives an overview of which simulations are done in this sensitivity study[10].

Table 4.1 *Overview of sensitivity analysis.*

	VGM-parameters					pref. flow		rooting pattern		evapo-transpiration		ground water
Irrigation	K_s	θ_s	α	λ	n	θ_{im}	F_m	dist.	depth	β	k_c	depth
I: 100%	x	x	x	x	x	x	x	x	x	x	x	x
II: 50%	x	x				x	x					x

The impact of the variation in input parameters is cross checked with the following so-called Vadose Zone Response Numbers (VZRN) (Bastiaansen, 1993):

Crop response indicators:

$VZRN_1$: relative transpiration (**RT**)

$$\frac{\sum T_a}{\sum T_p} \tag{4.1}$$

T_a : actual transpiration (cm/d)
T_p : potential transpiration (cm/d)

$VZRN_2$: relative evaporation (**RE**)

$$\frac{\sum E_a}{\sum E_p} \tag{4.2}$$

E_a : actual soil evaporation (cm/d)
E_p : potential soil evaporation (cm/d)

Water balance indicators:

$VZRN_3$: leaching fraction water balance ($\mathbf{LF_{wb}}$)

$$\frac{\sum Q_d}{\sum (I + P)} \tag{4.3}$$

Q_d : net downward percolation flux (cm/d)
I : irrigation application (cm/d)
P : precipitation (cm/d)

---

10 The variation in soil parameters concerns only the first soil layer of Field 4. The parameters of the second layer are kept constant.

Soil moisture indicator:

$VZRN_4$: moisture storage change (MSC)

$$\frac{\Delta W_{2.10}}{W_{2.10}^{init}} \tag{4.4}$$

$\Delta W_{2.10}$: change in moisture storage of the total soil profile (2.10 m) over a certain time period Δt (cm)

W^{init} : initial moisture storage of the total soil profile od 2.10 m (cm)

The moisture storage at a certain time t is calculated as follows:

$$W_{2.10}^{t} = \sum_{i=1}^{n} \theta_{a_i} * D_i \tag{4.5}$$

$\theta_{a,i}$: actual moisture content (cm^3/cm^3)

D_i : depth of compartment i (cm)

n : number of compartments in total soil profile

Soil salinity indicators:

$VZRN_5$: leaching fraction salt balance (LF_{sb})

$$\frac{\sum Q_d * EC_d}{\sum P * EC_P + \sum I * EC_I} \tag{4.6}$$

EC_d : electical conductivity of the percolating water (dS/m)

EC_P : electrical conductivity of the precipitation (dS/m)

EC_I : electrical conductivity of the irrigation water (dS/m)

$VZRN_6$: salt storage change (SSC)

$$\frac{\Delta S_{2.10}}{S_{2.10}^{init}} \tag{4.7}$$

$\Delta S_{2.10}$: change in salt storage of the total soil profile (2.10 m) over a certain time period Δt (dS/m*cm)

S^{init} : initial salt storage of the total soil profile (2.10 m) (dS/m*cm)

The salt storage at a certain time t is calculated as follows:

$$S^t_{2.10} = \sum_{i=1}^{n} EC_{sw} * \theta_{a_i} * D_i \qquad (4.8)$$

EC_{sw} : electrical conductivity of the soil water (dS/m)
$\theta_{a,i}$: actual moisture content (cm^3/cm^3)
D_i : depth of compartment (m)
n : number of compartments of the total soil profile

For calculating these six Vadose Zone Response Numbers (VZRN) for this sensitivity study, the total calibration period is used as time period Δt (day 1 - day 365 see section 3.2.1). The effects of varying the input parameters on these Vadose Zone Response Numbers is illustrated with pressure heads at different depths, with moisture content profiles, and with EC_e profiles (at day 365).

The simulations done in this sensitivity study are representative for the long term. This means that the environmental parameters and the irrigation management do not change over time. To simulate this 'constant' physical environment and irrigation management, the initial conditions of the simulations should represent this 'constant' environment and management of the past. Therefore, one year with the same environmental parameters and management variables is simulated prior to the one year simulations for the sensitivity analysis. This means that for simulations which are representative for the long term, the moisture storage change is zero (MSC=0, equilibrium state). If the initial conditions do not reflect the constant physical environment and irrigation management, the moisture storage change will not be zero and the initial moisture condition will have a disturbing influence on the water and salt balances. Since these simulations are not representative for the long term, they are not very useful in a sensitivity analysis.

In principle, the same reasoning holds for the salt storage change (SSC). However, the salt storage change is not necessarily zero over one year, as the salt storage changes over a number of succesive years, till an equilibrium situation is reached (SSC=0). Therefore, the initial salt concentrations cannot be determined in the same way as the initial moisture conditions. The initial salt concentrations are based on measured salinity data (EC_e June '94).

The initial EC_{sw} is determined as followed:

$$EC_{sw} = EC_{e,measured} * \frac{\theta_s}{\theta_{a,calculated}} \qquad (4.9)$$

In this way, the initial salt storage for a certain irrigation management is the same for all simulations, except for simulations with varying θ_s:

$$S_{2.10}^{init} = \sum_{i=1}^{n} EC_{sw} * \theta_{a_i} * D_i = \sum_{i=1}^{n} EC_e * \theta_{s_i} * D_i \qquad (4.10)$$

As the initial conditions have to be entered in the form of EC_{sw}, they will vary for different physical parameters and management variables. Since the initial salt concentration is assumed to be the same for the mobile and immobile part, the immobile amount of salts differs for the different simulations, and therefore can influence the simulation results.

4.2 Soil hydraulic parameters

The VGM-parameters describe the soil hydraulic functions and are the most important input parameters for calibration of the model. During the calibration process, many simulations were performed to obtain a better understanding of the meaning and significance of these soil hydraulic parameters. The VGM-parameters were varied one-by-one and their effect on the above described VZRN's and pressure heads was studied.

In this paragraph, the sensitivity of the saturated hydraulic conductivity and the saturated moisture content are discussed in detail, since these two parameters give the best insight into the transport of water through the soil profile. The other three shape-parameters are more abstract and their physical meaning is less clear. Simulations for K_s and θ_s are performed at two irrigation management situations (I=100% and II=50%), while the shape parameters are only tested for one irrigation management (I=100%).

4.2.1 Variation of saturated hydraulic conductivity

Different simulations were done to study the sensitivity of the saturated hydraulic conductivity. The hydraulic conductivity is varied from 4.0 cm/d to 36.0 cm/d, which is approximately the range for a 'loamy' (loam/silt loam/very fine sandy loam) soil, given in the different tables with VGM-parameter sets (Carsel and Parrish, 1988; Rawls et al., 1982; Wösten et al., 1987). The results are shown in Table 4.2.

As can be seen in Table 4.2, changing the saturated hydraulic conductivity within the above mentioned limits hardly effects the Vadose Zone Response Numbers.

Table 4.2 *Variation of saturated hydraulic conductivity.*

irrigation	run	K_s	RT	RE	LF_{wb}	LF_{sb}	SSC
I: 100%	ref_I	12.0	0.91	0.43	0.21	1.39	-0.20
	A_I.1	36.0	0.91	0.43	0.21	1.42	-0.27
	A_I.2	4.0	0.91	0.43	0.21	1.38	-0.19
II: 50%	ref_{II}	12.0	0.59	0.41	0.00	0.01	0.25
	A_{II}.1	36.0	0.59	0.41	0.00	0.01	0.25
	A_{II}.2	4.0	0.59	0.41	0.00	0.01	0.25

In case of overirrigation (I), only the salt balance indicators show differences for different hydraulic conductivities. An increase in K_s results in an increase of the LF_{sb}, which means that more salts are leached out of the profile and the salt storage change becomes more negative. Since the LF_{wb} does not change when K_s is varied, it can be concluded that a higher LF_{sb} is caused by higher average salt concentrations in the percolating water. This can be explained by a lower actual moisture content and a faster movement of the salinity wave through the profile. Since the water is moving faster through the profile, there is less time for diffusion and the salt concentration of the percolating water will be higher. If the conductivity is low, the water moves slowly through the profile and salt concentration gradients will become smooth, resulting in a lower concentration of the percolating water.

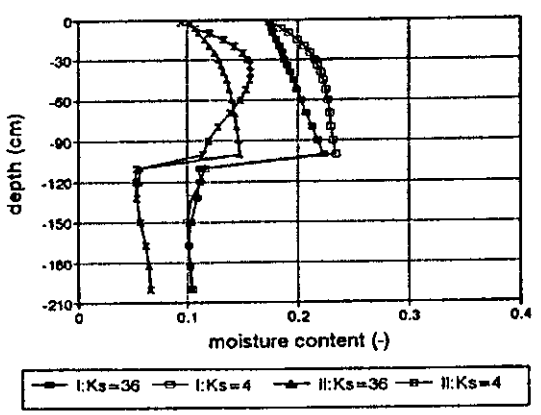

Figure 4.1 *Moisture content at day 365 at different hydraulic conductivities.*

When the field is underirrigated, the relative transpiration decreases considerably. All the apllied irrigation and precipitation is used by the crop and the net percolation flux almost becomes zero (LF_{wb}=0). This results in only a very low LF_{sb} and a considerable build up of salts in the soil (SSC > 0). Although the water and salts still move faster through the profile at a high K_s (see Figure 4.1 and Annex H.1.1), there is no effect on the Vadose Zone Response Numbers, since the percolation flux is zero.

As can be seen in Annex H.1.1, the EC_e is considerably higher in case of underirrigation and the overall moisture content is much lower. An increase in K_s results in a faster and more pronounced reaction on changes in moisture content (e.g. by irrigation or rainfall events) illustrated by sharper peaks in the pressure heads.

4.2.2 Variation of saturated moisture content.

Different simulations are done to study the sensitivity of the saturated moisture content on the behaviour of the system. The saturated moisture content is varied from 0.34 to 0.42,

which approximately corresponds with the range for a 'loamy' soil as derived from VGM-parameter sets by Wösten et al. (1987) (see Annex B).
The results are shown in Table 4.3.

Table 4.3 *Variation of saturated moisture content.*

irrigation	run	θ_s	RT	RE	LF_{wb}	LF_{sb}	SSC
I: 100%	ref_I	0.38	0.91	0.43	0.21	1.39	-0.20
	B_I.1	0.34	0.89	0.43	0.22	1.29	-0.17
	B_I.2	0.42	0.92	0.43	0.20	1.44	-0.21
II: 50%	ref_{II}	0.38	0.59	0.41	0.00	0.01	0.25
	B_{II}.1	0.34	0.59	0.41	0.00	0.01	0.26
	B_{II}.2	0.42	0.59	0.41	0.00	0.01	0.23

A change of the saturated moisture content within the abovementioned limits hardly effects the water balance indicators.

In case of overirrigation, a smaller saturated moisture content results in a slightly lower relative transpiration. The actual moisture content will be less and pressure heads will decline earlier after an irrigation event, resulting in a higher water stress for the crop (see Annex H.1.2). Since less water is transpired by the crop, the net percolation flux will be slightly higher (LF_{wb}). This implies that at lower values of θ_s, less salts will be leached out of the profile and the LF_{sb} is smaller. The salt storage change will be less negative.
For the underirrigated situation, the waterbalance indicators do not change for different saturated moisture contents. All the applied irrigation water and precipitation is transpired by the crop and there is hardly any percolation and leaching of salts. The build up of salts in the soil is equal to the amount of salts present in the applied irrigation water and precipitation. However, the salt storage change differs for different θ_s. This is caused by small differences in the initial amount of salts stored in the profile. As can be derived from Equation 4.10, at higher values of θ_s, the initial salt storage is higher, as well in the mobile as in the immobile part of the soil profile.

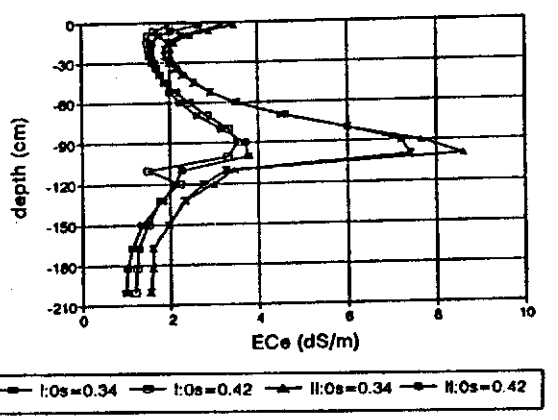

Figure 4.2 *EC_e profile at day 365 at different saturated moisture contents.*

In Figure 4.2 and Annex H.1.2, it is shown that, in general, the actual moisture content is lower at lower values of θ_s and the EC_e is slightly higher. However, the differences in EC_e are very small, which implies that the ratio θ_a/θ_s will approximately be constant (EC_{sw} is approximately constant). Therefore, the EC_e is a suitable parameter to express the soil

salinity, as it is not much influenced by the saturated moisture content of the soil. At lower values of θ_s, the soil gets saturated and desaturated earlier, pressure heads show larger peaks, and the wetting front moves faster through the profile.

4.2.3 Variation of shape parameters α, λ and n.

The VGM-parameters describe the K(h)-relation and the h(θ)-relation. The shape parameters α and n determine both curves, while λ only effects the K(h)-relation (see Equations 2.5 and 2.7). The shape factor α is varied from 0.008 to 0.032, λ from -3.0 to 1.0, and n from 1.2 to 2.0, hereby covering a large textural range. In Annex H.1.3, the effect of varying the shape parameters on the pressure heads is shown. In Figure 4.3, the effect of α, λ and n on the retention and conductivity curve is illustrated. By studying the abovementioned figures, a better understanding of the meaning and significance of the shape parameters can be obtained, which is useful during the calibration process.

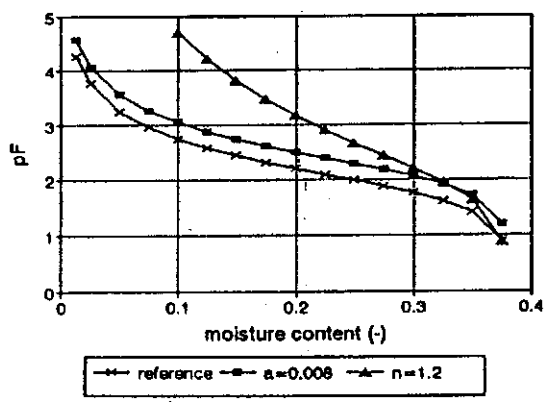

Figure 4.3a *Retention curve at different α and n.*

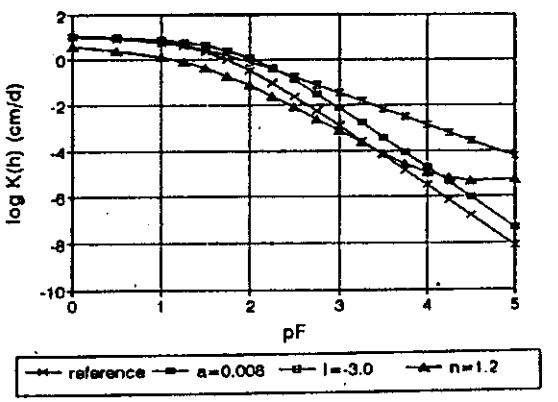

Figure 4.3b *Conductivity curve at different α, λ and n.*

When α is decreased, the air entry value is increased and air will enter the pores at higher pF-values. This results in more retention, higher conductivity and a wetter profile, since the start of drainage is delayed by lower values of α (Asher, 1993). For a given moisture content, the suction is higher at lower values of α, which can be observed in Figure 4.3.

The effect of λ on the conductivity curve is determined by the so-called flow path tortuosity. Since conductivity increases due to the presence of larger pores, it can be concluded that by decreasing λ, the flow path tortuosity is decreased due to an increase in the number of large conducting pores. This results in a higher conductivity for dry soils at lower values of λ.

When n is decreased, pore size distribution becomes larger and all the pores have different sizes. This results is more retention and a higher conductivity under dry conditions, while the conductivity is lower when the soil is wet. Consequently, the soil will drain over a larger range of suction.

The retention and conductivity curves determine the water balance, and consequently the salt balance, to a large extent. The effect of α, n and λ on the Vadose Zone Response Numbers is listed in Table 4.4.

Table 4.4 *Variation of shape parameters α, λ and n.*

run	α	λ	n	RT	ET	LF_{wb}	LF_{sb}	SSC
ref_1	0.016	-1.0	1.6	0.91	0.43	0.21	1.39	-0.20
$C_1.1$	0.008	-1.0	1.6	0.94	0.43	0.19	1.48	-0.25
$C_1.2$	0.016	1.0	1.6	0.89	0.42	0.23	1.42	-0.22
$C_1.3$	0.016	-1.0	1.2	0.86	0.42	0.24	1.48	-0.25

As stated before, a decrease in α results in an overall higher conductivity and more retention, which explains the higher relative transpiration. The drainage is delayed and the profile remains wet for a longer period of time after an irrigation application. Since more water is transpired by the crop, the net percolation will be less. However, more salts are leached out of the profile, since the conductivity and retention are higher. After an irrigation event, the excess of water will percolate, thereby leaching the main part of the salts present in the irrigation application. The salinity wave moves fast through the profile and the salt storage change will be more negative.

Increasing λ results in a lower conductivity when the soil is dry. The water uptake by the crop is reduced and consequently the LF_{wb} will be increased. More salts are leached out of the profile and the salt storage change is more negative.

Decreasing n increases the retention of the soil, the conductivity is relatively decreased for a wet soil and increased when the soil is drying. Crop transpiration will be less, since pressure heads will decline sharply after an irrigation event and plants will face more difficulties extracting water. Since crop transpiration is decreased and the conductivity is relatively increased when the soil is drying, the overall leaching fraction will be higher. Consequently, more salts are leached out of the profile and the salt storage change wil be more negative.

4.3 Preferential flow

Preferential flow (PF) is determined by means of three input variables, i.e. the mobile fraction, the soil moisture content of the immobile fraction and the exchange coefficient between the mobile and immobile fraction. To test the sensitivity of these parameters, $\theta_{immobile}$ and F_{mobile} have been increased and decreased. The immobile moisture content is varied from 0.15 to 0.25 and the mobile fraction is varied from 0.5 to 0.7. The exchange coefficient is varied from 0 to 0.004. The results are listed in Table 4.5 and Annex II.2.

Table 4.5 *Variation of preferential flow parameters.*

run	F_m	θ_{im}	K_m	RT	RE	LF_{wb}	LF_{sb}	SSC
ref_I	0.6	0.20	0	0.91	0.43	0.21	1.39	-0.20
$D_I.1$	no preferential flow			0.98	0.43	0.17	2.02	-0.52
$D_I.2$	0.6	0.15	0	0.91	0.43	0.21	1.45	-0.23
$D_I.3$	0.6	0.25	0	0.91	0.43	0.21	1.31	-0.16
$D_I.4$	0.5	0.20	0	0.89	0.43	0.24	1.37	-0.19
$D_I.5$	0.7	0.20	0	0.94	0.43	0.19	1.42	-0.21
$D_I.6$	0.6	0.20	0.004	0.91	0.43	0.21	1.73	-0.37
ref_{II}	0.6	0.20	0	0.59	0.41	0.00	0.01	0.25
$D_{II}.1$	no preferential flow			0.56	0.41	0.01	0.07	0.15

First, the simulations with and without preferential flow are considered (i.e. run $D_I.0$, $D_I.1$, $D_{II}.0$ and $D_{II}.1$). In case of overirrigation, the transpiration is lower in a soil with preferential flow paths. This is caused by the fact that transport of water and uptake of water by roots only takes place in the mobile fraction. Without preferential flow paths, more water can be stored in the soil and taken up by the roots, while in case of preferential flow, the water can only be stored in the mobile fraction and consequently the wetting front moves faster through the profile. In case of a large mobile fraction, the percolation is faster and relatively less water can be taken up by the roots and the leaching fraction will increase. As can be seen in Annex H.2.1, pressure heads will drop earlier after an irrigation application and drainage of the profile is accelerated by the presence of preferential flow paths. Although the LF_{wb} is increased by preferential flow, the LF_{sb} is decreased, as salts are fixed in the immobile fraction. Thus, without preferential flow, which can be interpreted as a uniform water distribution over the field, the salts will be leached more efficiently. This results in a higher LF_{sb}, a more negative salt storage change and lower EC_e values (see Figure 4.4).

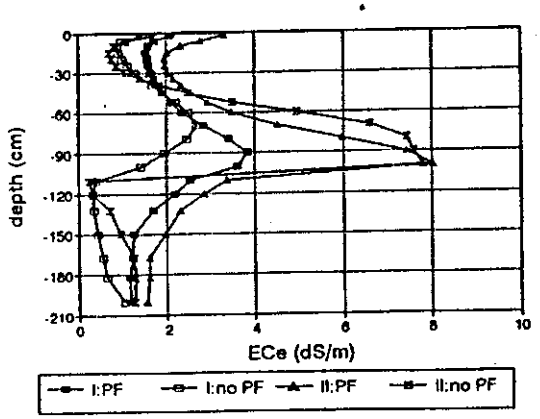

Figure 4.4 *EC_e profile at day 365 with and without preferential flow.*

When the field is underirrigated, the transpiration is lower for the simulation without preferential flow paths. Since the irrigation water is only applied to the mobile fraction, the moisture content in the mobile fraction will be higher than the moisture content in case preferential flow paths are absent and the irrigation water is applied to the total soil profile. Thus, when the field is underirrigated, the roots can extract water more easily in case preferential flow paths are present, as the moisture content in the mobile part is higher than in case preferential flow paths are absent. Since the field is underirrigated the LF_{wb} is almost zero, only slightly more water percolates without

preferential flow paths, thereby resulting in a higher LF_{sb}. The absolute build up of salts in the profile is approximately the same, as almost no salts are leached out of the profile. However, the salt storage change is higher in case of preferential flow paths, since the initial salt storage is lower compared to the initial salt storage in the profile without preferential flow paths. Obviously, EC_e values will fluctuate more (as well in time as throughout the profile) without a fixed amount of salts present in the immobile volume (see Figure 4.4).

Secondly, the sensitivity of $\theta_{immobile}$ is studied (runs D_1.2 and D_1.3). The transpiration, percolation and pressure heads are not changed by changing the immobile moisture content within the abovementioned range. Therefore, the water balance indicators do not change. However, the salt balance is affected (i.e. an increase in the immobile moisture content yields an increase in the amount of salts which are fixed in the immobile part). Thus, less salts are leached and EC_e values are generally higher (see Annex H.2.2).

Thirdly, the effect of F_{mobile} on the water and salt balance is studied (runs D_1.4 and D_1.5). Increasing the mobile fraction results in a higher crop transpiration, as more water can be stored in the mobile part and taken up by the crop (see Annex H.2.2). The percolation flux will consequently be less at higher F_{mobile}. By increasing F_{mobile}, less salts are kept in the immobile soil volume and the LF_{sb} will be higher.

Finally, the influence of the exchange coefficient K_{mobile} on the salt balance is studied (run D_1.6). The higher K_{mobile}, the higher the displacement of salts from the immobile fraction to the mobile fraction. Consequently, more salts are leached out of the profile, resulting in a higher LF_{sb} and lower EC_e values (see Figure 4.5). The displacement of salts from the immobile to the mobile part is the most at the highest concentration gradients e.g. at the 'EC_e-peak in the profile'.

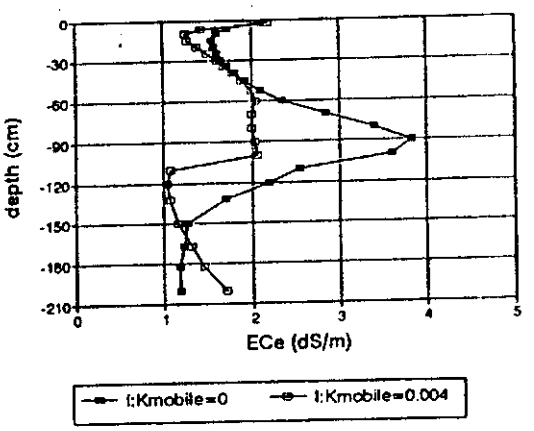

Figure 4.5 *EC_e profile at day 365 at different K_{mobile}*

4.4 Root water uptake

The root water uptake in the model is determined by two factors: the rooting depth and the root distribution function. The model SWAP offers the possibility to describe the root water uptake by different root distribution functions, e.g. the Feddes (1978) and Prasad (1988) distribution. Simulations for an overirrigated field were carried out to determine the sensibility of the root distribution and rooting depth. The results are listed in Table 4.6.

Table 4.6 *Variation of root water uptake parameters.*

run	root distribution	depth wheat	depth cotton	RT	RE	LF_{wb}	LF_{sb}	SSC
ref_1	Prasad	110	160	0.91	0.43	0.21	1.39	-0.20
$E_1.1$	Feddes	110	160	0.90	0.43	0.22	1.38	-0.19
$E_1.2$	Prasad	150	200	0.93	0.43	0.20	1.30	-0.15
$E_1.3$	Prasad	70	120	0.89	0.43	0.23	1.44	-0.28
$E_1.4$	fallow	fallow	fallow	0	0.44	0.84	1.84	-0.43

Considering the distribution of roots, it can be seen that the differences in the Vadose Zone Response Numbers are negligeable. The differences between the two distributions functions have a more pronounced effect on the waterbalances of individual layers at different depths, instead of on the total balances. At deeper depths, uptake will be higher for the Feddes distribution, as rooting density is higher. In the upper soil layer, the uptake will be more for the Prasad distribution, which has a higher root density in the upper soil layers. When the soil is wet, a high root density will cause a high water extraction. At depths with a high root density, pressure heads will increase more rapidly, resulti.g in an earl!urdecline o& 0he root water uptake compared to depths with less roots (Van Dam, 1993). Since the root water uptake in the upper layer is higher for the Prasad distribution, the actual moisture content will be less and the EC_e values will be higher in the upper soil layers (see Annex H.3.1). Deeper in the profile, the EC_e is higher for the Feddes distribution, as more water is extracted at deeper depths compared to the Prasad distribution.

If the rooting depth is considered, it can be seen that a higher rooting depth results in a higher root water uptake (higher RT) and a lower flux to the groundwater (lower LF_{wb}) (see Table 4.6). When roots still grow at deeper depths, pressure heads will decline because of extraction and the total root water uptake will increase (see Annex H.3.2). When the rooting depth is shallow, extraction will be relatively higher in the upper soil layers, which is the result of a higher rooting density, according to the Prasad distribution. However, root water uptake is slightly more efficient in case of deeper rooting depths. Obviously, the efficiency of the root water uptake is not only determined by the rooting depth itself, but also by the soil type. In case of a highly conductive soil, root water uptake is more efficient with deeper rooting depths, since the wetting front is moving fast through the profile and less water is lost by percolation compared to the situation with a shallow root system.

Concerning the salt balance, the leaching fraction (LF_{sb}) shows the same trend as for the water balance. More water is taken up by the crops at deeper rooting depths, and consequently less salts are leached out of the profile. This results in a less negative salt storage change. At shallow rooting depths, the accumulation of salts is smaller and is located higher in the profile, since the water uptake is relatively higher in the upper soil layers. In the fallow situation, the leaching fraction will obviously be very high and almost all salts are leached out of the profile (see Figure 4.6).

Root distribution and rooting depth are mostly determined by the type of crop. In most cases, the root distribution will be somewhere in between the Prasad and Feddes distributions, as they are both very strong schematic representations. In irrigated fields, roots will generally be more dense in the upper soil layers, since roots will grow there, where they can extract water in the easiest way. This also means that roots will avoid dense layers, or layers where salts are accumulated. This 'adaptive' behaviour of plant roots to their changing environment cannot be described by the model.

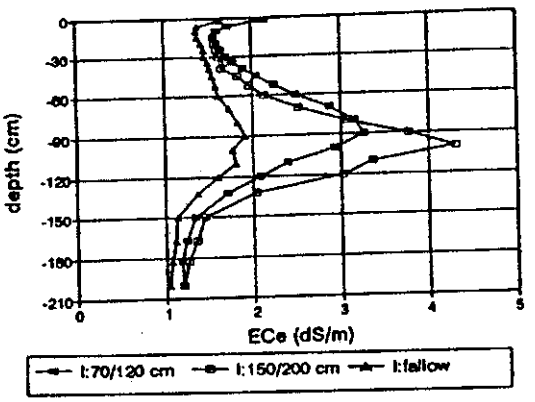

Figure 4.6 *EC_e profile at day 365 at different rooting depths.*

4.5 Evapotranspiration

Potential evapotranspiration is determined by the calculated reference evapotranspiration and the crop factors for the different development stages. Actual transpiration is determined by the root water uptake, and the actual soil evaporation is determined by the value of the Boesten-parameter. The sensitivity of the crop factors and Boesten-parameter is tested and the results are listed in Table 4.7.

The Boesten-parameter is a texture dependent variable. Unfortunately, an overview of the Boesten-parameter for the different soil textures is not yet established. Generally, the Boesten- parameter is varied from 0.54 to 0.95, using higher values for sandier soil, as evaporation from the bare soil will take place more easily. In this study, the Boesten parameter was varied from 0.63 to 1.89[11].

Factors affecting the value of the crop coefficient are mainly the crop characteristics (e.g. crop height, crop roughnes, ground cover), the crop planting or crop sowing data, rate of crop development and length of growing season, climatic conditions and the frequency of rain and irrigation. Crop factors are varied from 125% to 75% of the values of the reference situation, which are the averages given by Doorenbos and Pruitt (1977).

[11] Although 1.89 may seem to be an unrealistic high value, it is used in this study, since previous calibrations on SWAP had yielded Boesten parameters of 2.5 (Asher, 1993).

Table 4.7 *Variation of Boesten parameter and crop factors.*

run	β	k_c	RT	RE	LF_{wb}	MSC	LF_{sb}	SSC
ref_1	0.63	100%	0.91	0.43	0.21	-0.01	1.39	-0.20
$F_1.1$	1.89	100%	0.88	0.74	0.10	-0.02	1.19	-0.09
$F_1.2$	0.63	125%	0.82	0.39	0.11	-0.01	1.34	-0.16
$F_1.3$	0.63	75%	0.97	0.49	0.36	0.00	1.61	-0.29

A higher Boesten-parameter results in a higher bare soil evaporation, which consequently decreases the flux to the groundwater and diminshes the amount of salts that are leached from the profile. This results in a higher relative evapotranspiration (RE), a lower leaching fraction (LF_{wb} and LF_{sb}) and a less negative salt storage change. The larger soil evaporation affects the water and salt balance mainly in the upper soil layer, as illustrated in Annex H.4.1. The moisture content decreases and EC_e values increase. Especially in the beginning of the growing season, when the soil cover is still very low, the influence of the Boesten parameter is considerable. The percolation and desalinization is largely influenced by the amount of bare soil evaporation.

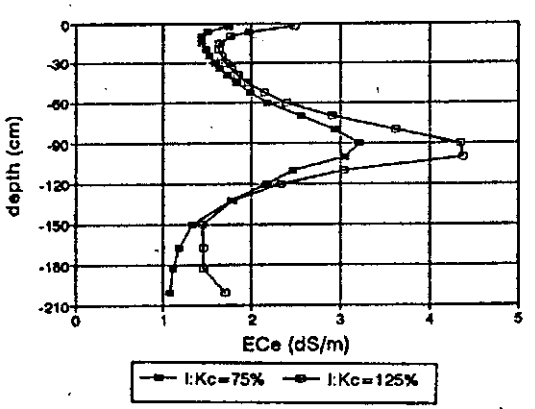

Figure 4.7 *EC_e profile at day 365 at different crop factors.*

Increasing the crop factors, increases the potential evaporation. This means that the absolute evapotranspiration may increase as well, but relatively less water can be transpired and evaporated. The effect of increasing the potential evapotranspiration is dominant over the absolute increase in evapotranspiration, which explains the lower values of RT and RE at higher crop factors. As absolute evapotranspiration is higher at higher crop factors, the irrigation surplus is less high and the leaching fraction (LF_{wb} and LF_{sb}) decreases. Less salts are removed from the soil profile, resulting in a less negative salt storage change and higher EC_e values (see Figure 4.7).The opposite holds for decreasing the potential evapotranspiration by decreasing crop factors. A lower ET_p will result in a lower suction of the soil, which means that pressure heads will not decline as sharply as when ET_p is higher and the relative evapotranspiration will be higher (see Annex H.4.2). At higher crop factors, the moisture content is lower due to higher atmospheric demand and higher suction. Consequently, the salt accumulation in the profile is higher, since the bottom flux is reduced. Concluding, the crop transpiration has a very large influence on the percolation flux and consequently on the (de)salinization.

4.6 Groundwater table depth

Two different options are studied, which describe the bottom boundary condition of the system, i.e. a groundwater table at a depth that free drainage can be assumed (more than 4 m) and a ground water table at 2.0 m depth. The influence of the groundwater table on the water and salt balances is studied for both an over- and underirrigated field. The results are listed in Table 4.8.

Table 4.8 *Variation of bottom boundary conditions.*

run	bottom boundary	RT	RE	LF_{wb}	LF_{sb}	SSC
ref_I	free drainage	0.91	0.43	0.21	1.39	-0.20
$G_I.1$	groundwater depth 2.0 m	0.93	0.43	0.29	1.54	-0.27
ref_{II}	free drainage	0.59	0.41	0.00	0.01	0.25
$G_{II}.1$	groundwater depth 2.0 m	0.79	0.43	-0.28	-0.40	0.35

In case of overirrigation, a groundwater table at 2.00 m depth causes a slightly higher relative transpiration than for the free drainage condition. This can be explained by a higher overall moisture content, resulting in a lower suction, so that the plant roots can extract water more easily (see Annex H.5). The leaching fraction (LF_{wb}), increases because the profile is much wetter, and consequently, the flux at the bottom of the profile will be higher. Thus, the leaching of salts is much higher and the salt storage change is more negative (see Figure 4.8). When the groundwater table rises, the leaching fraction increases and more salts are leached from the profile. Because the field is overirrigated, capillary rise hardly occurs, and the salt concentration of the groundwater does not influence the salinity profile.

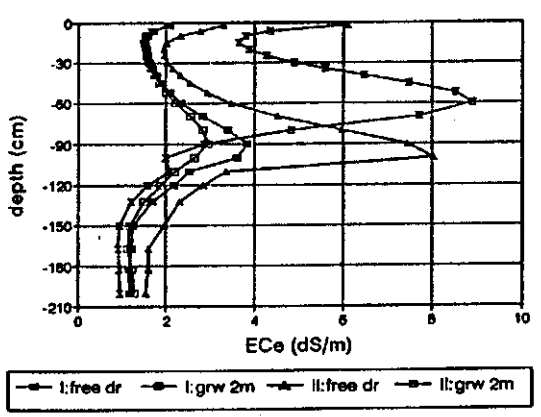

Figure 4.8 *EC_e profiel at day 365 at different groundwater table depths.*

When the underirrigated situation is considered, a groundwater table at 2.00 m depth causes a much higher moisture content in the profile, since capillary rise occurs when the soil starts drying. Pressure heads are prevented from declining because of this capillary rise and more water is available for the crop, resulting in a considerable increase in transpiration. Due to capillary rise from the groundwater, there is a net upward flux, which causes the negative leaching fractions (LF_{wb} and LF_{sb}). The salt storage change is higher in case of a groundwater table at 2.0 m depth, as there is a build up of salts due to the applied irrigation water, and due to capilláry rise from the ground water. The salts will rise in the profile, resulting in a EC_e-peak closer to the surface (see Figure 4.8).

Thus, in case of underirrigation, a higher groundwater table has a positive effect on the plant transpiration, but a negative effect on the salt balance of the profile. The quality of the groundwater determines the salinity hazard that is created by underirrigating the field, as it influences the input of salts from the bottom of the profile.

4.7 Discussion of sensitivity analysis

4.7.1 Sensitivity of parameters in relation to measurements and calibration

Soil hydraulic parameters
The soil hydraulic functions are very important for the calibration process, since pressure heads and moisture contents are strongly affected by the values of the VGM-parameters. To keep the number of calibration parameters as small as possible, it is recommended to measure the saturated hydraulic conductivity in the field (e.g. by auger hole method) and the saturated moisture content in the laboratory, as these two parameters are rather easy to determine. The shape parameters can be fixed later in the calibration process. Instead of altering the VGM-parameters one-by-one, another method can be used to quantify the effects of a different texture on the behaviour of the system. This method is known as 'scaling' and only the so-called scale factor has to be adapted in order to change the VGM-parameters and thereby the retention and conductivity curves (Feddes et al., 1995).

Preferential flow
Using the concept of preferential flow has a very large influence on the behaviour of the system, especially on the transport of salts. As explained in section 3.1.1, preferential flow can be seen on different scales--on the scale of the soil profile and on the field scale. When preferential flow on the soil profile scale is used, measurements should be done in the field to quantify the heterogeneity of water flow through the soil profile (e.g. by means of tracer experiments).

There is considerable difficulty in translating the concept of preferential flow paths of a non-uniform water distribution and heterogeneous infiltration for the field scale. In order to reduce the effects of preferential flow on the calibration results, it is recommended to keep the immobile moisture content and the immobilesalts as low as possible (i.e. a low F_{mobile} and $\theta_{immobile}$). An alternative approach to simulating non-uniform water distribution and heterogeneous infiltration is to do several simulations with different quantities of irrigation water. Afterwards, the water and salt balances have to be averaged in a certain way[12]. Again, this procedure is very difficult to calibrate.

Root Water uptake
In general, the behaviour of the system is not very sensitive to the root distribution and rooting depth. However, the rooting depth influences the pressure heads and moisture

---

[12] Kuper and Van Waijen (1993) did similar simulations with the SOWATSOL model to account for nonuniform water distribution and heterogeneous infiltration. The field was divided into two equal parts and one part was irrigated with 50 % and the other with 150 % of the original irrigation application.

contents at different depths; therefore, the rooting depth is an important parameter in the calibration process. Since the development of the roots is determined by the type of crop, the density of the soil layers, etc., the rooting depth should be measured in the field when the crop is fully grown.

Evapotranspiration
Although the water and salt transport is very sensitive to the bare soil evaporation and the crop transpiration, the Boesten parameter and crop factors are not very important in the calibration process. since these parameters are very difficult to measure[13], they are often directly derived from literature and, if necessary, only slightly adjusted during calibration.

4.7.2 Sensitivity of parameters in relation to management of environment

Soil hydraulic parameters
There is little known about the way the **VGM**-parameters are influenced by cultural practices of the farmer (e.g. hoeing, planking, ploughing, manure applications etc.). It is obvious, for example, that continuos ploughing at a fixed depth will result in a plough pan being formed and the saturated conductivity and saturated moisture content will decrease at that depth.

Not only cultural practices have their impact on the soil structure, but also the irrigation management practices of the farmer may effect the soil structure and thereby the **VGM**-parameters. Excessive irrigation with sodium rich tubewell water will cause sodification of the soil and will result in soil structure loss. In sodic soils, the clay particles are dispersed and will fill conductive pores, resulting in a dense impermeable soil (Summer et at., 1993). For these sodic soils, the saturated hydraulic conductivity and the available soil moisture are reduced, which may lead to waterlogging and to longer periods of excessive wettness (So and Aylmore, 1993). This will also lead to less efficient leaching of salts and the sodification will increase even more (see section 4.2).

Preferential flow
When the preferential flow concept at field scale is translated into a non-uniform water distribution over the field, a higher immobile fraction can be interpreted as a higher non-uniformity of the water distribution over the field. Farmers' practices influence the uniformity of the water distribution and infiltration over the field. Since a non-uniform water distribution and heterogeneous infiltration reduces the leaching of salts (see section 4.3), farmers will try to prevent this heterogeneity. the water distribution over the field will be more uniform when the farmer divides his field into smaller bounded units and irrigated those units seperately. A second practice for increasing the uniformity of water distribution is levelling of the field.

Groundwater table depth
The groundwater table depth is an important environmental parameter for the farmer, since

---

[13] Boesten parameters can be determined by doing lysimeter experiments (Boesten and Stroosnijder, 1986).

it influences the water and salt transport to a large extent. Therefore, the farmer should adapt his irrigation management according to the prevailing groundwater conditions. When the groundwater table is at a depth that capillary rise occurs, the water and salt balances are significantly influenced, especially when the salt concentration of the groundwater is high. In case the groundwater is of poor quality, the farmer should give sufficient irrigation applications to reduce or prevent capillary rise, since the capillary rise is transporting a lot os salts into the root zone. If the quality of the groundwater is good, less water can be applied and capillary rise is a useful source for water uptake by the crop, without the danger of salinization.

CHAPTER 5 SHORT TERM ANALYSIS OF 'MANAGEMENT VARIABLES'

5.1 Introduction

In this chapter, the short term effects of the so-called management variables on soil salinity and crop transpiration are discussed. These variables include the quantity, quality and the frequency of the irrigation applications, which are determined by the ways that farmers decide to irrigate their fields. The way the farmer irrigates a field is dependent on a lot of factors, such as the availability of canal water, the availability of tubewell water, the soil type, the salinity level of the fields, the crop which is grown, the farmer's perspectives about salinity, etc.

To understand the short term effects of the management variables on soil salinity and crop transpiration, several simulations with a different irrigation management were undertaken. The results of the different management simulations are compared with the results of the reference management simulation. This analysis is valid for the short term, which means that only one agricultural year is simulated with an irrigation management that differs from the reference irrigation management. The reference management scenario was simulated one year prior for determining the initial moisture conditions. The long term effects of different irrigation management scenarios are discussed in Chapter 6.

In Table 5.1, an overview is given of the simulations which are performed for one agricultural year, having a wheat-cotton cycle. These simulations were done for four different soil types, corresponding with the soil types of the calibrated sample fields. Six Vadose Zone Response Numbers (see section 4.1) were used as performance indicators.

Table 5.1 *Overview sensitivity study management variables.*

management variable	
quantity	reference - overirrigation - underirrigation
frequency	reference - low frequency - high frequency
quality	reference - canal - tubewell - low quality rauni
initial salinity	reference - high salinity level

The reference irrigation management will be discussed below, while the other management simulations are described in the following sections. The reference situation includes a crop calendar, an irrigation pattern (quantity, quality and frequency) and an initial salinity level.

Crop calendar
The crop calendar is based on the average wheat-cotton cycle in the research area. The reference situation comprises the two growing seasons, including their pre-sowing irrigations. Although the Agricultural Department of Hasilpur advises to sow wheat from November 15th

to November 30th, in the reference simulation, wheat is sown on December 20th[14]. This relatively late sowing is directly related to the wheat-cotton cycle, since cotton is not removed from the field before the end of November. The wheat is harvested after 120 days (April 20th). Afterwards, there is a fallow period, in which the field is prepared for sowing cotton, which is done on June 1st. The cotton crop is removed from the field after 195 days (December 15th). Afterwards, the next sowing of wheat takes place on December 20th and the next cycle starts.

Irrigation pattern
The irrigation pattern for the reference situation is based on the recommendations of the Hasilpur Agricultural Department and Ayub Agricultural Research Institute in Faisalabad. For wheat and cotton, the following irrigation pattern is advised (see Table 5.2)

Table 5.2 *Irrigation pattern cotton and wheat for reference simulation.*

	wheat		cotton	
quantity	rauni[15] other total	: 15.0 cm : 7.5 cm : 52.5 cm	pakki rauni[15] kachi rauni[15] other total	: 10.0 cm : 7.5 cm : 7.8 cm : 80.0 cm
frequency	rauni first interval	: 2-3 weeks before sowing : 3 weeks after sowing : 2 weeks	pakki rauni kachi rauni first interval	: 3 weeks before sowing : 1 week before sowing : 6 weeks after sowing : 2 weeks
quality	rauni other	: 0.2 dS/m (canal water) : 1.5 dS/m	rauni other	: 0.2 dS/m (canal water) : 1.5 dS/m

Initial salinity level
in order to compare the effects of the different irrigation managements on soil salinity, the initial amount of salts in the profile should be the same for all simulations for the four fields. The total amount of salts in the profile is set at 150 dS/m * cm for all the four fields, which approximates an EC_e value of 2.0 dS/m throughout the profile. Since the initial moisture content and the saturated moisture content slightly differ for the four soil types, the initial EC_e is not exactly 2.0 dS/m for all the four fields.

In the following sections, the effects of varying the different management parameters are discussed. In section 5.2, the effects of different quantities of irrigation water are discussed

---

14 According to Pintus (1995), 49 % of the fields in the 8 sample watercourses of the research area were sown from December 15th to December 31th.

15 The pre-sowing irrigations are called the rauni irrigations. For the wheat crop, only one rauni is given before sowing. Often, this rauni for wheat is applied when the cotton crop is still at the field. Two pre-sowing irrigations are applied for the cotton crop, i.e. the pakki rauni (first pre-sowing irrigation) and the kachi rauni (second pre-sowing irrigation).

(field 2). Section 5.3 deals with the effects of different irrigation frequencies for Field 1. The effects of different irrigation water qualities are discussed in section 5.4 (Field 3), while in section 5.5 the effects of a different initial salinity level are discussed for Field 4. Finally, in section 5.6, the results of the different irrigation management scenarios are compared for the four soil types.

5.2 Quantity of irrigation applications

5.2.1 Irrigation scenarios for different quantities

Three simulations were done to study the short term effects of different quantities of irrigation water on the water and salt balance of the system. The quantities of the irrigation applications were set at four-third (133%) and two-third (67%) of the reference quantity (100%), to simulate a situation with over- and underirrigation (see Table 5.3).

Table 5.3 *Irrigation scenarios at different quantities.*

crop	irrigation pattern	reference	overirrigation	underirrigation
wheat	rauni others (5) total	15.0 cm 7.5 cm 52.5 cm	20.0 cm 10.0 cm 70.0 cm	10.0 cm 5.0 cm 35.0 cm
cotton	1st rauni 2nd rauni others (8) total	7.5 cm 10.0 cm 7.8 cm 80.0 cm	10.0 cm 13.3 cm 10.4 cm 106.7 cm	5.0 cm 6.7 cm 5.2 cm 53.3 cm

All other variables (e.g. the frequency, the water quality etc), were kept the same as for the reference simulation. The abovementioned scenarios are simulated for all of the four soil types (see section 5.6). In the next section, the sensitivity of the quantity of irrigation water is discussed on the basis of the simulations for the soil type of Field 2 (sandy loam).

5.2.2 Results and discussion

To understand the effects of different quantities of irrigation water on the water and salt balance, six VZRN's (see section 4.1) are used. They are determined for the two growing seasons, which are defined from the day before the first rauni irrigation to the harvest of the crop (see Table 5.4).

Table 5.4 *VZRN's for wheat and cotton at different irrigation water quantities (Field 2).*

crop	quantity	RT	RE	LF_{wh}	SMC	LF_{sb}	SSC
wheat	reference	0.93	0.56	0.39	0.16	1.10	-0.04
	overirrigation	0.94	0.56	0.53	0.18	1.19	-0.10
	underirrigation	0.85	0.56	0.24	-0.02	1.26	-0.07
cotton	reference	0.90	0.43	0.24	0.52	1.19	-0.13
	overirrigation	0.95	0.43	0.39	0.51	1.27	-0.28
	underirrigation	0.74	0.43	0.09	0.54	0.49	0.24

Crop indicators

For both crops, the relative evaporation is not influenced by a different irrigation quantity. The relative evaporation for the cotton crop is less than for the wheat crop, because cotton does not cover the soil as much as the wheat crop (especially not in the beginning of the growing season). Therefore, the potential evaporation will be higher for cotton than for wheat and the relative evaporation will be less. In Figure 5.1, the cumulative RE and RT are illustrated for the cotton crop (see Annex I.1 for the wheat crop). For both crops, the relative evaporation is increased after the rauni irrigation(s). After the rauni irrigation(s), the soil will dry out till the first irrigation after sowing, resulting in a decreasing relative evaporation. For both crops, the relative transpiration is increased for larger irrigation quantities and decreased for smaller quantities (see Table 5.4). For the cotton crop, the relative transpiration decreases during the initial stage, since the soil cover is increasing and the moisture content in the profile is decreasing. After the first irrigation, the relative transpiration increases and, in case of the reference situation, stays at about the same level during the rest of the growing season. In case of overirrigation, the cotton crop obtains a slightly higher relative transpiration. For the underirrigated situation, the relative transpiration decreases during the mid-season stage, since the potential transpiration is the highest during that period. Afterwards, in the late season stage and at harvest, the relative transpiration stays at the same level because the potential transpiration is low and a smaller quantity of water is needed to fulfill the crop water requirements.

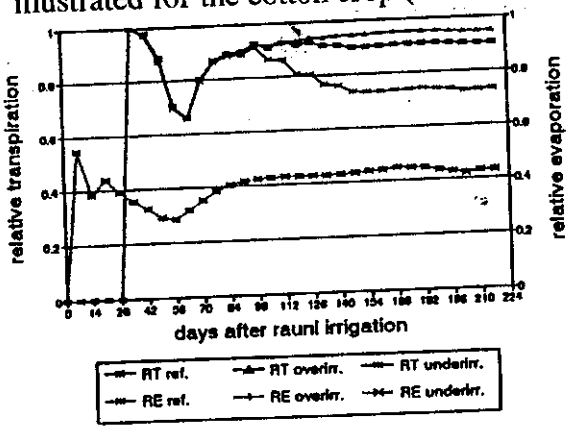

Figure 5.1 *Cumulative RT and RE for cotton at different irrigation quantities.*

Water balance indicators

In Table 5.4, it can be seen that for both crops the leaching fraction increases for the over irrigation scenario and decreases in case of underirrigation. The cumulative leaching fraction for cotton is illustrated in Figure 5.2 (see Annex I.1 for wheat). After the first rauni irrigation, the leaching fraction slightly increases, as the soil is very dry and almost all of the irrigation water will be stored in the profile. After the second rauni, the leaching fraction

increases more rapidly with larger irrigation quantities. At smaller irrigation quantities, the leaching fraction is lower, since relativily more water is taken up by the roots, thus less water will percolate.

Moisture storage indicator

In Table 5.4, it can be seen that the moisture storage slightly increases during the wheat season, except in the case of underirrigation. However, the moisture storage change for the cotton season gives an unrealistic view, since the rauni for wheat is included in the growing season and this rauni is applied when the cotton is still standing on the field.

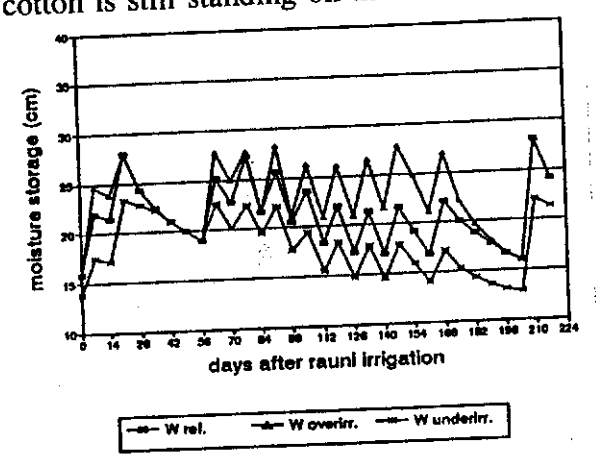

Figure 5.3 *Moisture storage cotton at different irrigation quantities.*

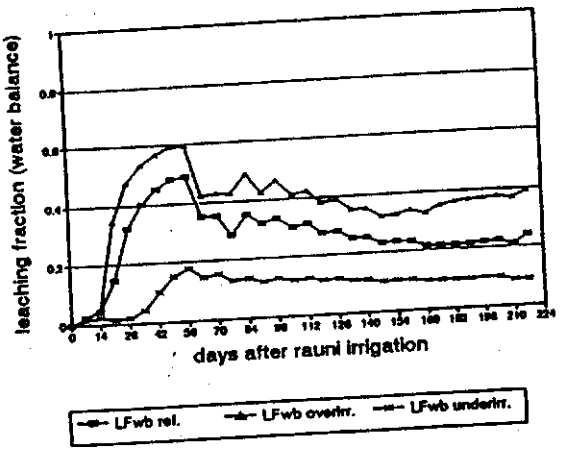

Figure 5.2 *Cumulative LF_{wb} for cotton at different irrigation quantities.*

In Figure 5.3, the moisture storage during the cotton season is illustrated (see Annex I.1 for wheat). The moisture storage is reflecting the irrigation pattern very well. The rauni irrigations increase the moisture storage, so the seeds will have sufficient water for germination. After sowing, the moisture storage decreases due to bare soil evaporation. For the rest of the season, the moisture storage increases directly after an irrigation event; for some time after the application, the moisture storage decreases, because of uptake and percolation. The larger the irrigation depths, the higher the moisture storage and the larger the fluctuations.

Soil salinity indicators

To obtain a better understanding of the soil salinity indicators, the total salt storage for the wheat season is illustrated in Figure 5.4.The salt storage change over the total wheat season is negative for all three simulations. The rauni irrigations leach a lot of salts from the soil, as the rauni irrigations consist of canal water. The higher rauni irrigations result in more salts being leached, as well as being leached more rapidly. During the wheat season, the salt storage stays at the highest level (approximately 140 dS/m * cm) for the underirrigation scenario. This is caused by the insufficient leaching of salts by the rauni irrigation. In comparing the reference and overirrigation scenario, a lot of salts are leached, but at the same time a lot of salts are added

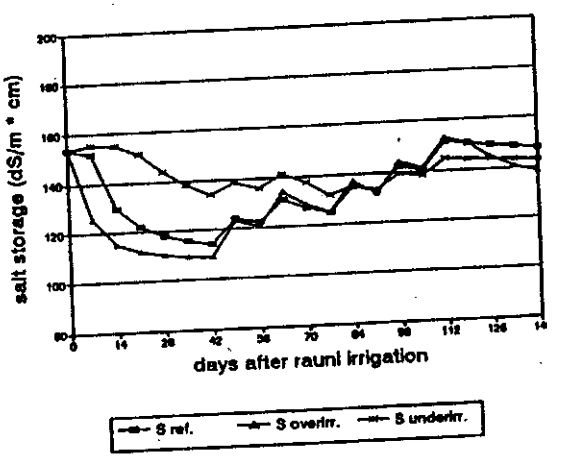

Figure 5.4 *Salt storage for wheat at different irrigation quantities.*

to the soil. Eventually, this leads to the highest salt storage at harvest for the reference scenario. The salt storage at harvest for the overirrigation simulation is the lowest, since a lot of salts are leached by the irrigation apllication at the end of the growing season. The LF_{sb} of the different scenarios are determined by the amount of salts which are added to the soil profile, and the amount of salts which is leached from the profile. The LF_{sb} is the highest for the underirrigation simulation, as the ratio of the amounts of salts in the percolation flux and the amounts of salts in the irrigation water are the highest (see Annex I.1). It can be concluded that not only the salt storage change over the total growing season is important, but also the salt storage during the growing season, especially at the salinity sensitive stages of the growing season.

In Figure 5.5, the salt storage during the cotton season is illustrated. The rauni irrigations of the reference and over irrigation scenarios are sufficient to leach the salts, so that the salt storage is below 150 dS/m*cm during the initial and development stage of the crop. In case of underirrigation, there is hardly any leaching of salts by the rauni irrigations, but the build up of salts during the growing season is less, as less salts are added to the soil. Finally, the amount of salts at the end of the mid-season stage is approximately the same for all scenarios. During the last irrigation and the rauni for wheat, a lot of salts are leached for the overirrigation scenario. This explains the highest LF_{sb} and the most negative salt storage change over the season (see Table 5.4). For the reference scenario, the LF_{sb} is slightly lower and the salt storage change is less negative. In case of the underirrigation scenario, the irrigation applications are not sufficient to leach the salts at the end of the cotton season. This results in a positive salt storage change and a LF_{sb} smaller than 0.5.

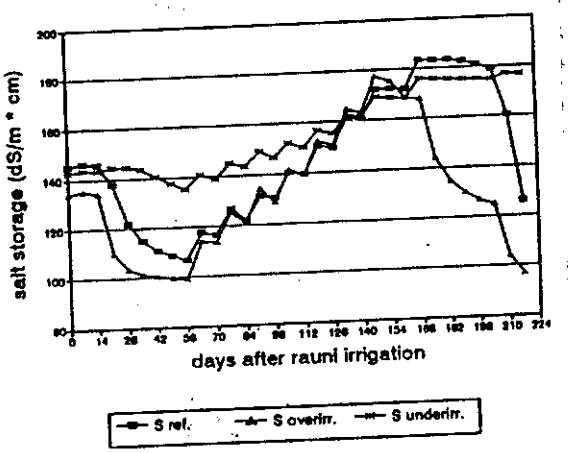

Figure 5.5 *Salt storage for cotton at different irrigation quantities.*

5.3 Frequency of irrigation applications

5.3.1 Irrigation scenarios for different irrigation intervals

Besides the reference simulation, two scenarios were simulated to study the effect of different frequencies of irrigation applications on the water and salt balance of the system. For the wheat crop the number of irrigation events was set at three and seven, representing an irrigation regime with a low and high application frequency, respectively. For the cotton crop, the number of events was fixed at six and eleven during one growing season (see Table 5.5). The date and the quantity of the rauni irrigations was not changed. The date of the first irrigation after sowing was not changed either, only the interval between the irrigation applications was changed, consequently changing the irrigation depth, since the total quantity of irrigation water was kept constant. All other variables (e.g. the quality of the irrigation water) were kept the same as for the reference scenario.

Table 5.5 *Irrigation scenarios at different irrigation intervals.*

crop	irrigation pattern	reference	low frequency	high frequency
wheat	number of applications depth interval	5 applications 7.5 cm 17 days	3 applications 12.5 cm 30 days	7 applications 5.4 cm 13 days
cotton	number of applications depths interval	8 applications 7.8 cm 15 days	6 applications 10.4 cm 20 days	11 applications 5.7 cm 10 days

The abovementioned scenarios were simulated for all of the four soil types. In section 5.6, the results of the analysis for the different management variables will be correlated with the different soil types. In the next section, the sensitivity of the irrigation interval is discussed on the basis of the simulations for the soil type of Field 1 (loamy sand).

5.3.2 Results and discussion

In Table 5.6, the cumulative VZRN's over the two growing seasons are given for the simulations with different irrigation intervals (additional graphs are given in Annex G.2).

Table 5.6 *VZRN's for wheat and cotton at different irrigation frequencies (Field 1).*

crop	frequency	RT	RE	LF_{wb}	MSC	LF_{sb}	SSC
wheat	refrence	0.84	0.54	0.46	0.08	1.17	-0.07
	low	0.65	0.49	0.58	0.02	1.39	-0.15
	high	0.95	0.60	0.37	0.17	0.99	0.00
cotton	reference	0.84	0.42	0.30	0.45	1.30	-0.22
	low	0.75	0.41	0.35	0.52	1.19	-0.15
	high	0.91	0.43	0.26	0.36	1.40	-0.27

Crop indicators

From Table 5.6, it can be concluded that an increased irrigation interval decreases the relative transpiration of cotton and wheat, and decreasing the interval will increase the relative transpiration considerably. Field 1 is a sandy, very permeable soil and has a low water holding capacity. In case of the low frequency scenario, the large irrigation events will saturate the soil and will move fast through the profile. In this way, the roots can extract water during a short period of time only. Once the wetting front has passed, the suction in the soil will increase and root water uptake will be limited. Therefore, in sandy soils, a shorter irrigation interval with smaller application depths results in a more efficient root water uptake and a higher relative transpiration. In Figure 5.6, the cumulative relative transpiration and evaporation is illustrated for wheat (see Annex I.2 for cotton).

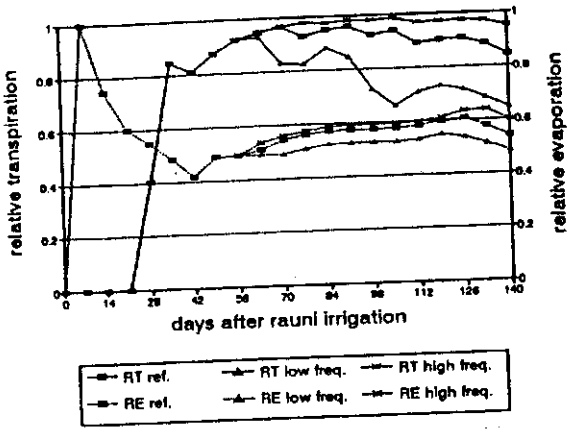

Figure 5.6 *RT and RE for wheat at different irrigation frequencies.*

At shorter irrigation intervals, the relative soil evaporation will increase, since the upper soil layer stays relatively wet for a longer period of time. This effect is less pronounced than the change in the relative transpiration, because the soil evaporation is only determined by the conditions in the upper soil layer and not the whole rooting zone.

Water balance indicators

At a lower irrigation frequency, less water can be taken up by the roots and in between two irrigation applications more water will percolate to the groundwater (see Figure 5.7 and Annex I.2). The leaching fraction will be higher at larger irrigtion intervals, as can be seen in Table 5.6. At shorter intervals, the root water uptake is more efficient and the leaching fraction will decrease. This holds as well for both the wheat and cotton crops, although the effects are more pronounced for the wheat season, as the interval for the different scenarios is varied over a wider range (see Table 5.5).

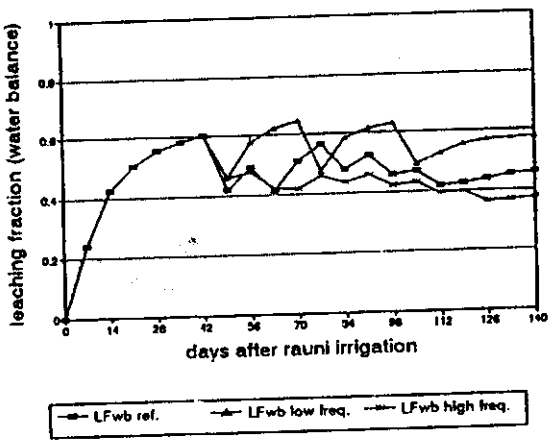

Figure 5.7 *LF_{wb} for wheat at different irrigation frequencies.*

Moisture indicators

In Annex I.2, the moisture storage of the soil profile is shown for different irrigation intervals. It can be observed that after an irrigation event the moisture storage increases the most for the low frequency situation, since the quantity of each application is larger. Between two applications, the moisture storage declines the most for the low frequency simulation, since it takes longer before the drying process is interrupted by the following irrigation application. For the wheat season, the total moisture storage change is the highest for the high frequency simulation. The moisture content is the highest at the end of the growing season, as the last irrigation is given very late in the season. For the cotton crop, the moisture storage change is the highest for the low frequency simulation as the moisture storage at the end of the growing season is the same for all scenarios (due to the rauni application for wheat), and the initial moisture storage is the lowest for the low frequency simulation (see Table 5.6 and Annex I.2).

Salinity indicators

For the wheat season, the leaching fraction of the salt balance shows the same trend as the water balance. The longer the irrigation interval the more water percolates, and consequently

the more salts are leached below the root zone, resulting in a higher leaching fraction of salts and a lower salt storage at the end of the growing season (see Annex I.2). For the high frequency simulation, the percolation of salts is so little that the salt storage change is positive.

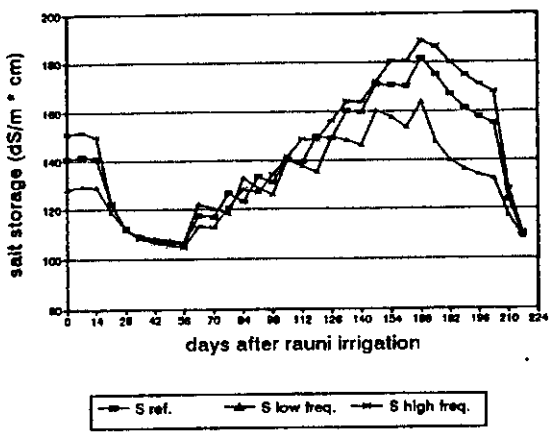

Figure 5.8 *Salt storage for cotton at different irrigation frequencies.*

For the cotton season, the effects of different intervals are less pronounced, because the changes in the intervals are relatively smaller. Still, more salts are leached during the growing season, at longer irrigation intervals (not including rauni irrigations at the end of the season). During the mid- and late-season stage of the growing season, the salt storage is significantly lower for the low frequency scenario as compared with the high frequency scenario (about 10 %). The rauni irrigation neutralizes these differences at the end of the growing season. The salt storage change for cotton shows a different trend for the three simulations as compared with wheat (see Table 5.6), which is caused by the different salt storage that is present at the beginning of the cotton season. Therefore, it is better to look to the absolute values of the salt storage (Figure 5.8).

5.4 Qualitiy of irrigation water

5.4.1 Irrigation scenarios for different qualities.

To study the effect of different qualities of irrigation water on soil salinity and crop transpiration, four scenarios are simulated (see Table 5.7).

Table 5.7 *Irrigation scenarios at different irrigation water qualities (dS/m).*

crop	reference	high quality (canal)	low quality (tubewell)	low rauni quality
wheat	rauni : 0.2 others : 1.5	all : 0.2	all : 3.0	rauni : 1.5 others : 1.5
cotton	rauni : 0.2 others : 1.5	all : 0.2	all : 3.0	rauni : 1.5 others : 1.5

An irrigation application with EC of 0.2, 3.0 and 1.5 dS/m represents an application of respectively canal water, low quality tubewell water and average quality tubewell water. All other factors (e.g. quantity, frequency etc.) were kept constant. The abovementioned scenarios were simulated for all of the four soil types. In the next section, the sensitivity of the quality of the irrigation water is discussed on the basis of the simulations for the soil type of Field 3 (loamy soil). Separate attention will be paid to the results of the scenario with a low quality for the rauni irrigations.

5.4.2 Results and discussion

In Table 5.8, the VZRN's for the two growing seasons are given for the scenarios with irrigation water qualities (additional graphs are given in Annex I.3). First, the reference, canal and tubewell water scenarios are compared with each other, and secondly, the effect of a different quality of the rauni irrigation will be evaluated.

Table 5.8 *VZRN's for wheat and cotton at different qualities of irrigation water (Field 3).*

crop	quality	RT	RE	LF_{wb}	SMC	LF_{sb}	SSC
wheat	reference	0.99	0.61	0.32	0.27	1.32	-0.13
	high quality (canal)	0.99	0.61	0.32	0.26	7.26	-0.43
	low quality (tubewell)	0.98	0.61	0.32	0.28	0.70	0.31
	low quality rauni	0.99	0.61	0.32	0.27	1.17	-0.09
cotton	reference	0.97	0.46	0.17	0.60	0.74	0.20
	high quality (canal)	0.99	0.46	0.16	0.59	1.20	-0.05
	low quality (tubewell)	0.93	0.46	0.19	0.59	0.75	0.36
	low quality rauni	0.97	0.46	0.17	0.60	0.67	0.35

Crop indicators

For the wheat crop, a different quality of irrigation water does not influence the relative transpiration. When irrigating with low quality tubewell water, the concentration of salts in the soil water is not high enough to cause a reduction in transpiration due to increased osmotic pressure. In the next cotton season, the transpiration is reduced because the salt concentrations of the soil water are too high (see Figure 5.9 and Annex I.3). The reduction takes places after the rauni irrigations with tubewell water (during the initial and development stage), since the soil becomes very dry and the salt concentration is considerably increased due to this concentrating effect of the saline soil solution.

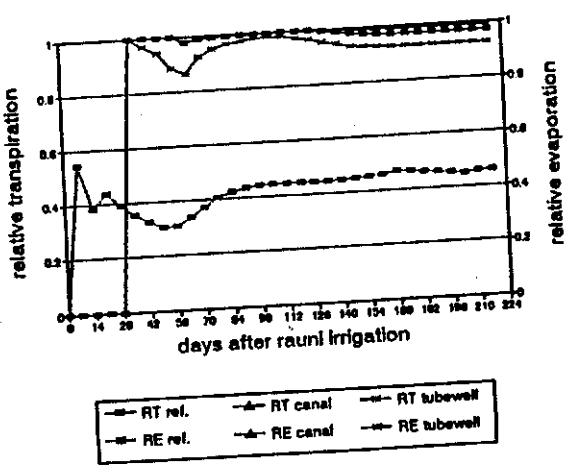

Figure 5.9 *RT and RE for cotton at different irrigation water qualities.*

The evaporation is not effected by the different qualities of irrigation water, since the soil evaporation is determined by the moisture conditions of the soil, which is not influenced by the amount of salts in the soil moisture.

Water balance indicators

For the wheat season, the leaching fraction does not change at different qualities of irrigation water. The water balance is not influenced by the salt balance, since the salt concentrations are too low to influence the root water uptake and thereby the other components of the water balance. In the next cotton season, the salinity level is more and more increased in case of irrigation with saline water and the transpiration is reduced. This results in an increased flux to the groundwater and the leaching fraction increases for the simulation with tubewell water. Vice versa, the leaching fraction is slightly decreased when canal water is used for irrigation (see Annex I.3).

Moisture indicators

Corresponding with the results of the water balance indicator, the moisture indicator for the wheat season hardly changes for the different irrigation quality scenarios. During the cotton season, the moisture content shows differences for the different scenarios. This can be explained by the fact that the osmotic pressure head on the total pressure head becomes significant and influences the moisture storage (see Figure 5.10). The total pressure head consists of the matrix pressure head and the osmotic pressure head. The more saline the soil water, the lower the osmotic potential. This results in a higher matrix potential, which consequently causes a somewhat higher moisture storage for saline soils. The salts will 'hold' the water by their osmotic behaviour.

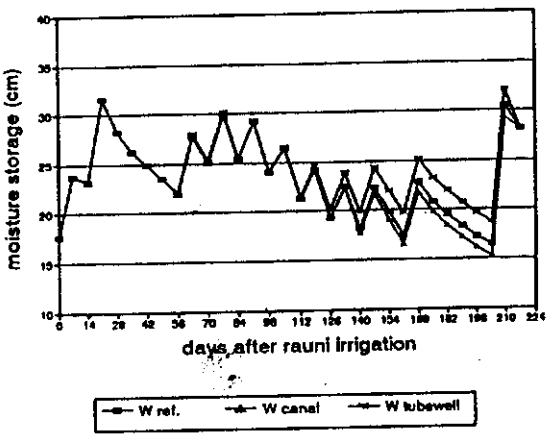

Figure 5.10 *Moisture storage for cotton at different irrigation qualities.*

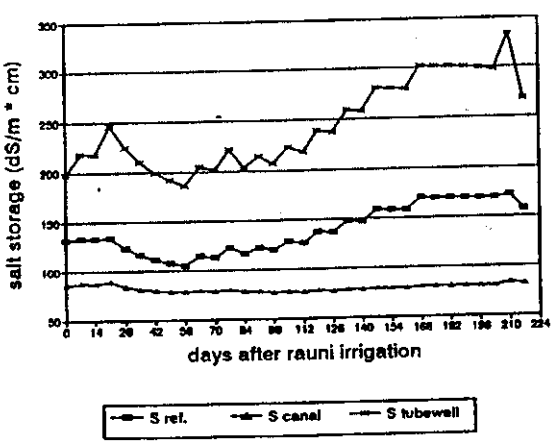

Figure 5.11 *Salt storage for cotton at different irrigation qualities.*

Salinity indicators

In Table 5.8, very large differences in the salinity indicators can be oberved for the wheat season. The amount of salts leached by irrigation with canal water is very high and consequently the salt storage change is the most negative and the LF_{sb} is very high (see Annex I.3). For the reference simulation, there is still a net decrease in the salt content and the LF_{sb} is much lower. For the tubewell irrigation scenario, the opposite trend can be observed; the salt storage change is positive and the leaching fraction of the salt balance is smaller than one.

For the cotton season, there is only a net leaching of salts for the scenario with canal water irrigation. However, the leaching fraction of salts over the cotton season is much lower as compared with the leaching fraction of salts over the wheat season. This is caused by the amount of immobile salts which are defined for the initial conditions (day 0 = one day

before the rauni application for wheat). Already, after one growing season, almost all the immobile salts are leached from of the profile for the case of canal water irrigation. In Table 5.9, the salt storage, divided over the mobile and immobile fraction, at the beginning and at the end of each growing season is given. It can be seen that for the reference and tubewell water scenario, the salt storage change is positive and salts accumulate in the mobile part of the soil, while the immobile salt storage remains approximately the same. The reason that the amount of salts in the immobile fraction hardly changes is because of a low K_{mobile}[16], and consequently, a lot of salts are leached from of the profile (see Figure 5.10).

Table 5.9 *Salt storage at different irrigation water qualities (dS/m*cm).*

crop	quality	S_{total}		S_{mobile}		$S_{immobile}$	
		begin	end	begin	end	begin	end
wheat	reference	153	134	70	60	83	74
	canal	153	87	70	15	83	72
	tubewell	153	201	70	124	83	77
cotton	reference	132	158	59	93	73	65
	canal	86	82	15	24	71	58
	tubewell	197	268	120	191	77	77

Quality of rauni irrigation

As can be seen in Table 5.8, the short term effects of a rauni application with low quality water are limited to the salinity indicators, as the overal salinity level is not high enough to influence the crop transpiration and thereby the water balance. For the simulation with rauni irrigations of low quality, the leaching of salts after the rauni irrigation is strongly reduced, although the total leaching fraction over the cotton season is only slightly lower (see Figure 5.12). While a canal water rauni leaches the salts before sowing and germination, a low quality rauni causes a build up of salts during the most salt sensitive stage of crop growth.

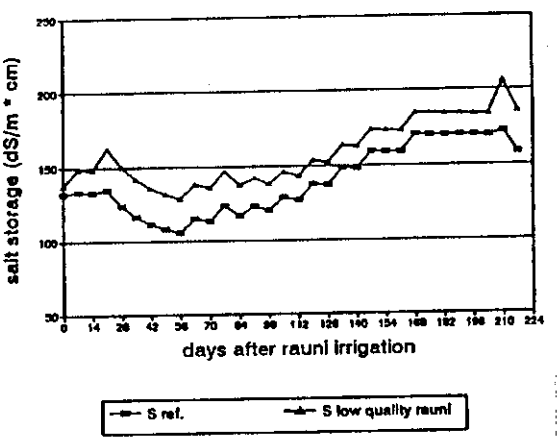

Figure 5.12 *Salt storage for cotton at different rauni qualities.*

16 During the calibration process, K_{mobile} was fixed at zero. This means there is no change between mobile and immobile part. For the simulations in Chapter 5 and 6, K_{mobile} is set at 0.00004, so the immobile salt storage *can* change over time. This means salinization or desalinization is also possible in the immobile fraction.

5.5 Initial salinity level

The reference irrigation scenario was simulated for all of the fields, while changing the initial salt storage in the profile. The electrical conductivity of the soil profile was increased from aproximately 2 dS/m to 5 dS/m, which corresponds with an amount of salts of 375 dS/m * cm. The results of the simulation with a high initial salt storage are discussed for the soil type of Field 4 (silty loam). The purpose of simulations with different initial salinity levels is to study the desalinization process for reclaiming soils.

Table 5.10 *VZRN's for wheat and cotton at different initial salinity levels (Field 4).*

crop	salinity level	RT	RE	LF_{wb}	SMC	LF_{sb}	SSC
wheat	reference	1.00	0.62	0.33	0.16	1.03	-0.01
	high salinity	1.00	0.62	0.33	0.16	2.51	-0.24
cotton	reference	0.99	0.46	0.15	0.44	0.59	0.27
	high salinity	0.99	0.46	0.15	0.44	0.78	0.0

A higher initial salinity level only influences the salinity indicators, and not the crop and water balance indicators. Even though the initial salinity level is very high, it does not affect the transpiration and, consequently, the water transport. This is caused by the fact that when defining the initial salinity level, a large part of those salts is stored in the immobile fraction. The immobile fraction does not take part in the water transport and no water can be taken up by the roots in the immobile fraction. Pressure heads are based on the osmotic potential in the mobile fraction and, therefore, a high salinity in the immobile fraction does not increase the osmotic potential and root water uptake is not effected by the salts in the immobile part. In Table 5.11, the salt storage at the beginning and end of the growing seasons, divided over the mobile and immobile fraction, is given.

Table 5.11 *Salt storage at different initial salinity levels (dS/m*cm).*

crop	initial salinity	S_{total}		S_{mobile}		$S_{immobile}$	
		begin	end	begin	end	begin	end
wheat	reference	153	151	57	60	96	91
	high salinity	382	292	144	69	239	223
cotton	reference	150	191	59	103	91	88
	high salinity	290	315	69	112	222	203

For the simulation with a high initial salinity, more than half of the mobile salts are leached during the wheat season, while the immobile salt storage slightly decreases. This results in a high leaching fraction of salts and a negative salt storage change. During the cotton season, salinization takes place and the salts in the mobile fraction are almost doubled. The leaching fraction of salts is smaller than one and the percolation of salts is higher in case of a high initial salinity level. Thus, relatively more salts are stored in the soil profile for the reference

simulation as compared to the simulation with high salinity, resulting in a higher salt storage change (see Table 5.10 and Annex I.4).

5.6 Relations between the different soil types and the management variables.

The effects of changing management variables on crop transpiration and soil salinity is compared for the four different soil types. The, analysis is done for two variables: the crop transpiration and the salt storage of the profile.

5.6.1 Crop transpiration

In Table 5.12, the potential transpiration and the actual transpiration for the reference situation are given. In addition, the relative deviation of the reference transpiration is given for the different scenarios in order to study the impact of the different scenarios upon the different soil types.

Table 5.12 *Impact of management scenarios on crop transpiration for four soil types.*

crop	field	T_{pot} (mm)	T_{act}/T_{pot}	$(T_{act,scenario} - T_{act,ref})/T_{act,ref}$ (%)							
			reference	2	3	4	5	6	7	8	9
wheat	1	272	0.84	2	-8	-23	13	2	-4	-1	-1
	2	272	0.93	1	-8	-20	6	2	-3	0	0
	3	272	0.99	0	-2	-5	1	0	-1	0	0
	4	272	1.00	0	-1	-2	0	0	0	0	0
cotton	1	637	0.84	4	-16	-14	9	4	-5	0	-1
	2	637	0.90	5	-19	-7	9	4	-5	0	0
	3	637	0.97	3	-18	-1	2	2	-5	-1	0
	4	637	0.99	1	-16	0	1	1	-4	-1	0

1 reference
2 overirrigation
3 underirrigation
4 low frequency
5 high frequency
6 canal water
7 tubewell water
8 low quality rauni
9 high initial salinity

From Table 5.12, it can be concluded that the effect of different management variables on the crop transpiration is different for the four soil types.

For the reference situation, the differences in relative transpiration can be explained by the differences in the soil hydraulic behaviour and by the division in the mobile and immobile parts. Fields 1 and 2 have the largest immobile fraction (F_{mobile}=0.55), which causes a decrease in transpiration, since water uptake can only take place in the mobile part. Besides, Fields 1 and 2 are the most sandy and, therefore, their permeability is higher and their retention lower than for Field 3 and Field 4. This explains the higher relative transpiration of Fields 3 and 4.

In relation to the reference transpiration of each soil type, it can be said that Scenarios 8 and 9 hardly influence the transpiration for any of the soil types.

The most pronounced differences between the soil types occurs for Scenarios 4 and 5. In these scenarios, the irrigation interval is increased and decreased, respectively . With increasing irrigation interval, the decrease in transpiration compared with the reference transpiration is the highest for the sandy soils. The opposite holds for decreasing the irrigation interval. The effect is more pronounced for the wheat season than for the cotton season, because the relative increase and decrease of the irrigation interval is higher than in the cotton season.

In case of over- and underirrigation, the effects on crop transpiration are more pronounced for the sandier soils. During the wheat season, an increase in irrigation quantity causes only an increase in transpiration for Fields 1 and 2, since the transpiration of Fields 3 and 4 is already at maximum level. Thus, the same quantity of water is more efficiently transpired by a crop grown on a loamy soil than a crop on a more sandy soil. In case of underirrigation, the decrease in transpiration for the wheat crop is higher for the sandier soils, which again implies that on a loamy soil the plant can transpire more effieciently, because of a lower permeability and a higher retention of the loamy soil compared with the more sandy soil. During the cotton season, this effect is less pronounced because irrigation intervals are relatively shorter.

When changing the quality of the irrigation water to canal or tubewell water, there will be an increase and decrease, respectively of the crop transpiration. The increase in transpiration only occurs when the crop is not transpiring at maximum level in the reference situation. This is the case for Fields 1 and 2 during the wheat season and for all fields during the cotton season. When irrigating with tubewell water, the transpiration is more decreased for the sandier soils, since the transpiration in the reference situation was already not at a maximum. Therefore, the extra fall in pressure heads, because of a higher salt concentration, has a more pronounced effect on the relative transpiration of the sandier fields. Another factor that influences the change in transpiration due to changing salt concentrations is the amount of salts which are stored in the immobile part of the soil, as these immobile salts do not influence the root water uptake.

5.6.2 Soil salinity

To understand the short term effects of different management scenarios on the salinity of the different soil types, the development of the total salt storage over the two growing seasons is followed. This is illustrated in the graphs of Annex I.5. The salt storage change over one

agricultural year is given in Table 5.13. The effects on the salt storage by the rauni irrigation for the wheat crop of the next cycle are ignored. Therefore, the salt storage change is calculated over exactly one year, instead of over two growing seasons, which covers more than one year by two weeks.

Table 5.13 *Salt storage change over one agricultural year for different scenarios.*

	reference	2	3	4	5	6	7	8	9
field 1	0.01	-0.22	0.10	-0.14	0.10	-0.35	0.31	0.03	-0.26
field 2	0.17	-0.18	0.14	0.00	0.16	-0.34	0.61	0.20	-0.20
field 3	0.10	-0.18	0.24	-0.01	0.14	-0.47	0.95	0.20	-0.30
field 4	0.27	0.04	0.41	0.29	0.30	-0.33	1.20	0.39	-0.16

The differences in salt storage change (SSC) between the four fields are caused by different soil hydraulic parameters, which determine the water flow and, consequently, the transport of salts. Besides, the preferential flow parameters determine the amount of salts stored in the immobile fraction and thereby the salt storage change (initial immobile salt storage is 110 dS/m*cm for Field 1, 105 dS/m*cm for Field 2, 84 dS/m*cm for Field 3 and 96 dS/m*cm for Field 4).

For the overirrigation scenario, the SSC over one agricultural year is the most negative for Field 1, since this field is the most sandy and the LF_{sb} is the highest. For Field 4, even the overirrigation scenario yields a positive salt storage change, as this soil has the lowest conductivity and, therefore, the lowest LF_{sb}. The immobile fraction is the lowest, so more salts can be stored in the mobile fraction. For the underirrigation scenario, the SSC is positive for all of the soil types. The build up of salts in the soil is the smallest for Field 1, the most permeable soil, with the largest immobile fraction, and is the largest for Field 4, the least permeable soil, with the smallest immobile fraction. This is illustrated in Figure 5.13, which shows the salt storage for the wheat season for the underirrigation scenario (see Annex I.5 for salt storage during the cotton season).

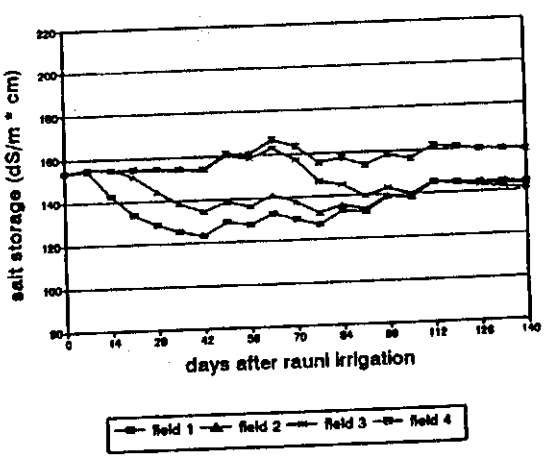

Figure 5.13 *Salt storage underirrigation scenario for four soil types (wheat).*

For Scenarios 4 and 5, the irrigation interval is changed. Varying the irrigation interval has a large impact on the SSC for the sandy soil of Field 1, since the transpiration is increased for shorter intervals. Thus, for shorter intervals (Scenario 4), less water is leached and the salt storage change is positive, while the SSC is negative for larger intervals (scenario 5). For field 4, changing the irrigation frequency hardly influences the SSC, as the water balance is not changed. Since the soil of Field 4 has a high retention and low conductivity, the transpiration reaches the potential for all the three scenarios with different irrigation intervals (see Annex I.5).

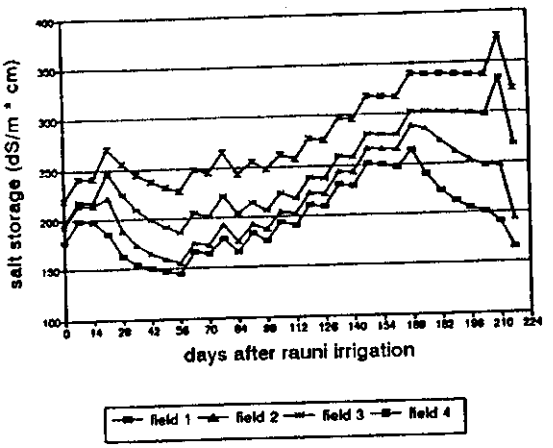

Figure 5.14 *Salt storage scenario with tubewell water for four soil types (cotton).*

For Scenario 6 (canal water irrigation), the SSC is almost the same for the four fields, as almost all the salts are leached from the mobile fraction and partly out of the immobile fraction. Since the amount of salts in the immobile fraction is the lowest for Field 3, the SSC is the most negative for Field 3. For the scenario with tubewell irrigation, the SSC is of course positive for all of the four fields. As said before, the build up of salts is the highest for Field 4, since the soil is the least conductive and the leaching fraction is the smallest (see Figure 5.14).

Scenario 8 shows approximately the same difference between the soil types as the reference simulation. If the rauni irrigation does not consist of canal water anymore, the SSC will be higher for all of the four fields. This extra build up of salts occurs because of a low quality rauni, which will be more pronounced for the more heavier soils (Fields 3 and 4) than for the sandy soils (Fields 1 and 2), which can be seen in Table 5.13 (see Annex I.5).

For Scenario 9, the differences in salt storage change for wheat between the four fields are illustrated in Figure 5.15 (see Annex I.5 for cotton). For Field 4, the salt storage is the least negative, while Field 1 has a much more negative SSC. Field 3 shows the most negative SSC, which can be explained by the fact that the amount of salts in the immobile fraction is much lower than for the other fields. This can also be seen in the SSC of Field 3 for the reference simulation. Based on conducitivity only, it is to be expected that Field 3 will have salt storage changes that are between Field 2 and Field 4. The deviation can be explained by the lower immobile salt content of Field 3.

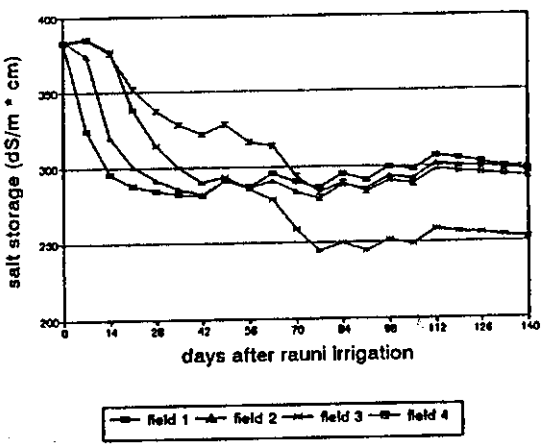

Figure 5.15 *Salt storage scenario with high initial salinity for four fields (wheat).*

CHAPTER 6 LONG TERM SCENARIOS

6.1 Introduction

In the previous chapter, a thorough analysis of the effects of the management variables on salinity and crop tranpiration was carried out for the short term, i.e. one agricultural year (two growing seasons). In this chapter, the effects of different irrigation management scenarios on salinity and crop transpiration are evaluated for the long term. The time span for these long term scenarios is set at ten years. By simulating a certain irrigation management scenario for ten successive years, trends in soil salinity and crop transpiration can be predicted.

Three scenarios are simulated for the four different soil types of the four sample fields (see section 6.2). A more comprehensive long term analysis is done for one of the four soil types, namely the loamy soil of Field 3 (see section 6.3).

6.2 Scenario analysis for four fields

6.2.1 Description of scenarios

The scenarios that are used for the long term simulations are mainly based on the simulations done in Chapter 5.

Scenario A
This scenario is called the reference scenario and corresponds with the reference irrigation management of Table 5.2 (section 5.1).

Scenario B
With respect to Scenario A, only the quantity of the irrigation applications is changed in Scenario B. An underirrigation scenario is the most interesting case in terms of varying the quantity of irrigation applications, as it has an increasing impact on soil salinity and a decreasing impact on crop transpiration. Therefore, the irrigation depths of Scenario B are reduced by one-third, corresponding with the underirrigation scenario of section 5.2.1 (Table 5.3).

Scenario C
In Scenario C, only the quality of the irrigation water is changed with regard to the reference scenario (A). Instead of an electrical conductivity of 0.2 dS/m for the rauni applications and 1.5 dS/m for the other irrigation applications, the electrical conductivity of all irrigation applications is set at 2.0 dS/m.

For these three long term scenarios, all other parameters were set at the same values as for the short term analysis in Chapter 5. The initial moisture conditions are calculated by simulating one year prior with the reference irrigation management (see section 5.1). The initial salt content of the profile is set at an EC_e of approximately 2.0 dS/m throughout the profile, which correspond with a total amount of salts of about 150 dS/m * cm (see section 5.1).

Scenarios A, B and C were performed for the soil types of the four sample fields in order to compare the long term effects of different irrigation management practices for different soils.

6.2.2 Results and discussion

The water balance components for the different scenarios do not change over the successive years, since there is no (positive or negative) soil moisture storage over one agricultural year. The soil moisture storage is zero over one agricultural year in case of a stationary situation. This means that the irrigation management is constant in time and in equilibrium with the environment[16]. The water balance components for the different scenarios are listed in Table 6.1.

Table 6.1 *Water balance components for Scenarios A, B and C.*

field	Scenario A			Scenario B			Scenario C		
	T_a/T_p	E_a/E_p	LF_{wb}	T_a/T_p	E_a/E_p	LF_{wb}	T_a/T_p	E_a/E_p	LF_{wb}
1	0.84	0.39	0.35	0.73	0.39	0.17	0.83	0.40	0.36
2	0.91	0.40	0.30	0.77	0.40	0.13	0.89	0.41	0.31
3	0.98	0.43	0.25	0.84	0.42	0.06	0.96	0.43	0.26
4	0.99	0.45	0.23	0.85	0.43	0.04	0.98	0.45	0.24

Scenario A

In the reference situation (Scenario A), the transpiration is the lowest for the most sandy soil and, therefore, the leaching fraction is the highest. In the heaviest soils (fields 3 and 4), transpiration is almost at potential and the leaching fraction is the lowest[17]. The difference in the water balances of the four soils influences the salt balance on the long term to a large extent. In Figure 6.1, the total amount of salts (S_{total}) and the leaching fraction of salts (LF_{sb})

---

16 The initial moisture conditions of the long term simulations are determined by simulating the same irrigation management one year prior. Hereby, a constant irrigation management is simulated (stationary situation).

17 Since the water balance components do not change over the successive years, the conclusions related to the water balance of Chapter 5 are not only valid for the short term, but also for the long term. Therefore, more attention will be paid to the consequences of different scenarios on the salt balances of the soils for the long term.

over the ten successive years is illustrated. Over the first year the leaching fraction of salts is smaller than one, which results in a build up of salts during the first year; more salts are added to the profile than leached. During second year, however, the leaching of salts is higher than the amount of salts added by irrigation, since part of the salts added during the first year is leached during the second year. In the process of time, the leaching fraction of salts will be one, and the amount of salts in the profile stays at the same level untill the irrigation management is changed. This process occurs in each soil type, but the components of the salt balances will differ for each soil, since the soil hydraulic characteristics and the occurance of preferential flow is not the same for each soil (see section 3.2).

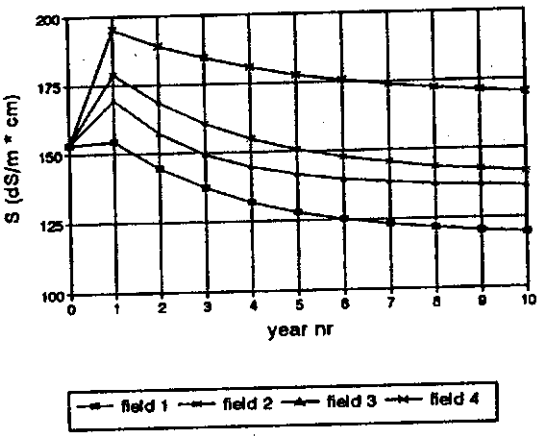

Figure 6.1a *Development of salt storage for reference scenario.*

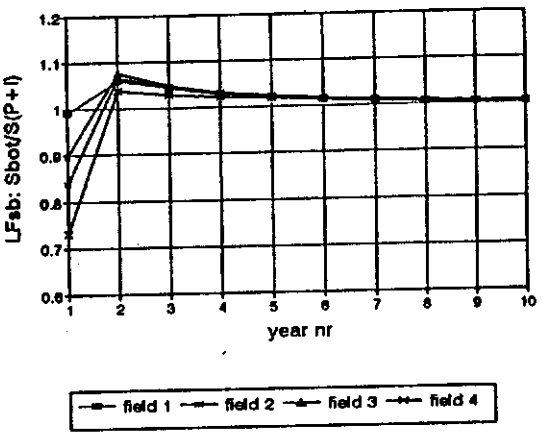

Figure 6.1b *Development of LF_{sb} for reference scenario.*

The differences between the soil types of the four fields result in a different salinization/desalinization process. For the sandier fields, a fast desalinization takes places, after two years for Field 1 and after three years for Field 2. Eventually, a desalinization will occur for Field 3 as well, but only after six years of applying the reference irrigation management. For Field 4, the equilibrium state shows salinization.

In the equilibrium state, the total amount of salts will be constant and the amount of salts in the immobile and mobile part of the soil will be constant as well. This means that there is no displacement of salts between the mobile and immobile fraction over the successive years. Obviously, during the agricultural year, there is still exchange of salts between the mobile and immobile fractions, because of salt concentration gradients caused by irrigation applications.

Scenario B

When the irrigation applications are decreased by one-third (Scenario B), the relative decrease in the relative transpiration is approximately 14 % for all soil types (see Table 6.1). Since the relative transpiration is different for the four soils, the relative decrease in leaching fraction is different for the four soil types (while the absolute decrease in leaching fraction is approximately 18 % for all soil types). This decrease in leaching fraction influences the salt balance to a large extent. In Figure 6.2, the development of the total amount of salts and the leaching fraction of salts are illustrated. In case of Scenario B, a build up of salts occurs for all soils, even for the sandy soil of Field 1. For Fields 1 and 2 the equilibrium state is reached quite soon, since these soils have a high conductivity. Field 3 and Field 4 are less

conductive and it takes more than ten years before a stationary salinity situation is reached. If the LF_{sb} of Field 4 is considered, it can be seen that the during the second year the build up of salts in the profile is even greater than during the first year after the change in irrigation management. After two years, there is still a salinization of the profile every year, but the build up of salts gradually becomes less every successive year. Even though the conductivities and the LF_{wb} for Fields 3 and 4 do not differ much, the differences between the different salt balances are very large, as the sensitivity to salinization is very high when the leaching fractions (LF_{wb}) are close to zero (see section 6.3).

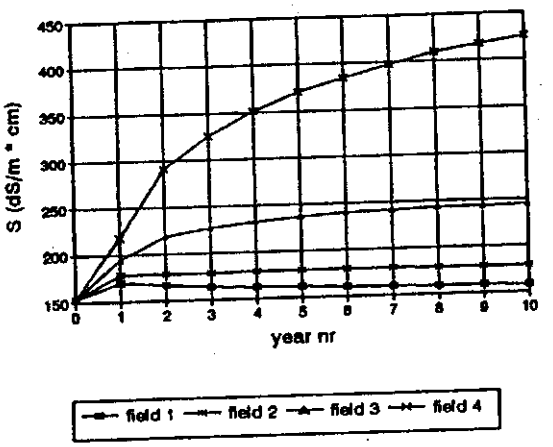

Figure 6.2a *Development of salt storage for Scenario B (underirrigation).*

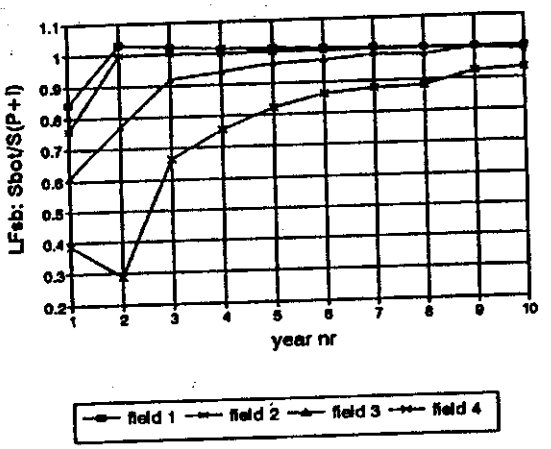

Figure 6.2b *Development of LF_{sb} for Scenario B (underirrigation).*

The build up of salts in the soil mostly takes place during the first year as can be seen in Figure 6.3.

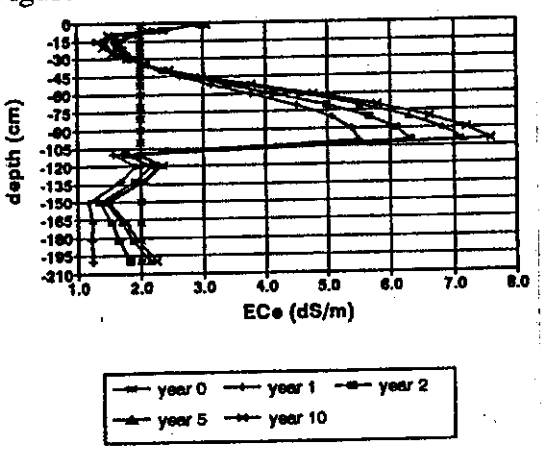

Figure 6.3 *EC_e profile for scenario B at day 365 for year 1,2,5 and 10 (field 3).*

In this Figure, the EC_eprofile of Field 3 is given at day 365 (one day before rauni for wheat) for the first, the second, the fifth and the tenth year with irrigation management Scenario B. The initial conditions are set at 2.0 dS/m throughout the profile, while after one year there is already an accumulation of salts in the root zone and the EC_e exceeds 5.0 dS/m. A reduction in crop transpiration only occurs in case the EC_e exceeds the average threshold value of 6.85 dS/m (cotton: 7.7 dS/m and wheat: 6.0 dS/m). Although the EC_e in the rooting zone exceeds this threshold value, there is no reduction in transpiration over the successive years due to an increase in soil salinity. This can be explained by the fact that root water uptake only takes place in the mobile part of the soil. This means that only the salts present in the mobile part of the soil determine the reduction in transpiration due to salinity. Approximately half of the amount of salts are stored in the immobile fraction of the soil, thereby not affecting the root water uptake. Concluding, there is no reduction in transpiration due to salinity, because a large amount of salts is stored in the immobile part of the soil and the salt concentrations in the mobile part of the soil are not limiting the root water uptake.

Scenario C

When the quality of the irrigation water is changed according to Scenario C, there is hardly any change in the water balance (see Table 6.1). Since the quality of the irrigation water is less good (higher EC), there is a slight decrease in relative transpiration and, consequently, a slight increase in the leaching fraction. However, there is no decrease in relative transpiration over ten years, which means that the excess of salts is adequately leached. Thus, there is no large build up of salts in the profile and no reduction in transpiration because of salinity stress will occur. In Figure 6.4, the development of the total amount of salts and the leaching fraction of salts is illustrated for Scenario C.

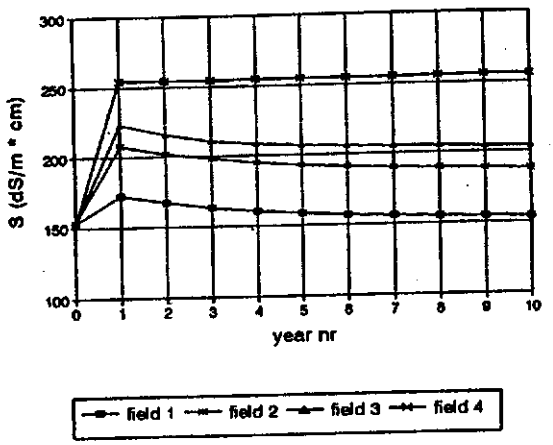

Figure 6.4a *Development of salt storage for Scenario C (low quality water).*

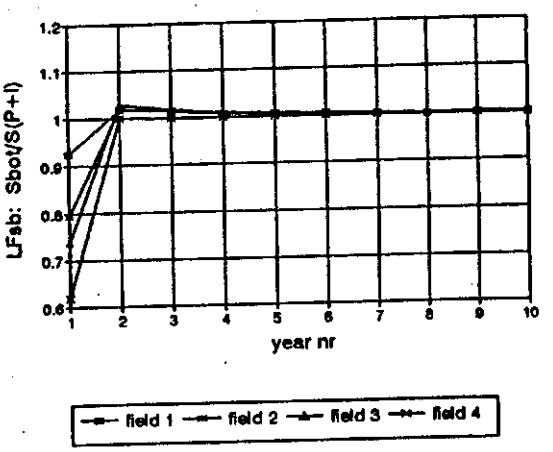

Figure 6.4b *Development of LF_{sb} for Scenario C (low quality water).*

Figure 6.4a resembles Figure 6.1a very much, the main difference is the level of the total amount of salts that is reached after a few years with the irrigation management of Scenario C. Since the electrical conductivity of the irrigation water is increased, and the leaching fraction does not change much compared to the reference scenario, the total amount of salts will be higher. For Scenario C, the soil profiles of Fields 2, 3 and 4 are salinized, while the salt level of Field 1 stays approximately at the same level. Another difference between Scenario A (reference) and Scenario C, is the fact that the equilibrium state is reached sooner for Scenario C (LF_{sb} is approximately one after five years instead of ten years). This can be explained by the fact that in the case of Scenario C, the percolation of water and salts does hardly change, while the amount of salts in the irrigation water is increased. This results in leaching fractions of salts which are closer to one and thus closer to the equilibrium state.

To make a better comparison between the effects on salinity for the different management scenarios, the development of the salt storage and the leaching fraction of salts (LF_{sb}) are put in one graph for one of the four soil types, i.e. Field 3 (see Figure 6.5).

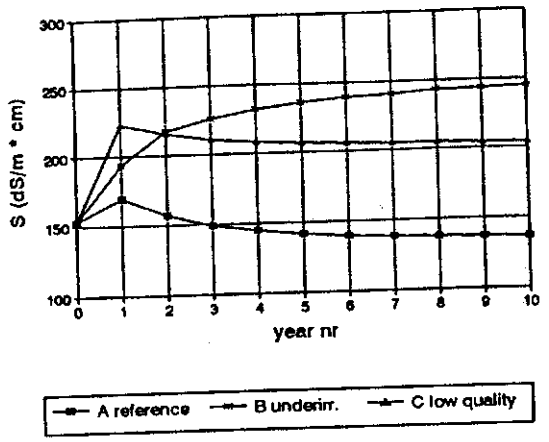

Figure 6.5a *Development of salt storage for Scenarios A, B and C (field 3).*

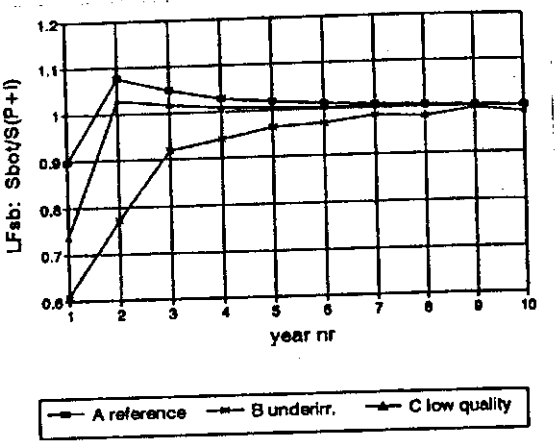

Figure 6.5b *Development of LF_{sb} for Scenarios A, B and C (field 3).*

A logical conclusion is that Scenario B (underirrigation) has the most negative impact on soil salinity and crop transpiration. Not only the soil salinity is increased, but the transpiration is reduced as well. Scenario C results in a higher soil salinity as well, but the salinity level is acceptable, since the leaching of salts is adequate. Neither for Scenario B nor for Scenario C, is the salt concentration in the soil moisture high enough to reduce the crop transpiration. Looking at the leaching fraction of salts, it can be concluded that it takes much longer to reach the equilibrium state for Scenario B (underirrigation). Since the water balance is greatly affected, it takes several years before an equlibrium in the salt balance is established.

By comparing the results of the three scenarios for the different soil types, a rough indication is obtained about the sensitivity of the different soil types for the different management scenarios over the long term. In the next section, a more detailed analysis is carried out for Field 3, in order to get a better understanding of the marginal effects of varying the quantity and quality of the irrigation water. In addition, the effect of a shallow groundwater is tested for different irrigation management scenarios.

6.3 Detailed scenario analysis

6.3.1 Description of scenarios

Quantity of irrigation water (underirrigation)
To obtain a better understanding of the long term effects of underirrigation on crop transpiration and salinity, different scenarios are developed. They can be divided into two classes i.e. underirrigation scenarios with an irrigation water quality which is the same as for the reference scenario (0.2 dS/m for rauni applications and 1.5 dS/m for other irrigation applications), and underirrigation scenarios with the irrigation quality of Scenario C (2.0 dS/m for all applications). The irrigation quantities are varied from 100 % to 50 % (in intervals of 10 %) of the reference irrigation application depths. Thus, six scenarios are

simulated to study the marginal effects of irrigation quantities on crop transpiration and salinity, for two different irrigation water qualities (totally 12 scenarios).

Quality of irrigation water
To study the long term effects of different irrigation water qualities on crop transpiration and soil salinity, three scenarios are simulated for two different irrigation quantities (totally 6 scenarios). The quality is varied from 1.5 dS/m to 2.5 dS/m (intervals of 0.5 dS/m) for all applications. The different quantities correspond with the quantities used in the reference Scenarios A and the underirrigation Scenario B (see section 6.2).

Groundwater table depth
Scenarios are performed to study the effect of a shallow groundwater table (150 cm depth) on crop transpiration and salinity. The scenarios concern two different quantities (quantity of Scenario A and of Scenario B, see section 6.2) and two different qualities (quality of Scenario A and of Scenario C), which yields four different irrigation management scenarios.

6.3.2 Results and discussion

Quantity of irrigation water (underirrigation)
Decreasing the quantity of irrigation water will have a large impact on the water balance components, since crop transpiration will be reduced and the leaching fraction will be smaller. The relative transpiration and leaching fraction for the different irrigation management scenarios are given in Table 6.2.

Table 6.2 *Water balance components for different underirrigation scenarios.*

scenario			T_a/T_p	LF_{wb}	scenario			T_a/T_p	LF_{wb}
nr	quantity	quality			nr	quantity	quality		
1	100%	A	0.98	0.25	7	100%.	C	0.96	0.26
2	90%	A	0.95	0.19	8	90%	C	0.94	0.20
3	80%	A	0.92	0.13	9	80%	C	0.90	0.15
4	70%	A	0.86	0.07	10	70%	C	0.84	0.09
5	60%	A	0.77	0.03	11	60%	C	0.75	0.05
6	50%	A	0.64	0.02	12	50%	C	0.62	0.04

In general, the relative transpiration is slightly lower for scenarios with a low irrigation water quality (Scenario C), and the leaching fraction is therefore slightly higher (absolute 2%).

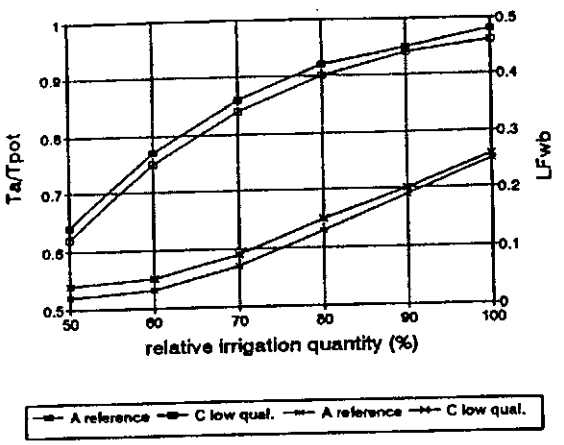

Figure 6.6 *Relative transpiration and leaching fraction as a function of irrigation quantity.*

In Figure 6.6, the relations between the irrigation quantity and the relative transpiration, respectively, and the leaching fraction (LF_{wb}) are shown for two different qualities of irrigation water. The decrease in relative transpiration and increase in leaching fraction is not linear (i.e. proportional) with decreases in irrigation water quantity. The marginal impact of the irrigation water quantity on the relative transpiration is lower for larger quantities of irrigation water. Consequently, the marginal impact on the leaching fraction is higher for larger quantities. For the two irrigation water qualities, this marginal impact is the same, since both curves have the same shape.

In Figure 6.7, the relation between the soil salinization and the leaching fraction (for the different underirrigation scenarios) is illustrated for two different qualities of irrigation water. The two curves have the same shape, only the salt storage in the soil profile is higher for the low quality water. This figure shows that when the leaching fractions are smaller than 0.1, the marginal impact on soil salinity is much higher than when the leaching fractions are greater than 0.1. Therefore, it is important to know at what quantity of irrigation water - so at what leaching fraction - the soil salinity will be sharply increased.

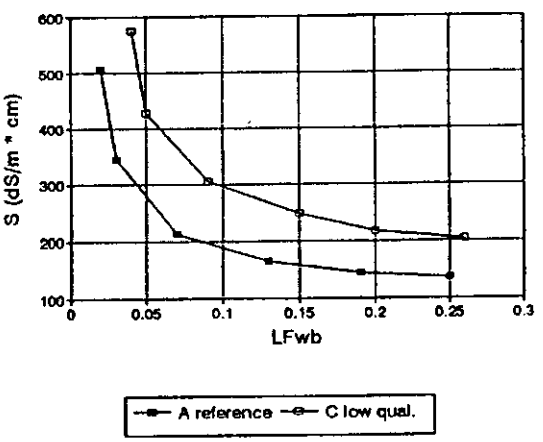

Figure 6.7 *Soil salinity as a function of the leaching fraction.*

The long term effect of different irrigation quantities on the salt balance are illustrated in Figure 6.8, which shows that if the irrigation quantity is reduced to 90 %, the final salinity level is decreased. This can be explained by the fact that the decrease in salts added to the soil profile by the reduced irrigation quantity is dominant over the fact that the leaching fraction is reduced by the reduced irrigation quantity. This means that the LF_{sb} is higher when the irrigation quantity is reduced by 10 %. For a reduction in quantity to 80 %, the same phenomenon occurs, but less pronounced. At a reduction to 70 % of the reference irrigation quantity, the leaching fraction is that much reduced (see Table 6.2) so that the amount of salts that are stored in the profile because of reduced leaching is larger than the reduction in added salts because of the reduced irrigation quantity. This reverse phenomenon becomes more and more pronounced when the irrigation quantity is further reduced. Thus, at a certain quantity of irrigation water, there is an optimum in terms of transpiration, leaching fraction and salinity.

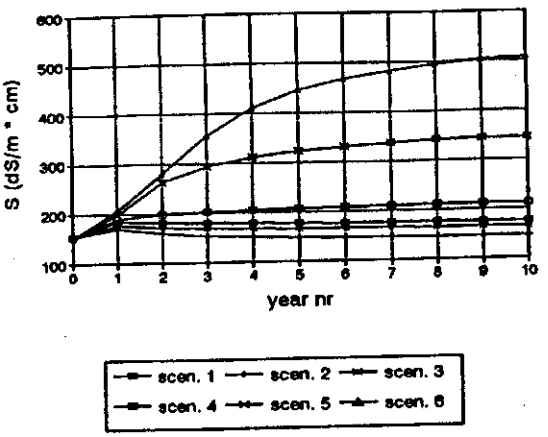

Figure 6.8a *Development of salt storage for different irrigation quantities.*

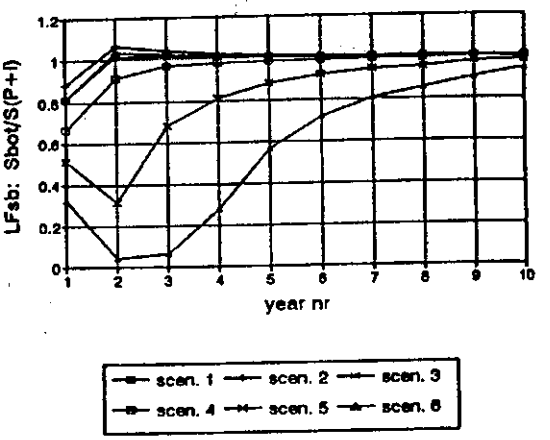

Figure 6.8b *Development of LF_{sb} for different irrigation quantities.*

Irrigation quality

The quality of the irrigation water will have an impact on the crop transpiration and the soil salinity. The transpiration and leaching fraction for the different irrigation water quality scenarios is listed in Table 6.3.

Table 6.3 *Water balance components for different irrigation quality (dS/m) scenarios.*

scenario			T_a/T_{pot}	LF_{wb}	scenario			T_a/T_{pot}	LF_{wb}
nr	quality	quantity			nr	quality	quantity		
13	1.5	A	0.97	0.25	16	1.5	B	0.83	0.06
14	2.0	A	0.96	0.26	17	2.0	B	0.81	0.08
15	2.5	A	0.95	0.26	18	2.5	B	0.80	0.09

The results listed in Table 6.3 lead to the conclusion that quality of the irrigation water does not influence the relative transpiration to a large extent; there is only a reduction of 2-3% due to the higher EC of the irrigation water.

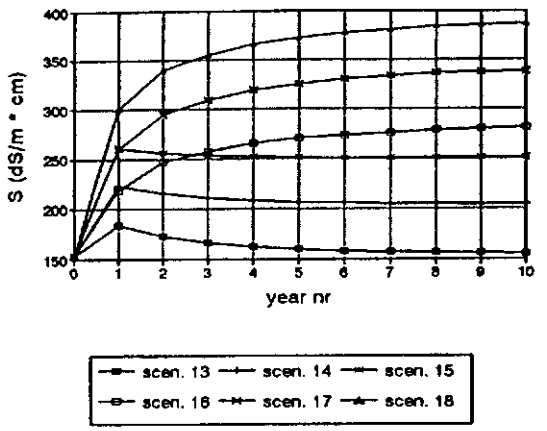

Figure 6.9a *Development of salt storage for different irrigation qualities.*

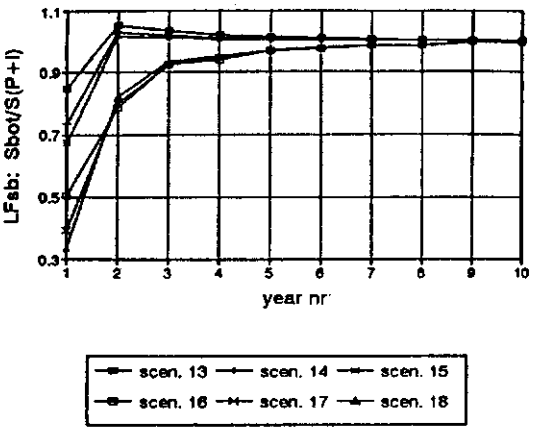

Figure 6.9b *Development of LF_{wb} for different irrigation water qualities.*

In Figure 6.9, the development of the total amount of salts and the leaching fraction of salts is illustrated for the six scenarios (Scenarios 13 - 18) In case of the reference irrigation quantity (overirrigated field), the final salinity level is approximately 150 dS/m * cm lower than in the case of underirrigation (Scenario B). This phenomenon is already explained in section 6.2. From Figure 6.9, it can also be seen that, for both of the irrigation quantities, a difference of 0.5 dS/m in the electrical conductivity of the irrigation water yields a difference of approximately 50 dS/m * cm in the final salinity level. This means that the increase in the amount of salts in the profile is approximately proportional with the increase in the electrical conductivity of the irrigation water.

Groundwater table depth

Four scenarios are performed with a groundwater table depth of 150 cm below the ground surface level. The water balance components for these four scenarios are listed in Table 6.4 and are compared with the water balance components for the case of a deep groundwatertable (free drainage).

Table 6.4 *Water balance components for different irrigation management scenarios with different groundwater table depths.*

scenario				T_a/T_{pot}	LF_{wb}	scenario				T_a/T_{pot}	LF_{wb}
nr	quant.	qual.	grw			nr	quant.	qual.	grw		
19	A	A	150	1.00	0.28	1	A	A	deep	0.98	0.25
20	A	C	150	0.99	0.28	7	A	C	deep	0.96	0.26
21	B	A	150	0.89	0.02	4	B[18]	A	deep	0.84	0.06
22	B	C	150	0.85	0.05	10	B[18]	C	deep	0.82	0.08

[18] The irrigation water quantity for Scenarios 4 and 10 does not exactly equals-two thirds (67%) of the reference quantity, but amounts to 70% of the reference quantity. Therefore, Figure 6.5 is interpolated to derive the RT and LF_{wb} at 67% of the reference quantity.

The conclusion is that the relative transpiration increases if a groundwater table is present at 150 cm depth. In case of underirrigation, the leaching fraction decreases, since capillary rise occurs when a shallow groundwater table is present.

In Figure 6.10, the development of the total amount of salts and the LF_{sb} are illustrated for the four management scenarios with a groundwater table at 150 cm depth. The quality of the groundwater is 2.0 dS/m.

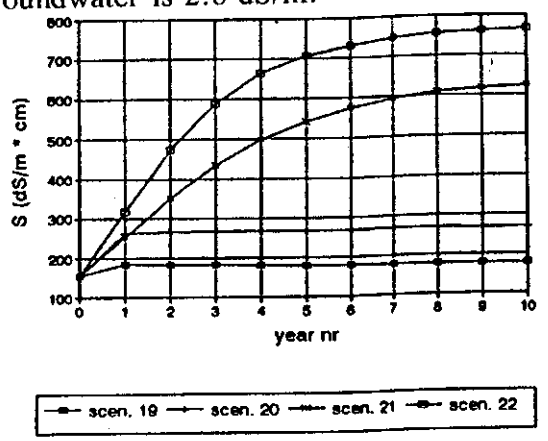

Figure 6.10a *Development of salt storage for scenarios with shallow groundwater table.*

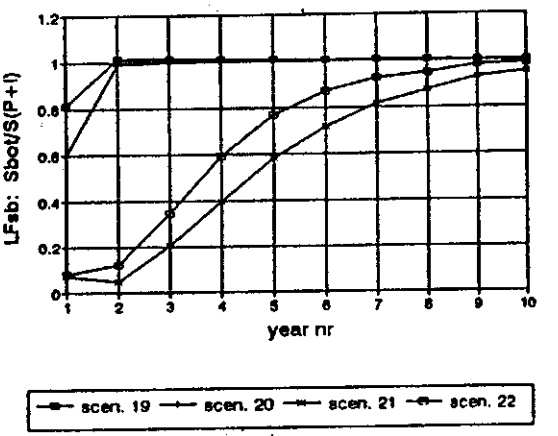

Figure 6.10b *Development of LF_{sb} for scenario with shallow groundwater table.*

In case of overirrigation (reference quantity), the final salinity level will be slightly increased for both the scenarios with different irrigation qualities (Scenarios 19 and 20). This increase is the same order of magnitude as for the scenarios with a deep groundwater table. Since the field is overirrigated, there is hardly any capillary rise, so the total salt storage and the leaching fraction of salts (LF_{sb}) show the same trends as for the scenarios with a deep groundwater table. For the underirrigation scenarios (Scenarios 21 and 22), the salt balances for a situation with and without a shallow groundwater show significant differences. For irrigation with the reference quality, the final salinty level will be higher than 600 dS/m * cm, while in case of a deep groundwater table the salinity level will not exceed 250 dS/m * cm. This large difference can be explained by the fact that capillary rise of the groundwater will bring more salts into the soil profile. Besides, the saturated part of the profile (below 150 cm) contributes largely to the total amount of salts. Moreover, the leaching fraction of salts is decreased and almost all the salts present in the applied irrigation water are stored in the soil profile. For the scenario with a low irrigation water quality (Scenario 22), the same phenomenon can be observed. The salinity level will be approximately 750 dS/m * cm and 350 dS/m * cm for a situation with a shallow and a deep groundwater table, respectively. Accordingly, with the build up of salts in the soil over several years, the LF_{sb} will gradually become higher and eventually reach one in the equilibrium state.

CHAPTER 7 CONCLUSIONS AND RECOMMENDATIONS

7.1 The use of the model SWAP93

Soil hydraulic functions
From the calibration process, it can be concluded that the Van Genuchten-Mualem (VGM) parameters influence the calibration results to a large extent (i.e. pressure heads and moisture contents). In case the values of the VGM-parameters (determined by means of pressure outflow measurements in the laborotory) are directly used as input data for the SWAP-model, the calibration does not yield satisfactory results. Therefore, it is recommended to derive the VGM-parameters from literature (Wösten et al., 1987) instead of carrying out costly and time consuming experiments in the laboratory. To reduce the number of calibration parameters, it is advised to measure the saturated hydraulic conductivity in situ in the field.

Soil salinity and preferential flow
Regarding the use of SWAP93 for simulating soil salinity, it can generally be concluded that the model overestimates the leaching of salts from the soil profile. This underestimation of the soil salinity can be explained by the underlying assumptions of the model concerning chemical and physical processes.

SWAP93 does not include any soil chemical processes, which can be a cause for the differences between measured and simulated soil salinity. Cation exchange processes and dissolution-precipitation processes influence the transport of salts and soil salinity to a certain extent. Therefore, it is recommended to study the influence of these chemical processes more thoroughly (e.g. by using numerical models that describe chemical interactions as well). Another possibility for investigating whether chemical processes significantly affect the salt balances is to do the same SWAP-calibration for the chloride-ion instead of the total amount of salts (expressed by the electrical conductivity). Since the chloride-ion is hardly involved in any chemical process, the results of the SWAP-calibration for the chloride-ion should yield more satisfactory results.

The physical reason for the underestimation of the soil salinity can be found in the assumption of the model that the infiltration of water is homogeneous over a field. In reality, the infiltration of water is very heterogeneous over a field, since the hydraulic conductivity is heterogeneous over a field and the distribution of water over a field is non-uniform. To account for these factors, the concept of preferential flow is used at the field scale. Hereby, the leaching of salts is decreased and the calibration of the soil salinity is improved. However, using the concept of preferential flow at the field scale has several disadvantages. The translation from the input parameters describing preferential flow at the soil profile scale (e.g. water repellent soils [(F_{mobile}, $\theta_{immobile}$ and K_{mobile})] to a non-uniform leaching at the field scale is very difficult, and should be studied in more detail. A limitation of the use of preferential flow related to the translation from soil profile to field scale, is the physical meaning of the exchange coefficient K_{mobile}. This coefficient determines the amount of salts in the immobile part and the influence of the initial conditions on the simulation results (initial amount of salts in the immobile part). Another restriction of using preferential flow

at the field scale is the large amount of salts that are stored in the immobile fraction, and therefore does not influence the root water uptake. Since roots only extract water from the mobile fraction, the crop transpiration is not reduced according to the total amount of salts in the soil, but according to the salt concentration in the mobile fraction. For the long term simulations, the build up of salts in the immobile part is considerable, but crop transpiration is not reduced since the salt concentration in the mobile part is not limiting the root water uptake.

Another way to adress the non-uniform water distribution over a field is to split the field into different parts with different amounts of irrigation water (e.g. 67%, 100% and 150%) and to take an average for the soil salinity of the whole field. At the writing of this report, this option is being tested and the preliminary results are very positive. It is recommended to study this option in more detail and to incorporate a kind of 'coefficient of uniformity' in SWAP in order to account for the non-uniform water distribution.

Extrapolation of SWAP93 from field level to watercourse level

This study is part of a larger multi-disciplinary research program that focuses on the whole Chishtian Sub-division (see Chapter 1). In this larger framework, the basic unit of analysis is the watercourse and, therefore, it is important to evaluate the use of SWAP93 at the watercourse level.

In this study, four sample fields were precisely calibrated for the prevailing physical conditions. Since the soil hydraulic properties are the most important calibration parameters, it can be concluded that the four fields correspond roughly with four different soil types. Although the calibration is done for a specific field, with a specific textural layering, the author thinks that the extrapolation from a specific field (e.g. Field 1) to a general soil type (e.g. loamy sand) is very well possible, as the soil physical behaviour of a certain soil type is adequately represented by the calibrated VGM-parameters. However, the preferential flow parameters might be more difficult to extrapolate, as it represents a certain non-uniformity in water distribution, which was not studied in detail during this research. Therefore, the author recommends to use SWAP93 for extrapolation purposes without the use of the preferential flow concept, but to adress the non-uniformity in water distribution by reducing the quantity of irrigtion water (via a kind of 'coefficient of uniformity').

The extrapolation of SWAP93 from a field soil type to a watercourse level, can be done by defining an average soil type for the whole watercourse. Another possibility is to do simulations for the dominant soil types present in the watercourse and, afterwards, use the weighted average as the final result for the whole watercourse. Besides the soil type, the cropping pattern and the irrigation quantity and quality should also be averaged for a watercourse. Although SWAP93 offers the possibility to model the water and salt balance of a field in a very detailed way, the model can also be used in a more simple way to describe the water and salt balance for a larger area. Obviously, the accuracy of the predictive capability is decreased when using SWAP93 at a larger scale, but the model can still be used to predict trends in soil salinity and crop transpiration. At the writing of this report, a study is being conducted to compare the results of using the SWAP93 model at the watercourse level and a simple water- and-salt balance model at the watercourse level. This study will provide more information about the possibilities and accuracy of using SWAP93 at the watercourse level.

7.2 The effects of irrigation management on soil salinity and crop transpiration

Quantity of irrigation water
The quantity of the irrigation applications affects the soil salinity and crop transpiration to a large extent. In case the irrigation quantity is reduced to 50% of the reference quantity, the relative crop transpiration on a loamy soil is reduced by 35% (from 0.98 to 0.64) and the leaching fraction is increased (from 0.25 to 0.02). On the long term, the salinity level on a loamy soil will be approximately three times higher than the soil salinity level for the reference quantity (from 175 dS/m*cm to 525 dS/m*cm).

Quality of irrigation water
The quality of the irrigation water does not influence the crop transpiration to a large extent, since cotton and wheat are salt tolerant crops[19]. In reality, a reduction in transpiration will not only occur due to soil salinity, but also due to sodicity. However, the negative effects of sodium on the soil structure and, consequently, on the crop transpiration are not taken into account by the SWAP-simulations. In sodic soils with a decreased saturated hydraulic conductivity and decreased saturated moisture content, the leaching of salts is less effective and the soil salinity will increase faster. The effects on the soil hydraulic parameters due to sodification should be studied in more detail, in order to incorporate the effects of sodicity in the SWAP-model by means of adapting the VGM-parameters.

On the long term, the soil salinity level is proportionally increased with the increase in the electrical conductivity of the irrigation water (an increase in irrigation water quality of 0.5 dS/m yields an increase in soil salinity of 50 dS/m*cm). Irrigation with low quality tubewell water (EC=2.5 dS/m) yields a final salinity level of approximately 250 dS/m*cm and 400 dS/m*cm for a leaching fraction of 0.25 and 0.07, respectively . Thus, even when a field is irrigated with tubewell water, the salinization can be controlled by applying an irrigation quantity which is sufficient to leach the excess of salts out of the soil profile.

The quality of the rauni application is very important, since a rauni application with canal water leaches the salts at the beginning of the growing season. If the rauni application is done with tubewell water, the germination can be hampered due to a high salinity level.

Frequency of irrigation
The frequency of irrigation has a large effect on the soil salinity and crop transpiration within the growing seasons. Decreasing the irrigation interval has a positive effect on the crop transpiration, while increasing the irrigation interval strongly decreases the crop transpiration. The effect on the soil salinity is inverse; namely, a positive effect while irrigating with a low frequency and an increase in soil salinity in case the irrigation interval is decreased.

---

19 The crop transpiration only shows a reduction if the salt concentration in the mobile part is higher than the critical salt concentration. Thus, a build up of salts in the soil due to low quality tubewell water does not necessarily result in reduced crop transpiration.

Soil types
The same irrigation management results in a different crop transpiration and soil salinity for the different soil types. The more sandy soils (Field 1 and Field 2) have a higher conductivity and a lower retention capacity than the loamy soils (Field 3 and Field 4). This results in a more efficient leaching of salts in the sandy soils, and at the same time a less efficient crop transpiration. In case the irrigation quantity is reduced to 50% of the reference quantity, the final soil salinity level is almost three times higher for a loamy than for a sandy soil. Consequently, the crop transpiration on a loamy soil is approximately 12% higher than on a sandy soil. If a field is irrigated with low quality tubewell water, the final soil salinity on a loamy field is almost two times higher than on a sandy field, while the crop transpiration is 15% higher than on a sandy field. In case the irrigation interval is decreased, the crop transpiraton on the loamy soil remains at the same level, while the transpiration on the sandy soil decreases by approximately 17%.

ACKNOWLEDGEMENT

This report is the result of a six-months thesis Agrohydrology at the Department of Water Resources, Wageningen Agricultural University. This thesis is part of the collaboration between the International Irrigation Management Institute of Pakistan (IIMI-Pakistan) and the Wageningen Agricultural University (WAU). Therefore, I spend one month in Wageningen and six months in Pakistan, working on this thesis, and enjoyed both periods a lot.

The first week I spend in Pakistan illustrated the above mentioned collaboration very well. One week of discussions, field visits and social talks with Marcel Kuper (IIMI), Pierre Strosser (IIMI) and Professor R.A. Feddes (WAU) was an excellent start of my stay in Pakistan.

I would like to thank Marcel Kuper for his supervision from IIMI's side: thanks for the discussions and the many advices and comments! From the Wageningen side, I would like to thank Jos van Dam for all the critical and supporting e-mails and faxes that - in spite of the distance - enabled us to discuss about my research.

Further, I would like to thank all IIMI-staff (including IIMI-students!) - whether based in Lahore or in Hasilpur - who made my stay in Pakistan an experience of great value.

Susanna Smets May, 1996

REFERENCES

Akbar, A., 1995. Simulation of soil water flow in the unsaturated zone using SWATRE model for optimal water table regime. Centre of Excellence in Water Resources Engineering, Lahore, Pakistan.

Asher, S., 1993. Calibration and application of SWATRE model for local conditions. Centre of Excellence in Water Resources Engineering, Lahore, Pakistan.

Barral, J.P., 1994. Development of a watercourse based model to assess the canal water supply at the farm level. IIMI-Pakistan.

Bastiaansen, W.G.M., 1993. Interpretation of field experiments to arrest rising water tables using SWASALT model. DLO-Winand Staring Centre, International activities report 29, Wageningen, The Netherlands.

Belmans, C., J.G. Wesseling and R.A. Feddes, 1983. Simulation of the water balance of a cropped soil: SWATRE. Journal of Hydrology, 63, vol. 3/4: 217-286.

Bhutta, M.N. and E.J. Van der Velde, 1992. Equity of water distribution along secondary canals in the Punjab, Pakistan. Irrigation and Drainage Systems, Vol. 6: 161-177.

Biggar, J.W., 1996. Water quality for agricultural and related uses. Department of Land, Air and Water Resources, University of California, Davis.

Black, T.A., W.R. Gardner and G.W. Thurtell, 1969. The prediction of evaporation, drainage and soil water storage for a bare soil. Soil Sci. Soc. Am. J., 33: 655-660.

Boesten, J.J.T.I. and L. Stroosnijder, 1986. Simple model for daily evaporation from fallow tilled soil under spring conditions in a temperate climate. Netherlands Journal of Agricultural Science, 34: 75-90.

Borg, H. and D.W. Grimes, 1988. Depth development of roots with time: An empirical description. Transactions of the ASAE vol. 29(1): 194-197.

Carsel, R.F. and R.S. Parrish, 1988. Developing joint probability functions of soil water retention characteristics. Water Resour. Res., Vol. 24: 755-769.

Celia, M.A., E.T. Bouloutas and R.L. Zarba, 1990. A general mass conservative numerical solution for the unsaturated flow equation. Water Resour. Res., Vol. 26: 1483-1496.

Dam, J.C. van, J.M.H. Hendrickx, H.C. van Ommen, M.H. Bannink, M. Th. van Genuchten and L.W. Dekker, 1990. Unsaturated soil water movement in hysteric and water repellent soils. Journal of Hydrology, 120: 359-379.

Dam, J.C. van, 1992. Preliminary simulations of water and salt transport at an irrigated field in Pakistan with SWATRE. Netherlands Research Assistance Project, Report no. 48, Lahore, Pakistan.

Dam, J.C. van, 1993. Simulation of water and solute transport to investigate irrigation management in Punjab, Pakistan. Consultancy report to IIMI-Pakistan. Department of Water Resources, Agricultural University, Wageningen, The Netherlands.

Dam, J.C. van, R.A. Feddes and P. Kabat (eds.), 1996 (in progress). Simulation model SWAP. Theory and model description.

Diepen, C.A. van, J. Wolf, H. van Keulen and C. Rappoldt, 1988. Crop growth simulation model WOFOST version 4.1. Documentation. SOW-88-01. Centre for World Food Studies, Wageningen, the Netherlands.

Doorenbos, J. and W.O. Pruitt, 1977. Crop water requirements. FAO Irrigation and Drainage paper no. 24. Food and Agricultural Organization of the United Nations, Rome.

Doorenbos, J. and A.H. Kassam, 1979. Yield response to water. FAO Irrigation and Drainage paper no. 33. Food and Agricultural Origanization of the United Nations, Rome.

Feddes, R.A., P.J. Kowalik and H. Zaradny, 1978. Simulation of field water use and crop yield. Simulation Monographs, Pudoc, Wageningen, The Netherlands.

Feddes, R.A., J.G. Wesseling and W. Wiebing, 1984. Simulation of transpiration and yield of potatoes with SWACRO model. In: F.A. Winiger and A. Stockli (eds.), Ninth Tri-annual Conference of the European Association of Potato Research (EAPR), Interlaken, 346-348.

Feddes, R.A., P. Kabat, P.J.T. van Bakel, J.J.B. Bronswijk and J. Halbertsma, 1988. Modelling soil water dynamics in the unsaturated zone - state of the art. Journal of Hydrology, vol 100: 69-111.

Feddes, R.A. and R.W.R. Koopmans, 1995. Agrohydrology. Lecture notes, Department of Water Resources, Agricultural niversity, Wageningen, The Netherlands.

Genuchten, M. Th., 1987. A numerical model for water and solute movement in and below the root zone. Res. Report, U.S. Salinity Laboratory, Riverside, CA.

Genuchten, M. Th. and R.J. Wagenet, 1989. Two-site/two region models for pesticide transport and degradation: Theoretical development and analytical solutions. Soil Sci. Soc. Am. J., 53: 1303-1310.

Haverkamp, R., et al., 1977. A comparison of numerical simulation models for one dimensional infiltration. Soil Sci. Soc. Am. Proc., 41: 285-294.

Hoogmoed, W.B. and J. Bouma, 1980. A simulation model for predicting infiltration into cracked clay soil. Soil Sci. Soc. Am. J., 44: 458-461.

IIMI, 1995. The effects of farmers irrigation and cultural practices on cotton and wheat production. Seasonal report 1 and 2, IIMI, Lahore, Pakistan.

IIMI, 1996. Analyzing large-scale irrigation systems in an integrated approach: application to the Chishtian Sub-division. Paper prepared for the Eleventh Internal Program Review, IIMI, Colombo, Sri Lanka.

IWASRI, 1995. Estimating soil hydraulic properties for two fields in the Chishtian Sub-division. International Waterlogging And Salinity Research Insitute, Lahore, Pakistan.

Kabat, P., B.J. Broek, van den and R.A. Feddes, 1992. SWACROP: A water management and crop production simulation model. ICID Bulletin 92, vol. 41 no. 2: 61-84.

Kelleners, J., 1993. Use of SWATRE to simulate the water and salt balance of an irrigated field in the Indus plain, Pakistan. NRAP report no. 56, Lahore, Pakistan.

Kijne, J.W. and M. Kuper, 1995. Salinity and sodicity in Pakistan's Punjab: A threat to sustainability of irrigated agriculture? IIMI-paper, Lahore, Pakistan

Kool, J.B. and J.C. Parker, 1987. Estimating soil hydraulic properties from transient flow experiments: SFIT user's guide. Report submitted to the Electric Power Research Institute, Palo Alto, California, USA.

Kuper, M. and E. Van Waijen, 1993. Farmers irrigation practices and their impact on soil salinity in the Punjab, Pakistan: Is salinity here to stay?. IIMI Internal Program Review, Colombo, Sri Lanka.

Maas, E.V. and G.J. Hoffman, 1977. Crop salt tolerance-current assesment. J. Irrigation and Drainage Div., ASCE 103: 115-134

Maas, E.V., et. al., 1990. Crop salt tolerance. In: Agricultural Salinity Assesment and Management. ASCE Manuals and Reports on Engineering Practice, no. 71, U.S.

Mualem, Y., 1976. A new model for predicting the hydraulic conductivity of unsaturated porous media. Water Resour. Res., 12: 513-522.

Pintus, F., 1995. Impact of irrigation, salinity and cultural practices on wheat yields. CEMAGREF, IIMI-Pakistan, University of Montpellier.

Prasad, R., 1988. A linear root water uptake model. Journal of Hydrology, Vol. 99: 297-306.

Rawls, W.D., D.L. Brakensiek and K.E. Saxton, 1982. Estimating soil water properties. Transactions, ASAE, 25(5): 1316-1320 and 1328.

Rinaudo, J.D., 1994. Development of a tool to asses the impact of water markets on agricultural production in Pakistan. CEMAGREF, IIMI-Pakistan, University of Montpellier.

Ritsema, C.J., L.W. Dekker, J.M.H. Hendrickx and W. Hamminga, 1994. How water moves in a water repellent sandy soil. Dynamics of fingered flow. Water Resour. Res., Vol. 30: 2519-2531.

Smith, M., 1992. CROPWAT, a computer program for irrigation planning and management. FAO Irrigation and Drainage paper 46, Food and Agricultural Organization of the United Nations, Rome.

So, H.B. and L.A.G. Aylmore, 1993. How do sodic soils behave? The effect of sodicity on soil physical behaviour. Australian Journal of Soil Research, Vol. 31: 761-777.

Strosser, P. and M. Kuper, 1992. Water markets in the Fordwah/Eastern Sadiqia area. IIMI-paper 30, Lahore, Pakistan.

Sumner, M.E., 1993. Sodic Soils: New Perspectives. Australian Journal of Soil Research, Vol. 31: 683-750.

Taylor, S.A. and G.M. Ashcroft, 1972. Physical Edaphology. W.H. Freeman and Co., San Francisco, 434-435.

U.S. Salinity Laboratory Staff, 1954. Diagnosis and improvement of saline and alkali soils. U.S. Department of Agricultural Handbook 60. U.S. Printing Office, Washington.

Wesseling, J.G., J.A. Elbers, P. Kabat and B.J. Broek, van den, 1990. SWATRE, instructions for input. Internal report, Winand Staring Centre.

Wijk, A.L.M. van, R.A. Feddes, J.G. Wesseling and J. Buitendijk, 1988. Effects of soil type and subsurface drainage on the yield of of agricultural crops. Report 31. ICW, Winand Stariong Centre, Wageningen, The Netherlands.

Working Group SWAP, 1994. SWAP Input Manual. DLO-Winand Staring Centre, Wageningen, The Netherlands.

World Bank, 1994. Pakistan- Irrigation and Drainage Issuses and Options. Washington, D.C., U.S.

Wosten, J.H.M. et al., 1987. Description of the water retention and hydraulic conductivity characteristics from the Staring Series with analytical functions. Soil Survey Institute Siboka, Wageningen, The Netherlands.

Wosten, J.H.M. and M.Th. van Genuchten, 1988. Using texture and other soil properties to predict the unsaturated soil hydraulic properties. Soil Sci. Soc. Am. J., 52: 1762-1770.

ANNEXES

ANNEX A MAP CHISHTIAN SUB-DIVISION

Map 1

Location of two sample watercourses in the Chishtian Sub-division

Map Showing the Location of Sample Watercourses

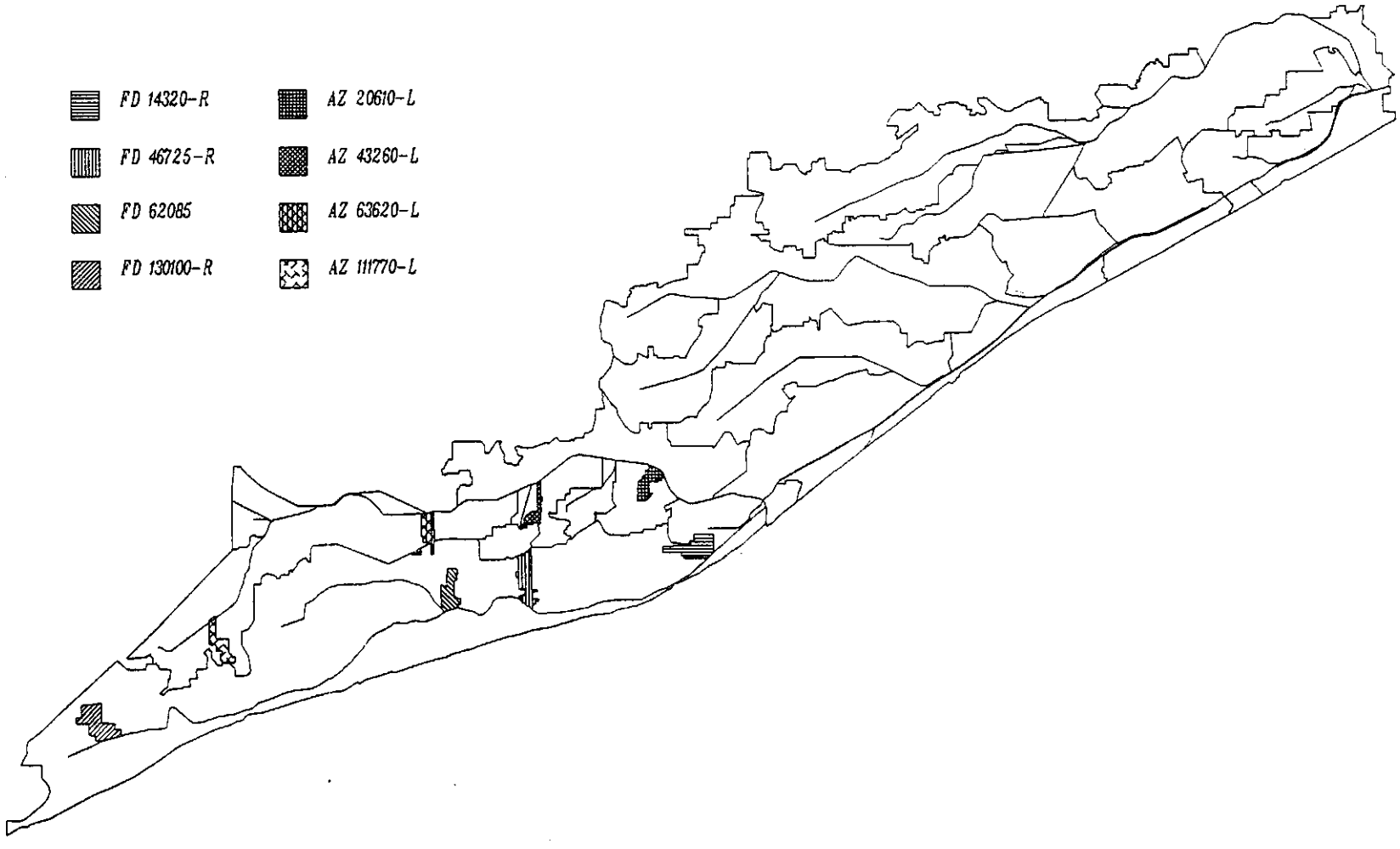

ANNEX B TABLES WITH VGM-PARAMETERS

VGM-parameters according to Rawls et al. (1982)

Table B.1 *VGM-parameters as derived by Rawls et al. (1982).*

texture	θ_r -	θ_s -	K_s cm/d	α 1/cm	n -
sand	0.020	0.417	504.0	0.138	1.592
loamy sand	0.035	0.401	146.6	0.115	1.474
sandy loam	0.041	0.412	62.16	0.068	1.322
loam	0.027	0.434	16.32	0.090	1.220
silt loam	0.015	0.486	31.68	0.048	1.211
sandy clay loam	0.068	0.330	10.32	0.036	1.250
clay loam	0.075	0.390	5.52	0.039	1.194
silty clay loam	0.040	0.432	3.60	0.031	1.151
sandy clay	0.109	0.321	2.88	0.034	1.168
silty clay	0.056	0.423	2.16	0.029	1.127
clay	0.090	0.385	1.44	0.027	1.131

VGM-parameters according to Carsel and Parrish (1988)

Table B.2 *VGM-parameters as derived by Carsel and Parrish. (1988).*

texture	θ_r -	θ_s -	K_s cm/d	α 1/cm	n -
sand	0.045	0.43	712.8	0.145	2.68
loamy sand	0.057	0.41	350.2	0.124	2.28
sandy loam	0.065	0.41	106.1	0.075	1.89
loam	0.078	0.43	24.96	0.036	1.56
silt	0.034	0.46	6.00	0.016	1.37
silt loam	0.067	0.45	10.80	0.020	1.41
sandy clay loam	0.100	0.39	31.44	0.059	1.48
clay loam	0.095	0.41	6.24	0.019	1.31
silty clay loam	0.089	0.43	1.68	0.010	1.23
sandy clay	0.100	0.38	2.88	0.027	1.23
silty clay	0.070	0.36	0.48	0.005	1.09
clay	0.068	0.38	4.80	0.008	1.09

VGM-parameters according to Wösten et al. (1987)

Table B.3 *VGM-parameters as derived by Wösten et al. (1987) (subsoils)*

code	texture	θs -	K_s cm/d	λ -	α 1/cm	n -
	top soil					
B1	fine sand	0.37	33.34	0.571	0.0208	1.646
B2	weakly loamy, fine sand	0.43	32.21	-0.304	0.0224	1.436
B3	loamy, fne sand	0.45	17.81	-0.213	0.0152	1.412
B4	strongly loamy, fine sand	0.42	54.80	0.177	0.0163	1.559
B7	light loam	0.40	25.10	0.248	0.0158	1.287
B8	moderately heavy loam	0.40	22.90	-3.578	0.0313	1.200
B10	loght clay	0.44	31.10	-6.552	0.0519	1.126
B11	moderately heavy clay	0.51	63.30	-8.067	0.1562	1.099
B12	heavy clay	0.57	98.20	-10.28	0.1689	1.068
	sub soil					
O1	fine sand	0.35	99.70	0.796	0.0220	2.186
O2	weakly loamy, fine sand	0.38	63.90	0.911	0.0182	1.870
O3	loamy, fine sand	0.34	44.60	-0.333	0.0265	1.543
O4	strongly loamy, fine sand	0.36	53.10	-0.520	0.0216	1.540
O5	coarse sand	0.33	223.0	0.873	0.0524	1.912
O8	light loam	0.42	26.40	-0.622	0.0248	1.321
O9	moderately heavy loam	0.41	24.00	-1.559	0.0280	1.283
O10	heavy loam	0.44	25.60	-2.220	0.0231	1.212
O11	light clay	0.42	61.00	-3.706	0.0420	1.125
O12	moderately heavy clay	0.49	10.80	-6.743	0.0384	1.113
O13	heavy clay	0.58	38.00	-12.54	0.1122	1.063
O15	silty loam	0.43	57.42	-2.077	0.0207	1.224

ANNEX C DETERMINATION OF SALINITY STRESS COEFFICIENTS

The soil water potential for the reduction of root water uptake consists of the matric head and the osmotic head according to:

$$h_{total} = h_{matric} + C * h_{osmotic} \quad (C.1)$$

$$h_{osmotic} = A + B * c \quad (C.2)$$

A,B,C : plant specific regression coefficients
c : salt concentration (dS/m)

The value of B is set at -360cm m/dS. The values of A and C can be determined with the help of the salt tolerance data of Maas, et al. (1990).

Example

threshold ECe value: 6.0 dS/m
slope: 7.1 % per dS/m

There is no reduction due to water stress at field capacity, which means pF = 2.0 and h_{matric} = -100 cm. It is assumed that the moisture content at field capacity is half the saturated moisture content, and the EC of the soil moisture is, therefore, two times the EC of the extract ($EC_e * 2 = EC_{sw}$).

Reduction in transpiration for wheat starts to occur at h_{total} = -700 cm ((500+900)/2). At this threshold point π = 12.0 dS/m (2*6) and there is no reduction due to salinity stress. The following equation can be derived:

$$-700 = -100 + (A - 360 * 12) * C \quad (C.3)$$

When h_{total} = 16000 cm, the reduction in transpiration is 100%. If this reduction is only caused by salinity stress, the osmatic potential will be:

$$\Pi = 6.0 + 100/7.1 * EC_e \quad (C.4)$$

At this point EC_e = 20.1 and EC_{sw} = 40.2. The following equation can be derived:

$$-16000 = -100 + (A - 360 * 40.2) * C \quad (C.5)$$

Combining Equations C.3 and C.5 yields the values for A and C of 3920 cm and 1.50, respectively.

ANNEX D HETEROGENEITY OF TEXTURE, SALINITY AND SODICITY

In Table 1.4, the results are shown for the textural analysis, which was done for the four sample fields in December'94. The texture varies substantially within a field (both in the horizontal and vertical directions), with coefficients of variation (CV) ranging from 0.09 to 0.75 (see Table D.1). These CV's are averages of the CV's at each depth, based on a sample size of 10 (IIMI, 1995).

Table D.1 *CV of texture percentages for the four sample fields, December'94.*

	CV % sand	CV % silt	CV % clay
Field 1	0.09	0.73	0.34
Field 2	0.21	0.50	0.33
Field 3	0.26	0.62	0.30
Field 4	0.34	0.75	0.53

The smaller the coefficient of variation for the different soil particles (sand, silt, clay), the more homogeneous is the texture of the field. It can be concluded that Field 1 has the most homogeneous texture, while the texture of Field 4 is the most heterogeneous.

The EC_e and SAR were also determined in December'94, and they show a strong heterogeneity as well. In Table D.2, CV's of the EC_e and SAR of the ten individual samples taken at each depth are listed, emphasizing the high variability in salinity and sodicity within the fields. Additionally, the minimum and maximum values of the EC_e and SAR are given in Table D.2.

Table D.2 *Minimum and maximum values of EC_e (dS/m) and SAR and their CV's for the four sample fields, December'94.*

	$EC_{e,\,min}$	$EC_{e,\,max}$	CV EC_e	SAR_{min}	SAR_{max}	CV SAR
Field 1	0.3	1.9	0.38	0.1	5.6	0.76
Field 2	0.5	3.7	0.45	0.6	14.5	0.71
Field 3	0.5	4.3	0.32	1.4	17.7	0.46
Field 4	0.5	6.1	0.49	0.9	12.7	0.41

The heterogeneity in salinity (CV's EC_e) is approximately the same for the four sample fields, while the sandier fields (Fields 1 and 2) are more heterogeneous concerning sodicity (CV's of SAR) than the heavier soils (fields 3 and 4).

ANNEX E COMPARISON OF CALIBRATED AND NOT CALIBRATED RESULTS

Since a lot of time and effort is spent on a detailed calibration of SWAP for the four sample fields, the question arises whether a routine wise calibration would still yield satisfactory results. Routine wise means, that the soil hydraulic functions are based on previous determined tables of VGM-parameters related to texture, and it means that the concept of preferential flow is not applied.

In this annex, a comparison is made between the results of the *'detailed'* (or *'calibrated'*) and the *'routine wise'* (or *'not calibrated'*) calibration for two of the four sample fields. The input data for the detailed calibration are listed in section 3.2. For the routine wise calibration, the VGM-parameter sets determined by Wösten (1987) are used (Table 3.2).

Field 1

In the routine wise calibration, this field is represented by a fine sandy top soil (B1) underlain by a fine sandy subsoil (O1). Figure E.1 shows the pressure heads at 60 cm depth for the detailed and routine wise calibrations. It can be concluded the pressure heads compare quite well, however, the effects of using the preferential flow concept are obvious.

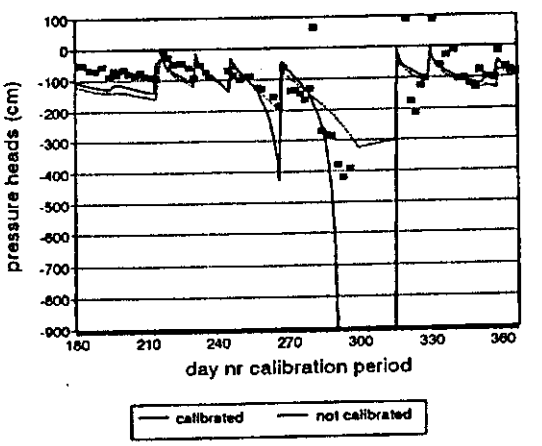

Figure E.1 *Pressure heads at 60 cm depth for field 1.*

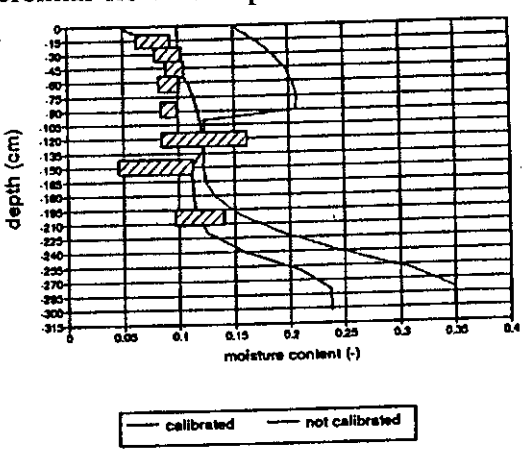

Figure E.2 *Moisture content at day 365 for field 1.*

The moisture content, however, is considerably overestimated by the routine wise calibration (see Figure E.2). Adjusting the VGM-parameter set and using the concept of preferential flow increases the percolation and reduces the overall moisture content in the profile (see Table F.1).

Table E.1 *Water balance components of field 1 (cm).*

	T_p	T_a	E_p	E_a	P+I	Q_{down}	ΔW
detailed	81.2	75.0	51.8	23.1	238.8	-141.4	42.3-42.2
routine	81.2	81.0	51.8	25.4	238.8	-130.6	63.6-63.7

The above differences in the water balance have a great impact on the salt balance. Since salts are 'fixed' in the immobile part, the percolation of salts is less for the detailed calibration than for the routine wise calibration (see Table E.2).

Table E.2 *Salt balance components of field 1 (dS/m * cm).*

	S_{P+I}	S_{down}	ΔS	$S_{immobile}$
detailed	78.6	-150.6	(57.0-129.3)=-72.3	49.7
routine	78.6	-189.2	(49.7-160.7)=-111.0	-

Concerning the simulated EC_e values, differences between the detailed and routine wise calibration can be explained by three factors, which determine the value of the EC_e i.e. the actual moisture content, the saturated moisture content and the amount of salts present. Figure E.3 shows the moisture content and EC_e at the end of the calibration period.

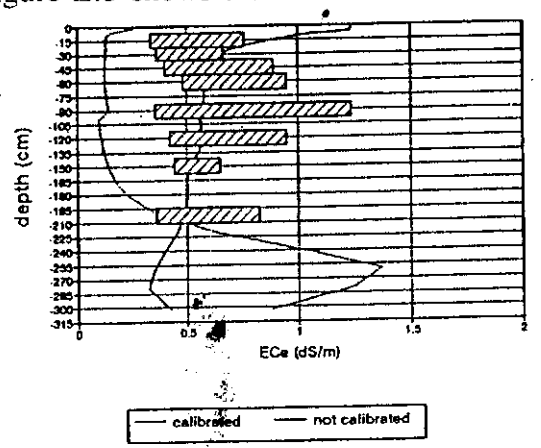

The amount of salts at the end of the calibration period is less for the routine wise calibration than for the detailed calibration. The actual moisture content for the routine calibration is higher than for the detailed calibration, but this is counteracted by a higher saturated moisture content for the routine wise calibration. This results in lower EC_e values for the routine wise calibration than for the detailed calibration and a greater deviation from the measured values.

Figure E.3 *EC_e profile at day 365 for Field 1.*

Field 4.

In the routine wise calibration, this field is represented by a strongly loamy fine sand top soil (B4), underlain by a weakly loamy fine sand (O2). Figure E.4 shows the pressure heads at 60 cm depth for the detailed and routine wise calibration.

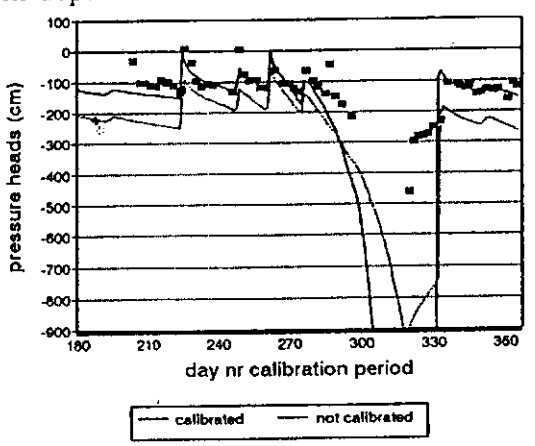

Figure E.4 *Pressure heads at 60 cm depth for Field 4.*

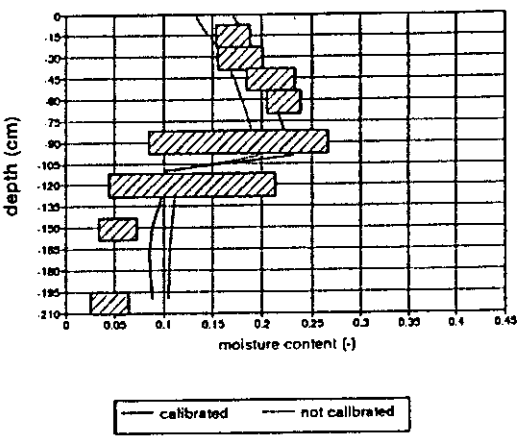

Figure E.5 *Moisture content at day 365 for Field 4.*

It can be concluded that the suction simulated by the routine wise calibration is overestimated compared to the detailed calibration, resulting in a lower overall moisture content (see Figure E.5).

For Field 4, the water balance differences between the detailed and the routine wise calibration are not remarkable (see Table E.3). Field 4 is less overirrigated as compared with Field 1, so the difference in the percolation flux is less. Again, more water percolates when the concept of preferential flow is used. However, the moisture content for the detailed calibration is slightly higher than for the routine wise calibration, since the differences in VGM-parameters yield a higher suction for the routine wise calibration. Besides, the moisture content in the immobile fraction (detailed calibration) is fixed at a rather high level.

Table E.3 *Water balance components of Field 4 (cm).*

	T_p	T_a	E_p	E_a	P+I	Q_{down}	ΔW
detailed	82.1	74.5	49.3	21.1	121.4	-23.4	30.2-29.8
routine	82.1	82.0	49.3	21.1	121.4	-20.7	29.3-29.4

In Table E.4, the differences in the salt balance between the detailed and routine wise calibration are given.

Table E.4 *Salt balance components of Field 4 (dS/m * cm).*

	S_{P+I}	S_{down}	ΔS	$S_{immobile}$
detailed	96.2	-133.6	(152.5-190.4)=-37.9	90.6
routine	96.2	-191.3	(114.9-209.0)=-94.1	-

The relatively small difference in the downward percolation flux results in a much larger difference in the leaching of salts. The salts are fixed in the immobile fraction and less salts are leached out of the profile.

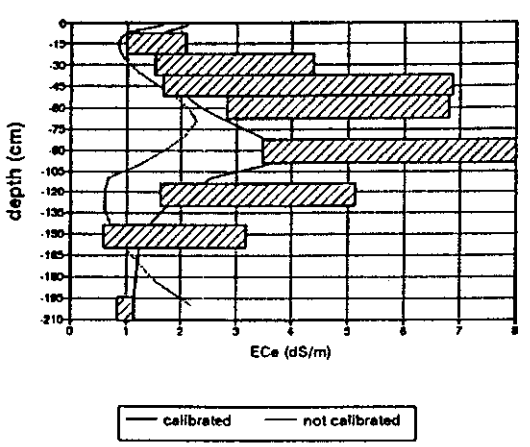

Figure E.6 *EC_e profile at day 365 for Field 4.*

The simulated EC_e values are lower for the routine wise calibration than for the detailed calibration, since the total amount of salts is lower. The saturated moisture content is slightly higher for the routine wise calibration, while the actual moisture content is a bit lower, which contributes to lower values of EC_e (see Figure E.6).

ANNEX F ADDITIONAL INPUT DATA CALIBRATION AND VALIDATION

Irrigation and rainfall validation period

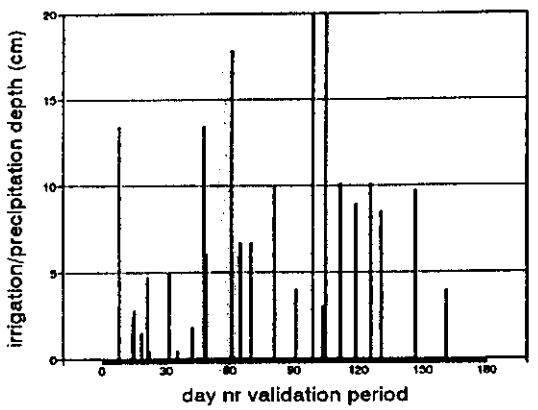

Figure F.1 *Irrigation and rainfall for validation period of field 1.*

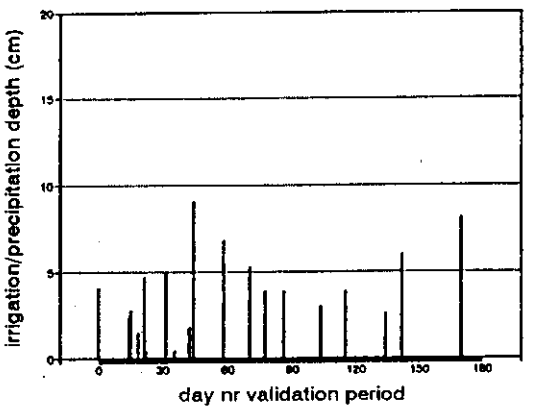

Figure F.2 *Irrigation and rainfall for validation period of field 2.*

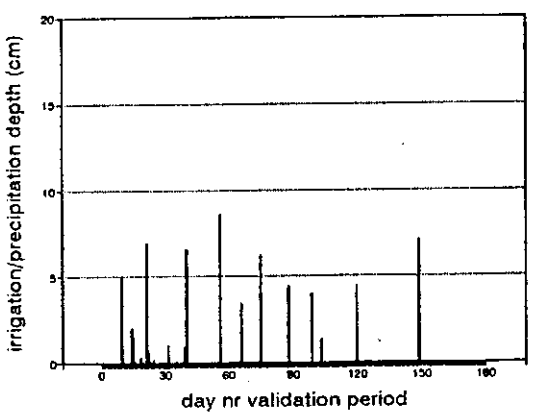

Figure F.3 *Irrigation and rainfall for validation period of field 3.*

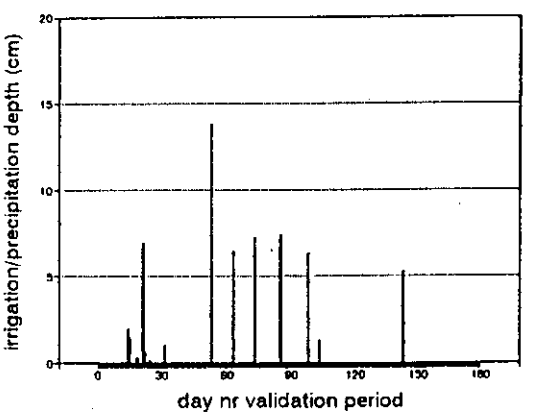

Figure F.4 *Irrigation and rainfall for validation period of field 4.*

Groundwater table validation period

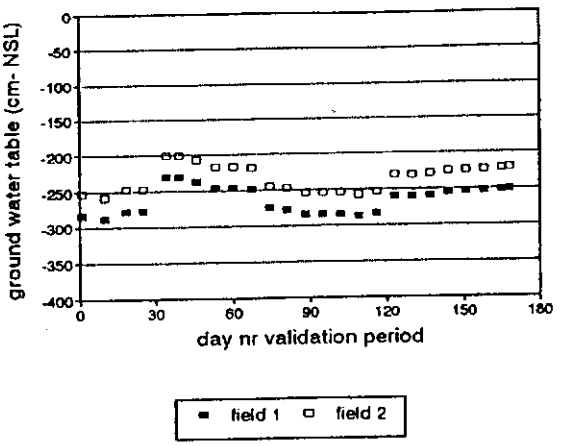

Figure F.5 *Groundwater table field 1 and 2 for validation period.*

Initial EC_e profiles (day 0 calibration period)

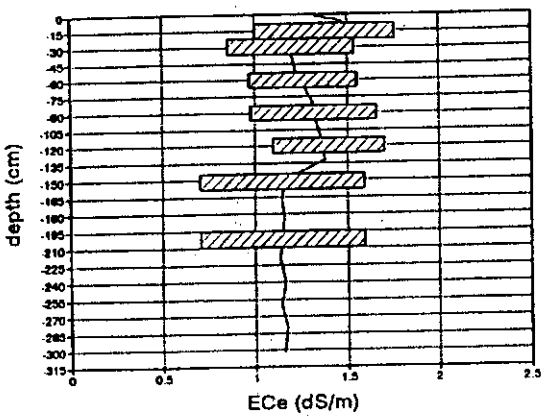

Figure F.6 *Initial EC_e profile of field 1.*

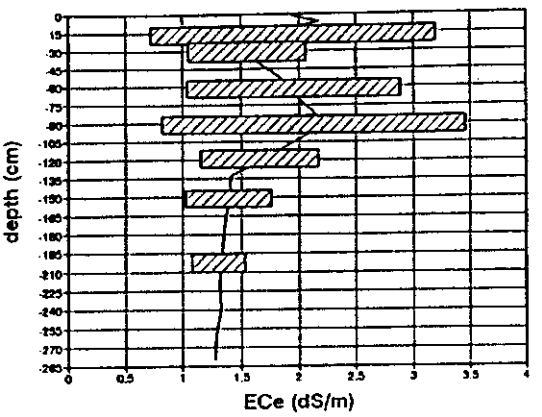

Figure F.7 *Initial EC_e profile of field 2.*

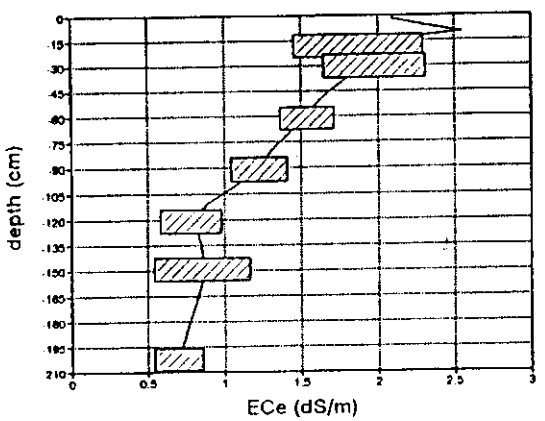

Figure F.8 *Initial EC_e profile of field 3.*

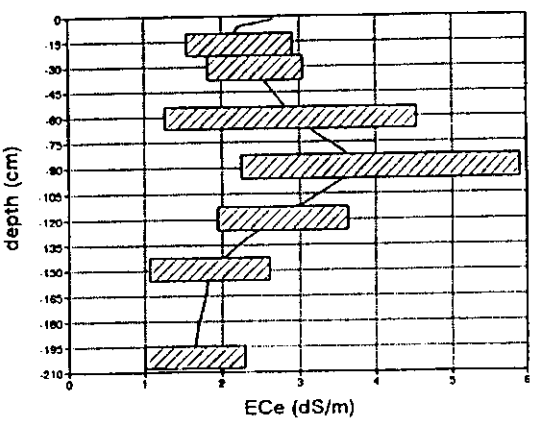

Figure F.9 *Initial EC_e profile of field 4.*

ANNEX G RESULTS OF CALIBRATION AND VALIDATION

G.1 FIELD 1

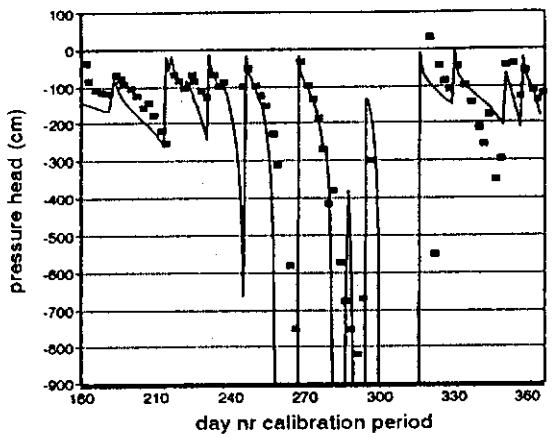

Figure G.1 *Pressure heads at 15 cm for calibration of field 1.*

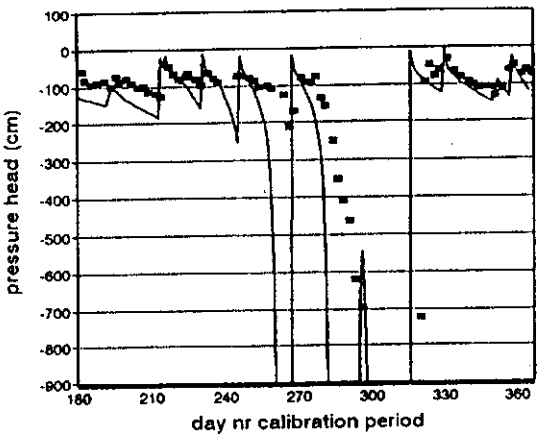

Figure G.2 *Pressure heads at 30 cm for calibration of field 1.*

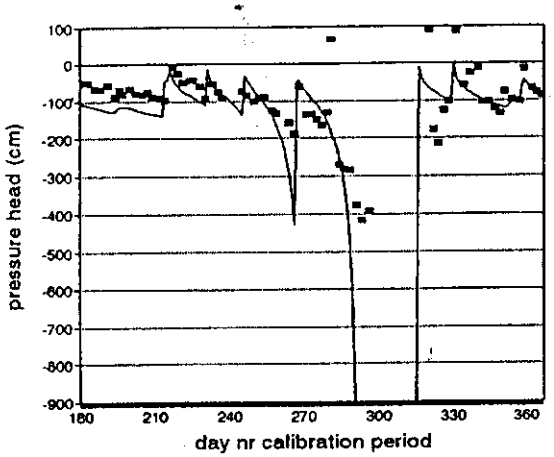

Figure G.3 *Pressure heads at 60 cm for calibration of field 1.*

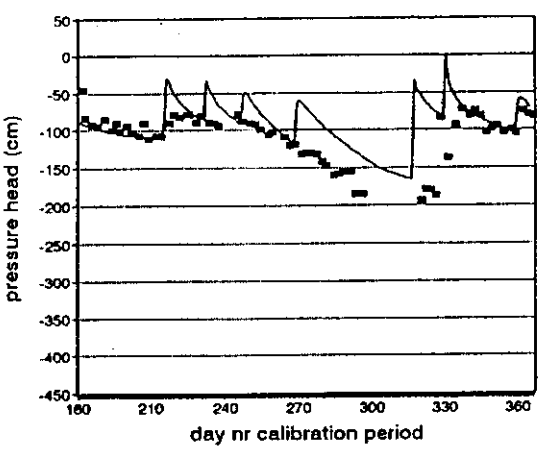

Figure G.4 *Pressure heads at 120 cm for calibration of field 1.*

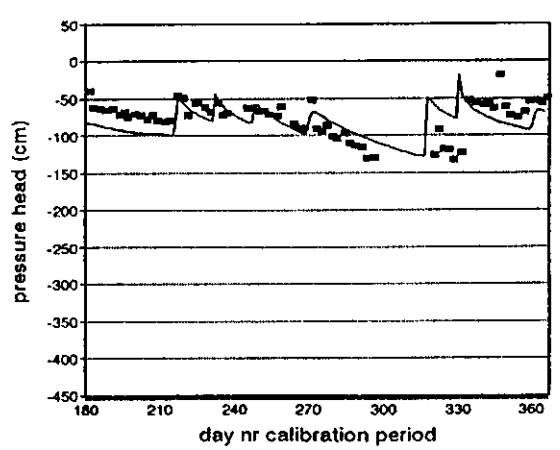

Figure G.5 *Pressure heads at 150 cm for calibration of field 1.*

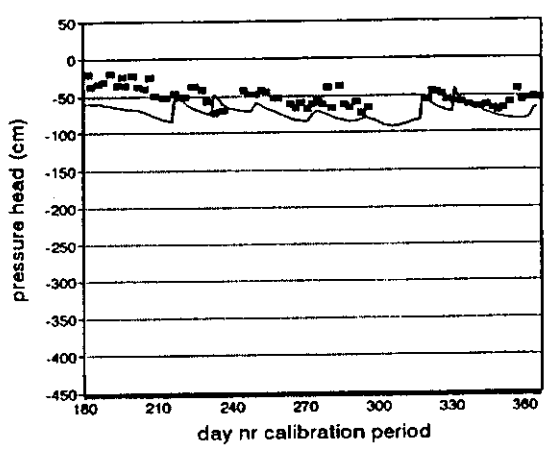

Figure G.6 *Pressure heads at 200 cm for calibration of field 1.*

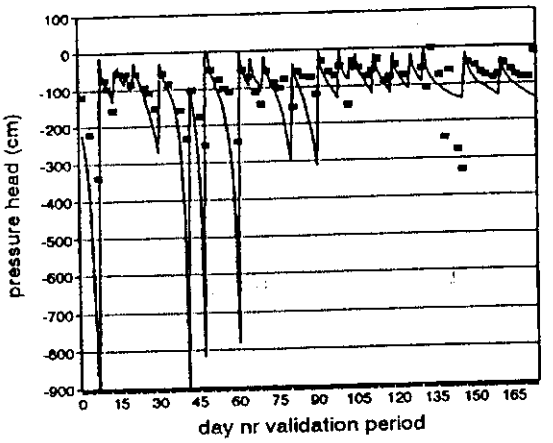

Figure G.7 *Pressure heads at 15 cm for validation of field 1.*

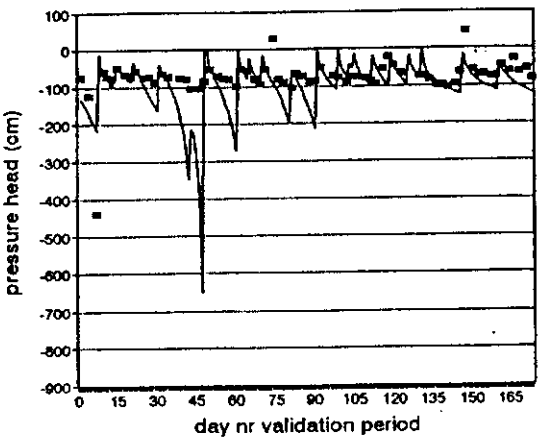

Figure G.8 *Pressure heads at 30 cm for validation of field 1.*

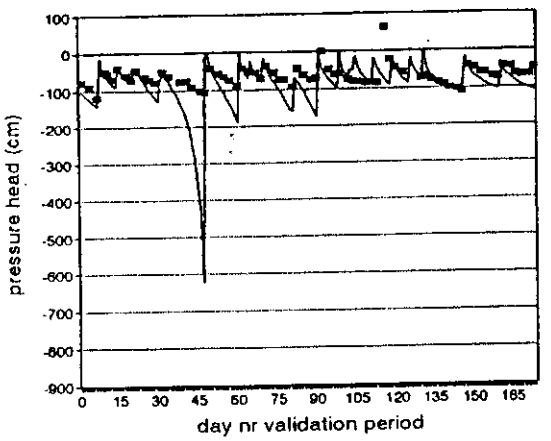

Figure G.9 *Pressure heads at 45 cm for validation of field 1.*

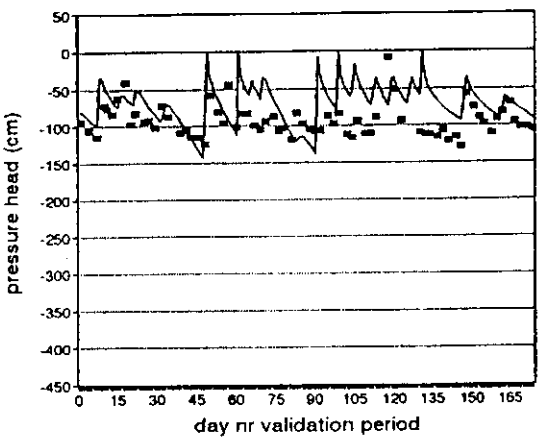

Figure G.10 *Pressure heads at 90 cm for validation of field 1.*

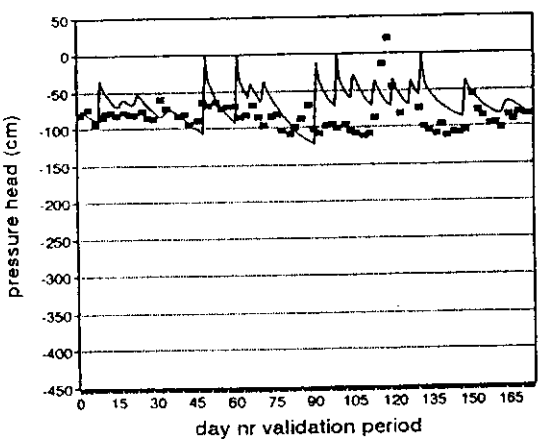

Figure G.11 *Pressure heads at 120 cm for validation of field 1.*

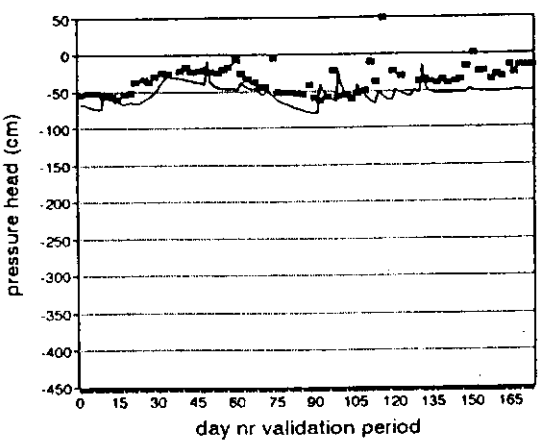

Figure G.12 *Pressure heads at 200 cm for validation of field 1.*

Table G.1 *Water balance components of field 1 (cm).*

	T_p	T_a	E_p	E_a	P+I	Q_{bottom}	ΔW
calibration	81.2	75.0	51.8	23.1	238.8	-141.4	0.1
validation	41.3	40.4	28.0	15.7	205.8	-166.7	3.1

Table G.2 *Salt balance components of field 1 (dS/m * cm).*

	S_{P+I}	S_{bottom}	ΔS	$S_{immobile}$
calibration	78.6	-150.6	(57.0-129.3)=-72.3	49.7

G.2 FIELD 2

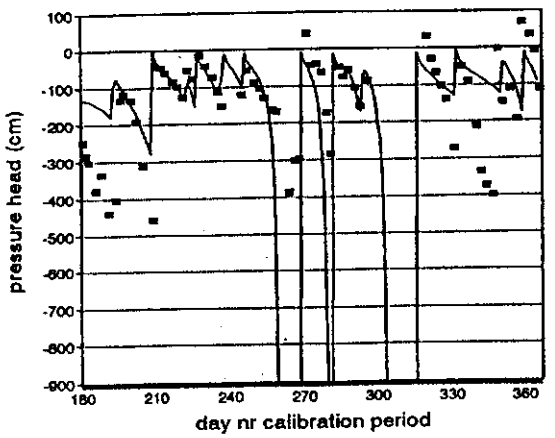

Figure G.13 *Pressure heads at 15 cm for calibration of field 2.*

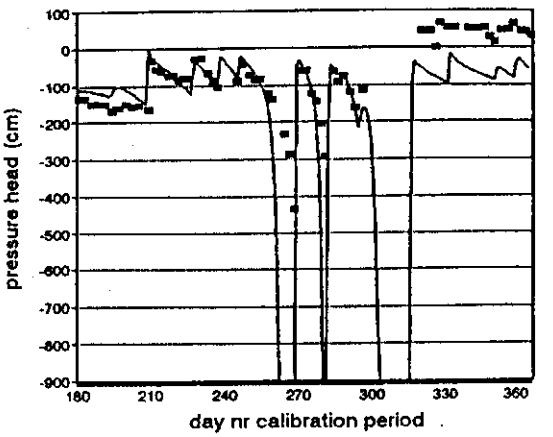

Figure G.14 *Pressure heads at 30 cm for calibration of field 2.*

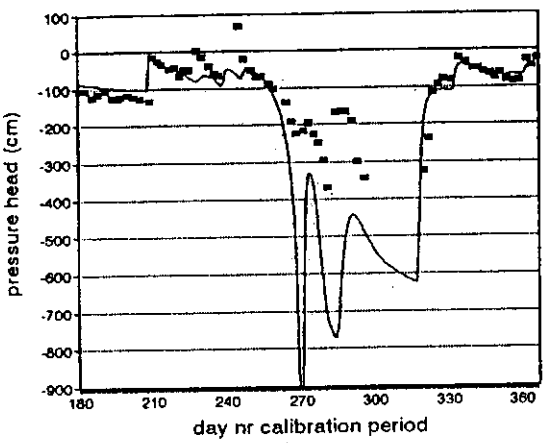

Figure G.15 *Pressure heads at 60 cm for calibration of field 2.*

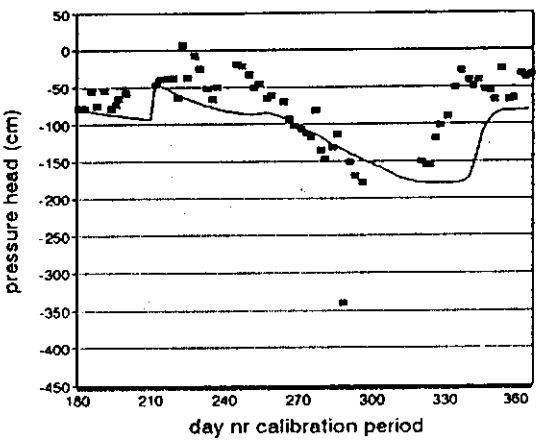

Figure G.16 *Pressure heads at 120 cm for calibration of field 2.*

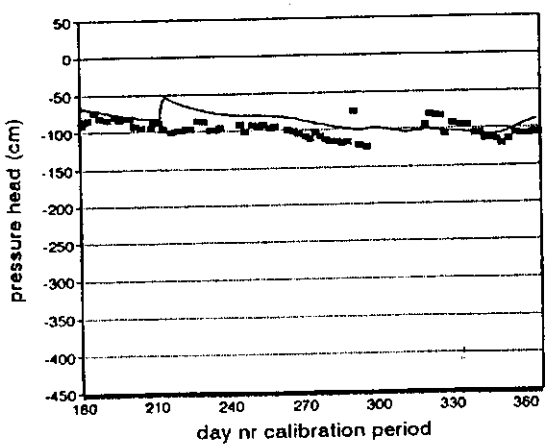

Figure G.17 *Pressure heads at 150 cm for calibration of field 2.*

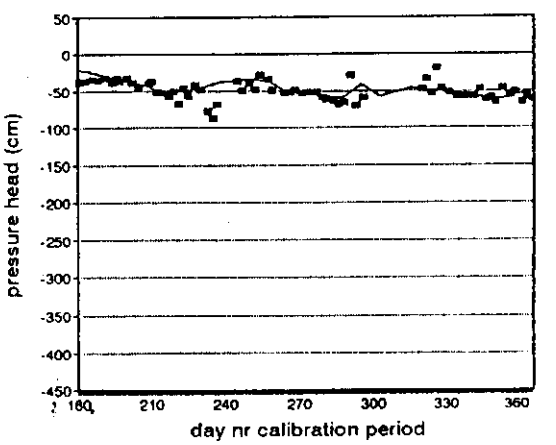

Figure G.18 *Pressure heads at 200 cm for calibration of field 2.*

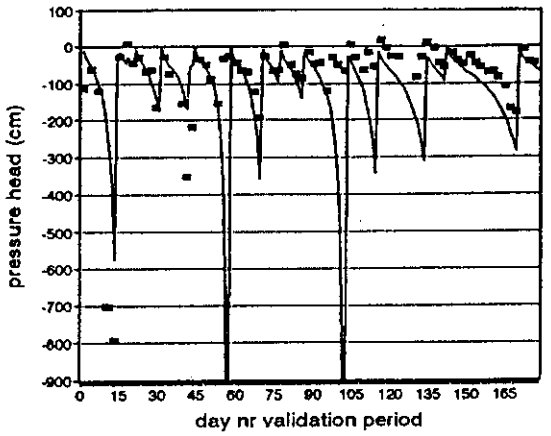

Figure G.19 *Pressure heads at 15 cm for validation of field 2.*

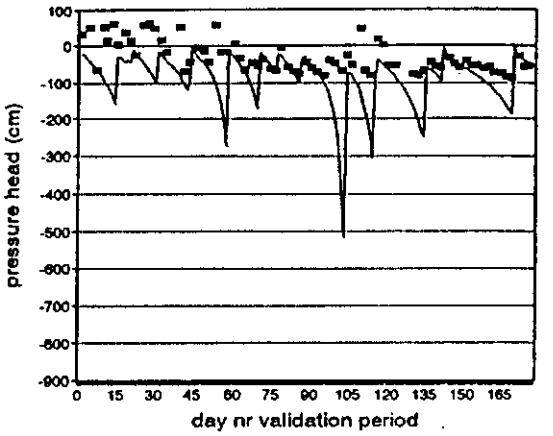

Figure G.20 *Pressure heads at 30 cm for validation of field 2.*

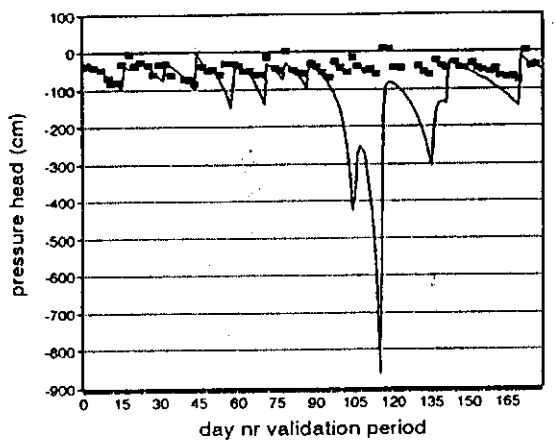

Figure G.21 *Pressure heads at 45 cm for validation of field 2.*

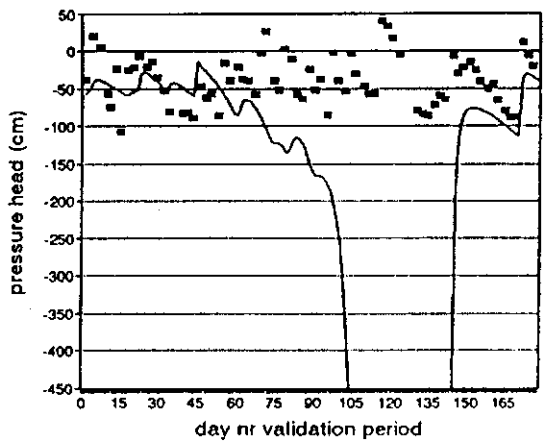

Figure G.22 *Pressure heads at 90 cm for validation of field 2.*

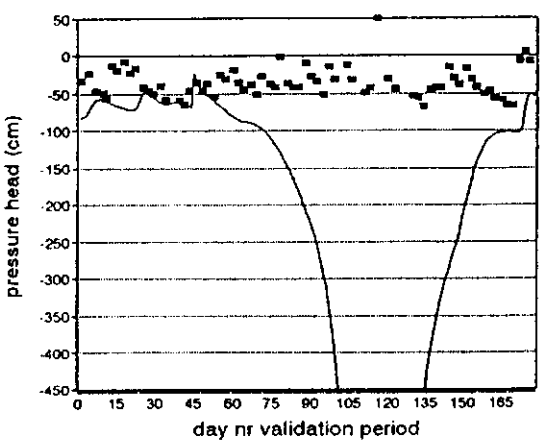

Figure G.23 *Pressure heads at 120 cm for validation of field 2.*

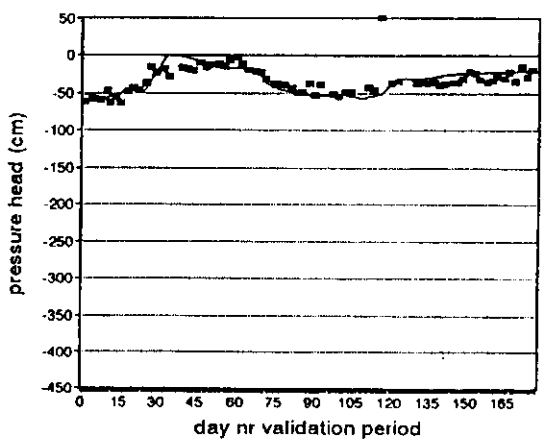

Figure G.24 *Pressure heads at 200 cm for validation of field 2.*

Table G.3 *Water balance components of field 2 (cm).*

	T_p	T_a	E_p	E_a	P+I	Q_{bottom}	ΔW
calibration	97.8	88.5	38.7	17.1	136.9	-42.8	0.3
validation	56.3	53.7	15.5	10.1	75.6	-6.2	7.3

Table G.4 *Salt balance components of field 2 (dS/m * cm).*

	S_{P+I}	S_{bottom}	ΔS	$S_{immobile}$
calibration	54.8	-98.6	(111.0-154.6)=-43.6	58.7

G.3 FIELD 3

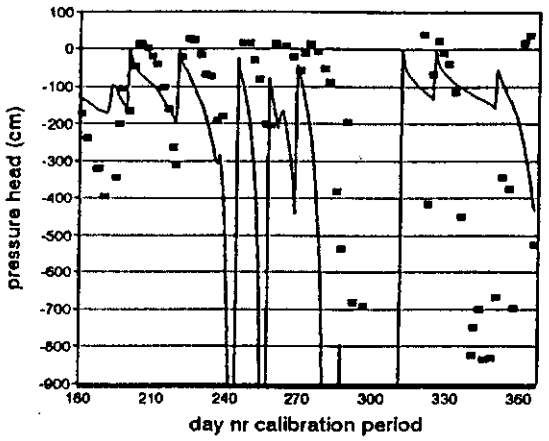

Figure G.25 *Pressure heads at 15 cm for calibration of field 3.*

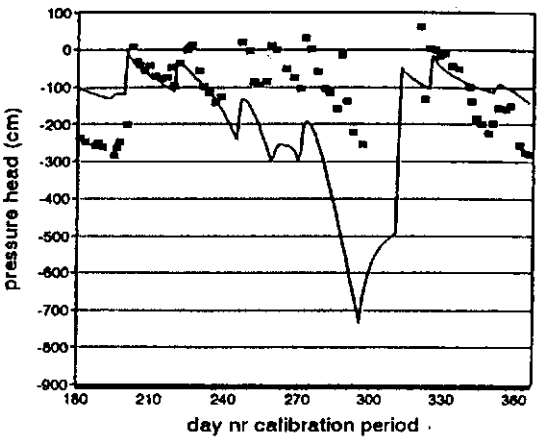

Figure G.26 *Pressure heads at 45 cm for calibration of field 3.*

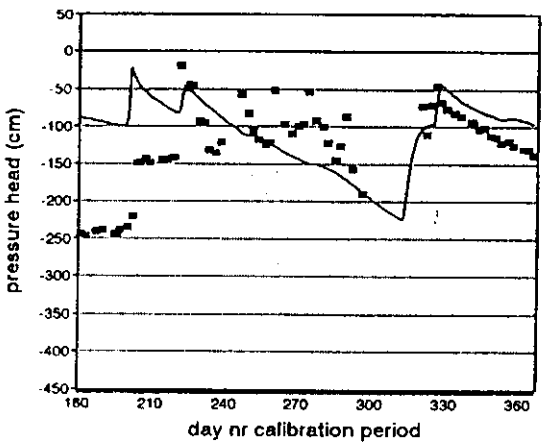

Figure G.27 *Pressure heads at 90 cm for calibration of field 3.*

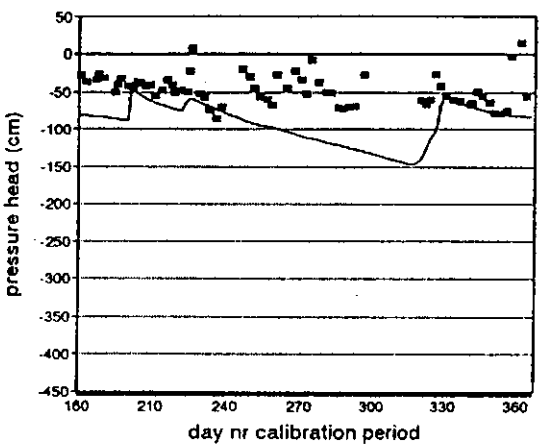

Figure G.28 *Pressure heads at 120 cm for calibration of field 3.*

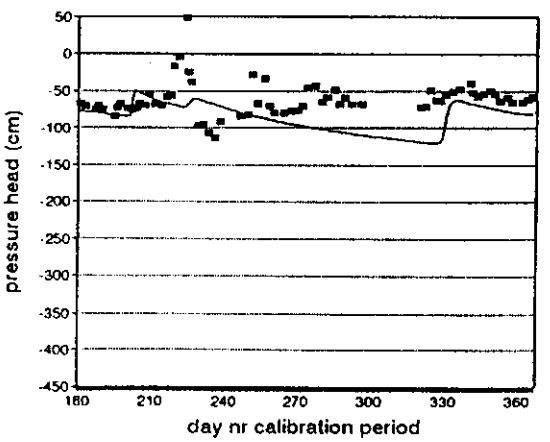

Figure G.29 *Pressure heads at 150 cm for calibration of field 3.*

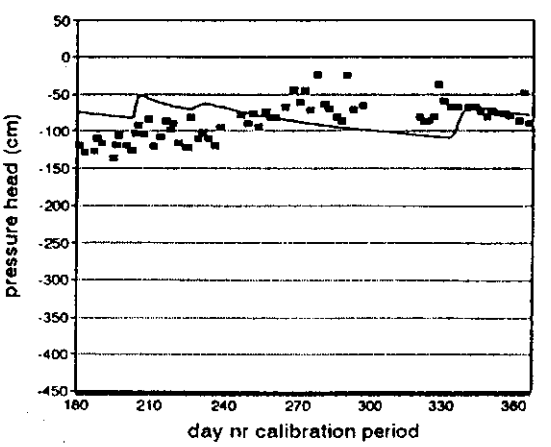

Figure G.30 *Pressure heads at 200 cm for calibration of field 3.*

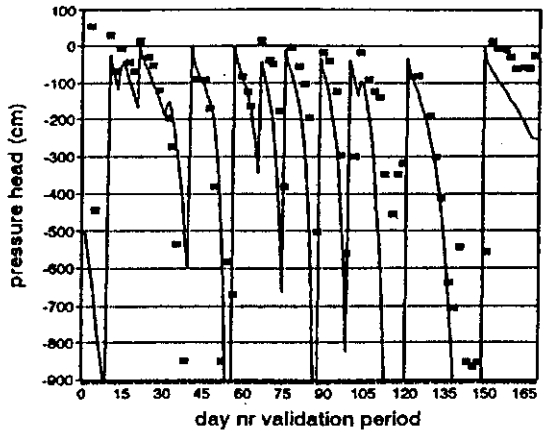

Figure G.31 *Pressure heads at 15 cm for validation of field 3.*

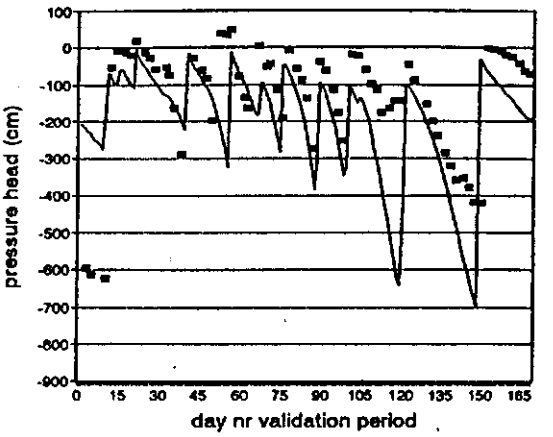

Figure G.32 *Pressure heads at 30 cm for validation of field 3.*

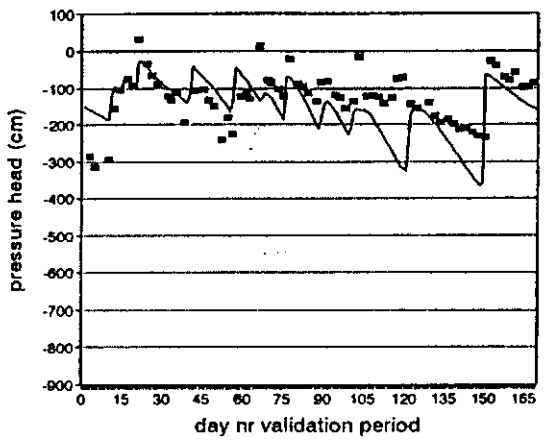

Figure G.33 *Pressure heads at 45 cm for validation of field 3.*

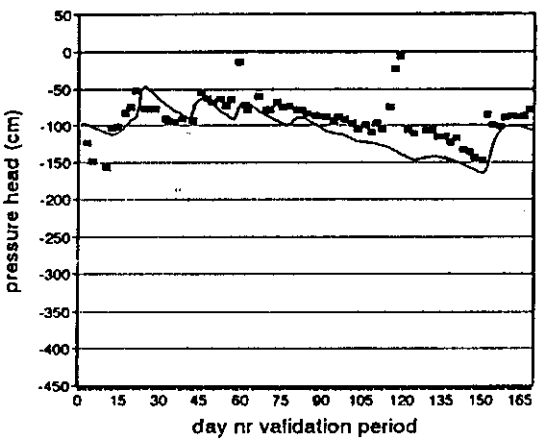

Figure G.34 *Pressure heads at 90 cm for validation of field 3.*

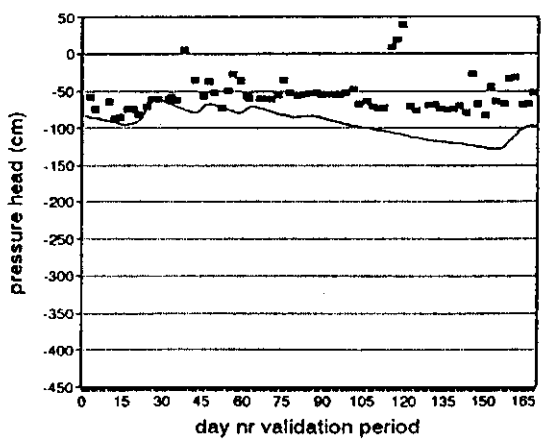

Figure G.35 *Pressure heads at 120 cm for validation of field 3.*

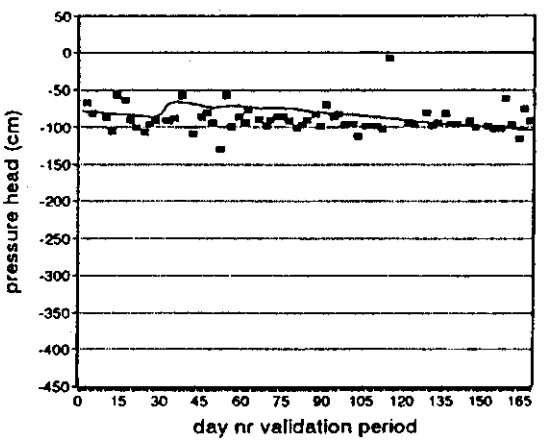

Figure G.36 *Pressure heads at 200 cm for validation of field 3.*

Table G.5 *Water balance components of field 3 (cm).*

	T_p	T_a	E_p	E_a	P+I	Q_{bottom}	ΔW
calibration	74.0	69.9	56.5	23.8	135.1	-41.4	0
validation	46.7	43.5	23.7	12.3	63.9	-11.2	2.2

Table G.6 *Salt balance components of field 3 (dS/m * cm).*

	S_{P+I}	S_{bottom}	ΔS	$S_{immobile}$
calibration	90.2	-103.9	(83.0-96.8)=-13.8	36.6

G.4 FIELD 4

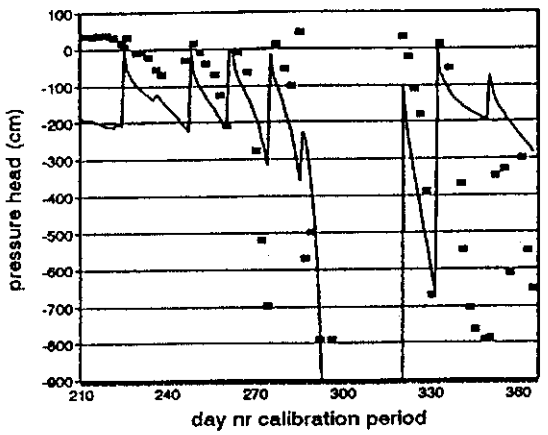

Figure G.37 *Pressure heads at 15 cm for calibration of field 4.*

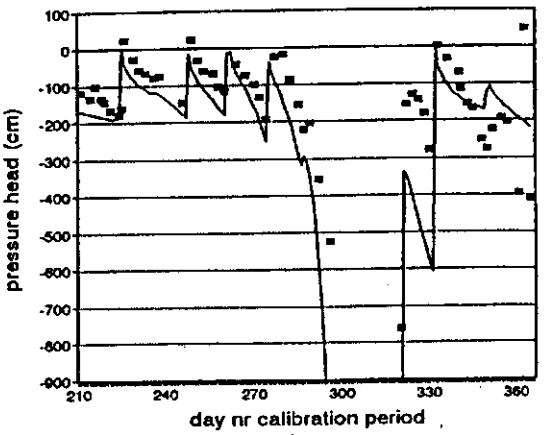

Figure G.38 *Pressure heads at 30 cm for calibration of field 4.*

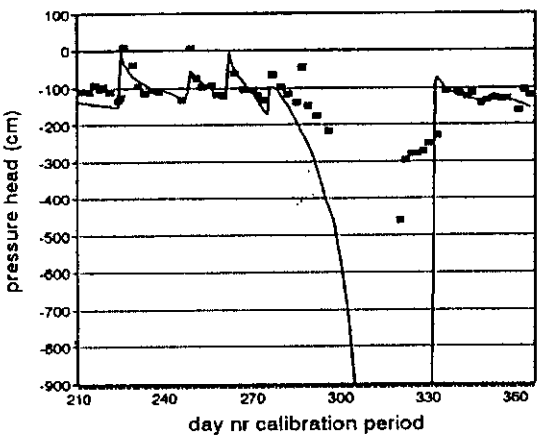

Figure G.39 *Pressure heads at 60 cm for calibration of field 4.*

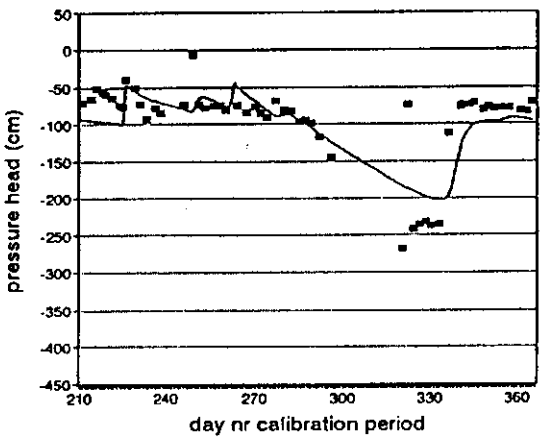

Figure G.40 *Pressure heads at 120 cm for calibration of field 4.*

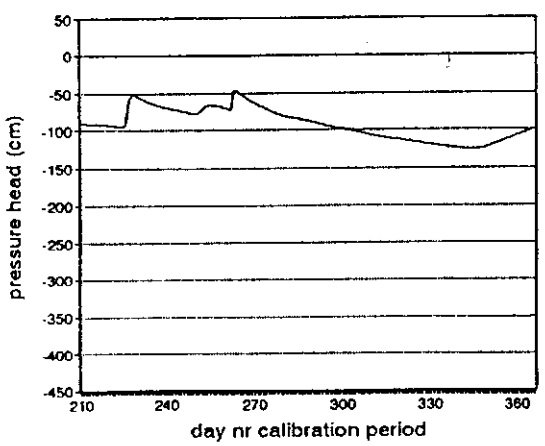

Figure G.41 *Pressure heads at 150 cm for calibration of field 4.*

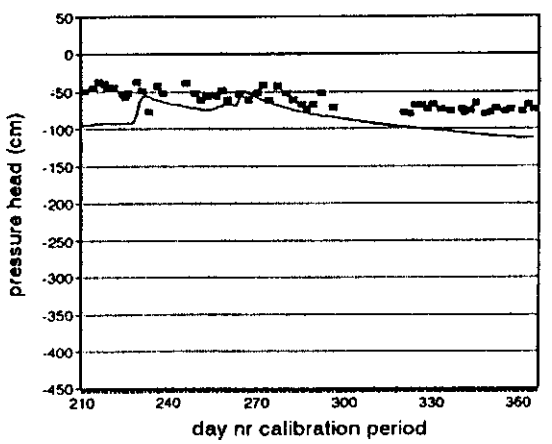

Figure G.42 *Pressure heads at 200 cm for calibration of field 4.*

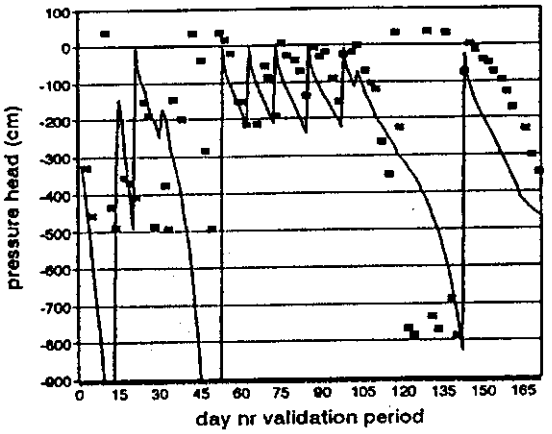

Figure G.43 *Pressure heads at 15 cm for validation of field 4.*

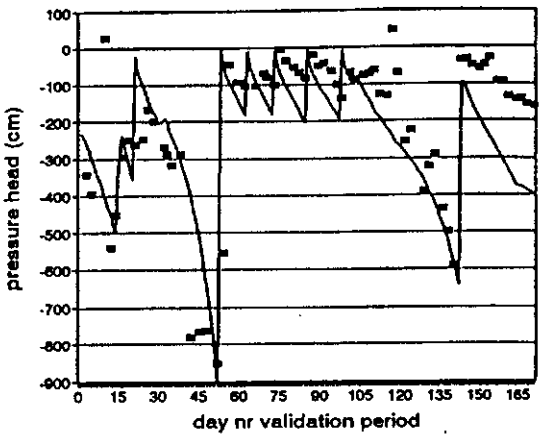

Figure G.44 *Pressure heads at 30 cm for validation of field 4.*

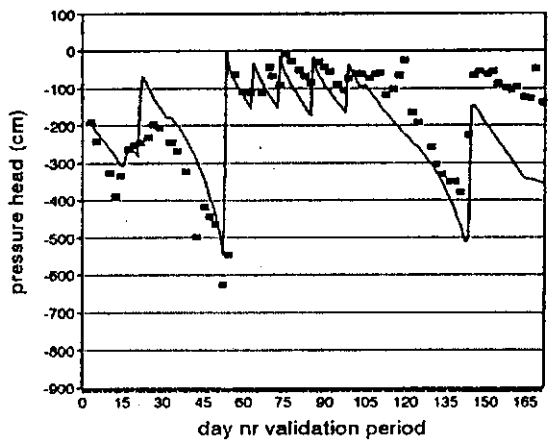

Figure G.45 *Pressure heads at 45 cm for validation of field 4.*

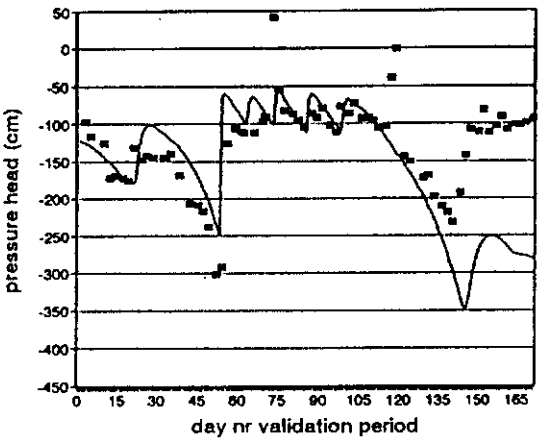

Figure G.46 *Pressure heads at 90 cm for validation of field 4.*

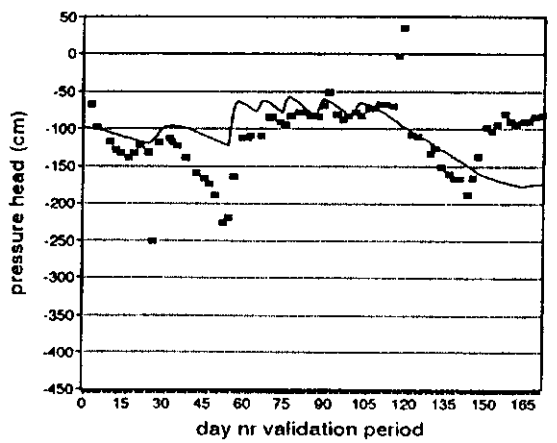

Figure G.47 *Pressure heads at 120 cm for validation of field 4.*

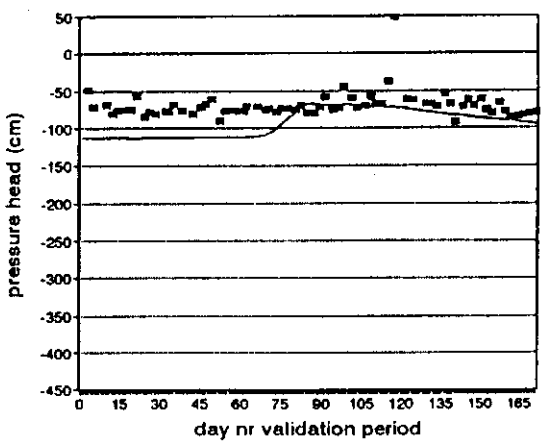

Figure G.48 *Pressure heads at 200 cm for validation of field 4.*

Table G.7 *Water balance components of field 4 (cm).*

	T_p	T_a	E_p	E_a	P+I	Q_{bottom}	ΔW
calibration	82.1	74.5	49.3	21.1	121.4	-25.4	0.4
validation	49.9	49.2	19.5	10.4	60.3	-5.0	4.1

Table G.8 *Salt balance components of field 4 (dS/m * cm).*

	S_{P+I}	S_{bottom}	ΔS	$S_{immobile}$
calibration	96.2	-133.6	(152.5-190.4)=-37.9	90.6

ANNEX H RESULTS OF SENSITIVITY ANALYSIS FOR ENVIRONMENTAL PARAMETERS

H.1 Soil hydraulic parameters

H.1.1 Saturated hydraulic conductivity

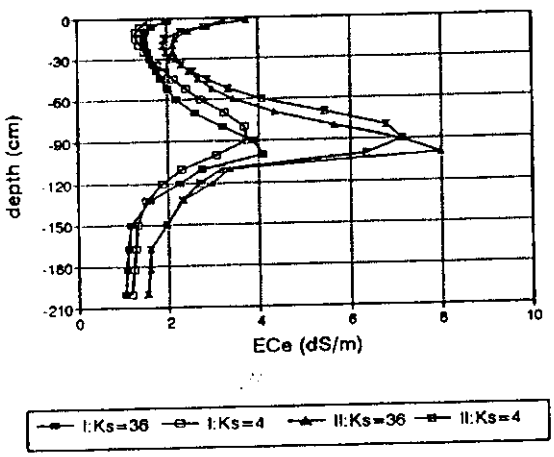

Figure H.1 *EC_e profile at day 365 at different saturated hydraulic conductivities.*

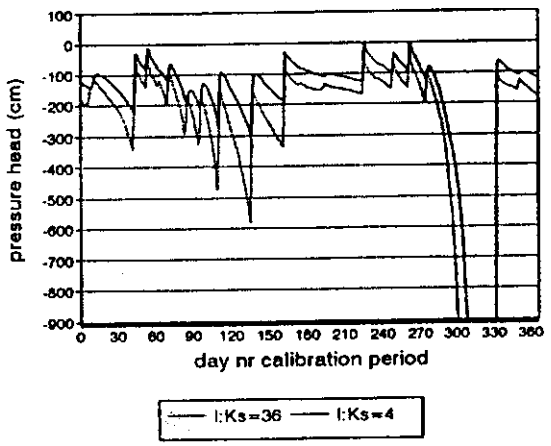

Figure H.2 *Pressure heads at 60 cm depth at different saturated hydraulic conductivities.*

H.1.2 Saturated moisture content

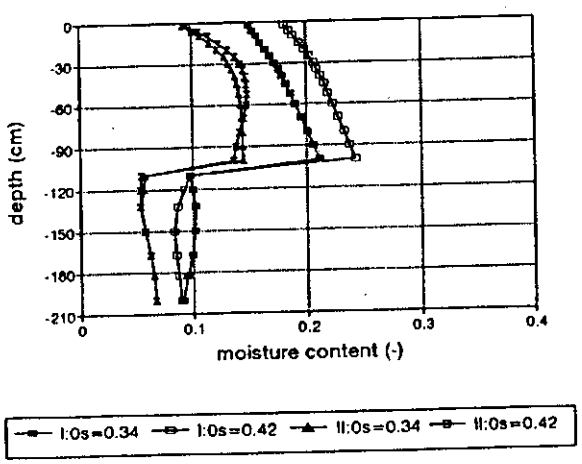

Figure H.3 *Moisture content profile at day 365 at different saturated moisture contents.*

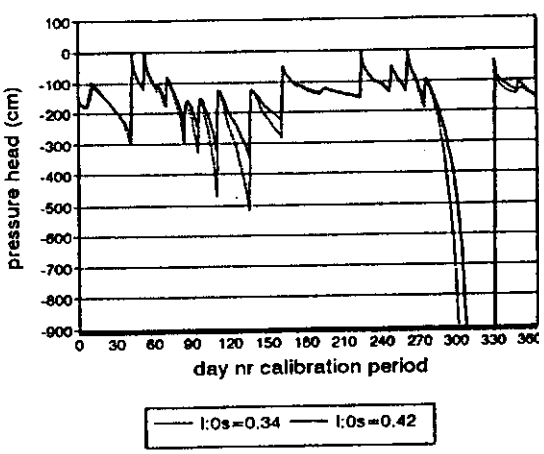

Figure H.4 *Pressure heads at 60 cm depth at different saturated moisture contents.*

H.1.3 Shape parameters alfa, labda en n

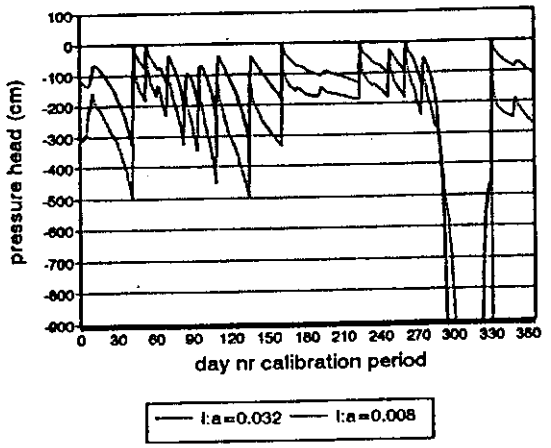

Figure H.5 *Pressure heads at 45 cm at different values of alfa.*

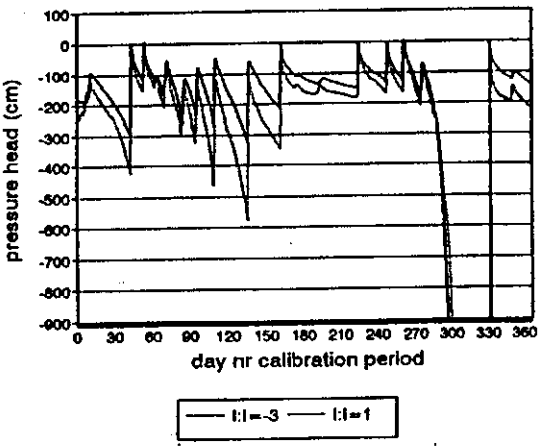

Figure H.6 *Pressure heads at 45 cm depth at different values of labda.*

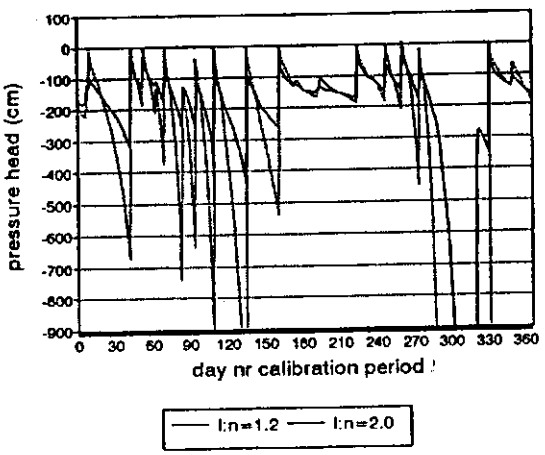

Figure H.7 *Pressure heads at 45 cm at different values of n.*

H.2 Preferential flow

H.2.1 No preferential flow

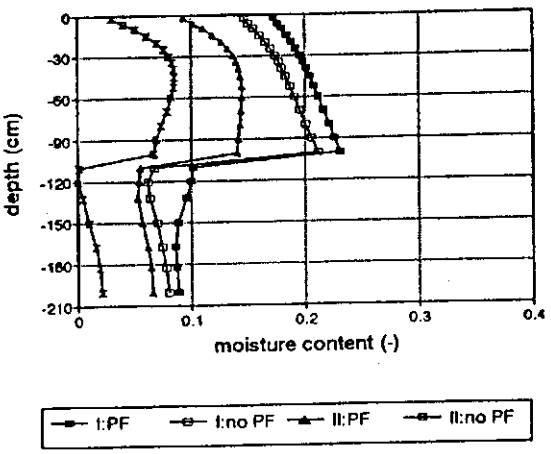

Figure H.8 *Moisture content profile at day 365 for no preferential flow.*

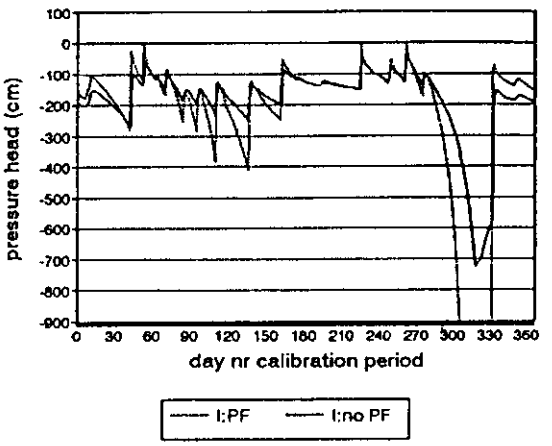

Figure H.9 *Pressure heads at 60 cm depth for no preferential flow.*

H.2.2 Immobile moisture content

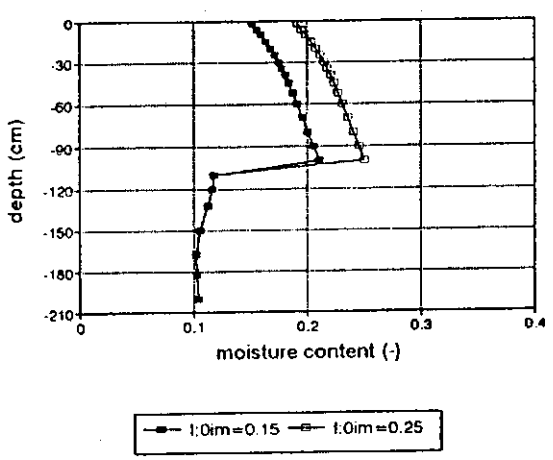

Figure H.10 *Moisture content profile at day 365 at different immobile moisture contents.*

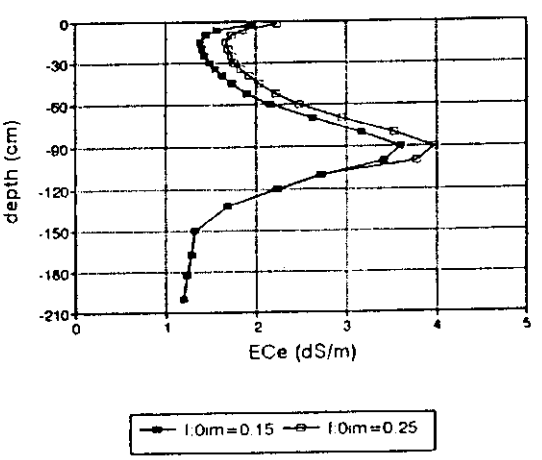

Figure H.11 *EC_e profile at day 365 at different immobile moisture contents.*

H.2.3 Mobile fraction

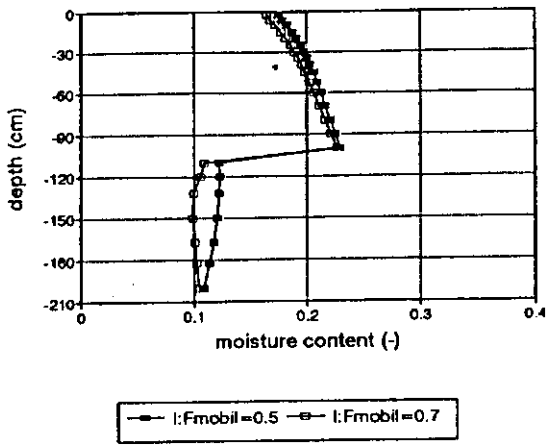

Figure H.12 *Moisture content profile at day 365 at different mobile fractions.*

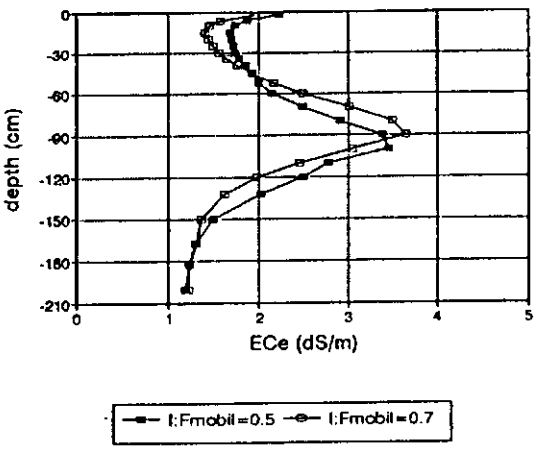

Figure H.13 *EC_e profile at day 365 at different mobile fractions.*

H.3 Root water uptake

H.3.1 Root distribution

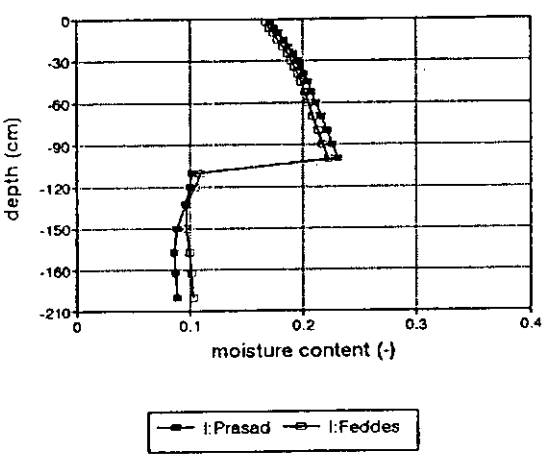

Figure H.14 *Moisture content profile at day 365 at different root distributions.*

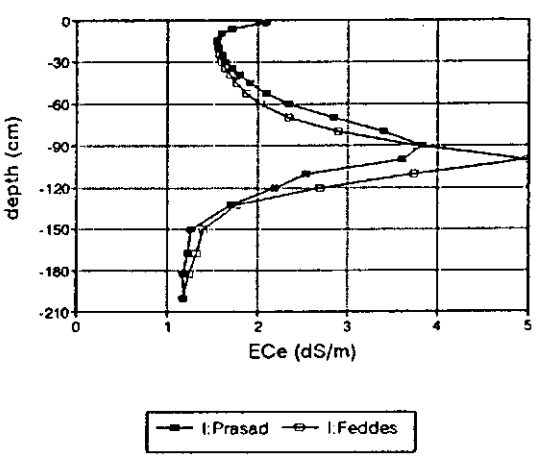

Figure H.15 *EC_e profile at day 365 at different root distributions.*

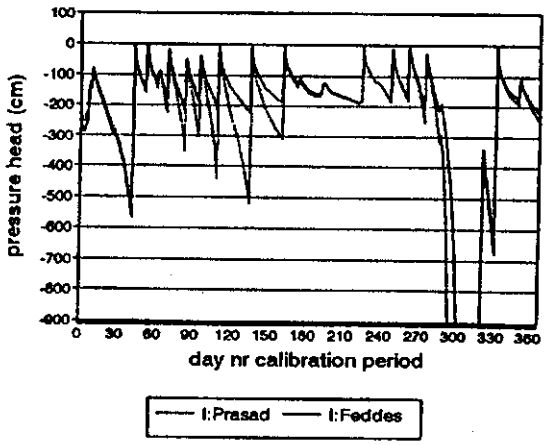

Figure H.16 *Pressure heads at 30 cm at different root distributions.*

H.3.2 Rooting depth

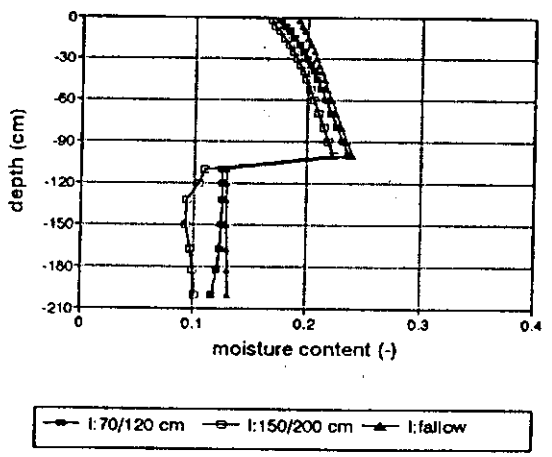

Figure H.17 *Moisture content profile at day 365 at different rooting depths.*

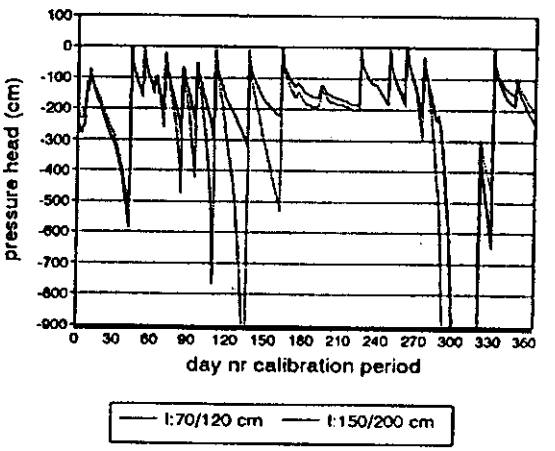

Figure H.18 *Pressure heads at 30 cm depth at different rooting depths.*

H.4 Evapotranspiration

H.4.1 Boesten parameter

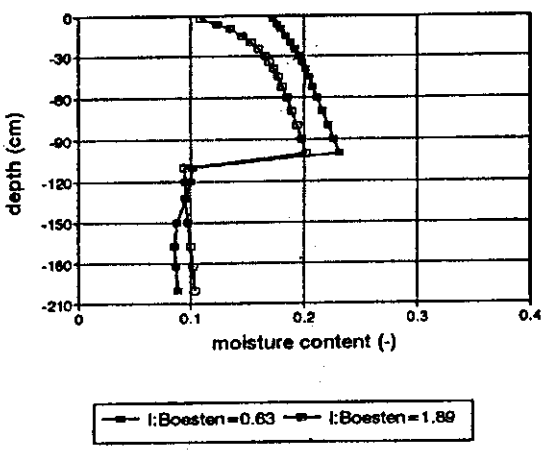

Figure H.19 *Moisture content profile at day 365 at different Boesten parameters.*

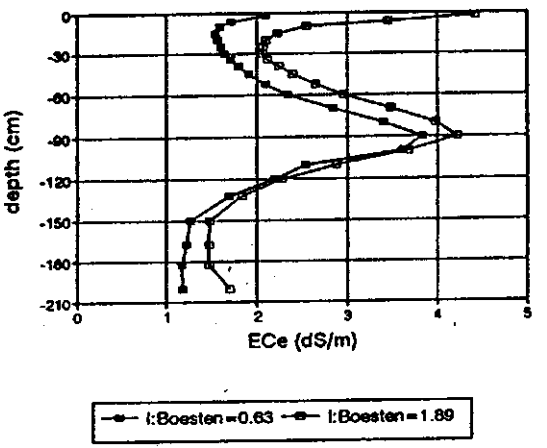

Figure H.20 *EC_e profile at day 365 at different Boesten parameters.*

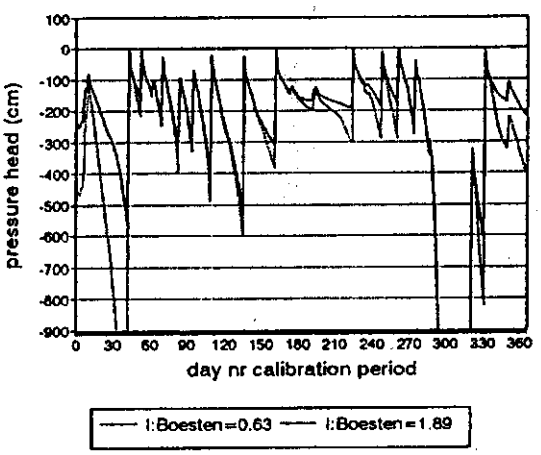

Figure H.21 *Pressure heads at 30 cm at different Boesten parameters.*

H.4.2 Crop factors

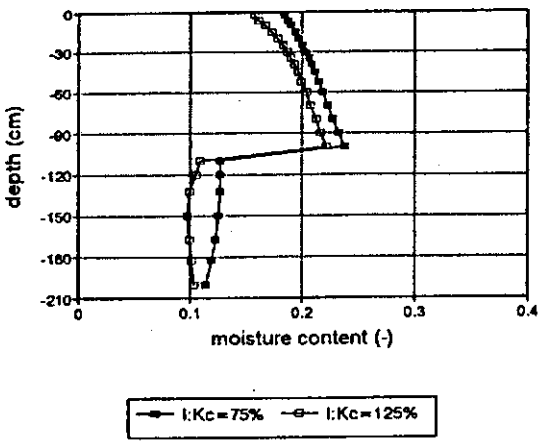

Figure H.22 *Moisture content profile at day 365 at different crop factors.*

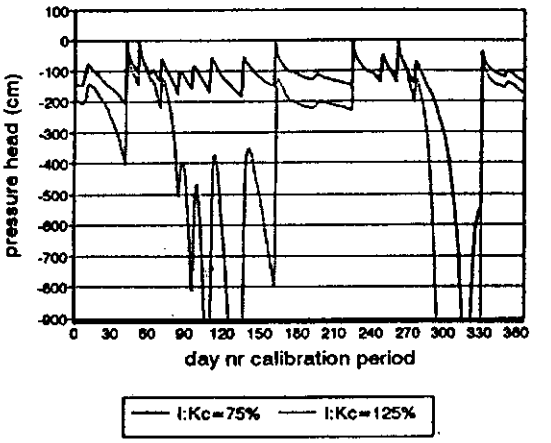

Figure H.23 *Pressure heads at 60 cm depth at different crop factors.*

H.5 Groundwater table depth

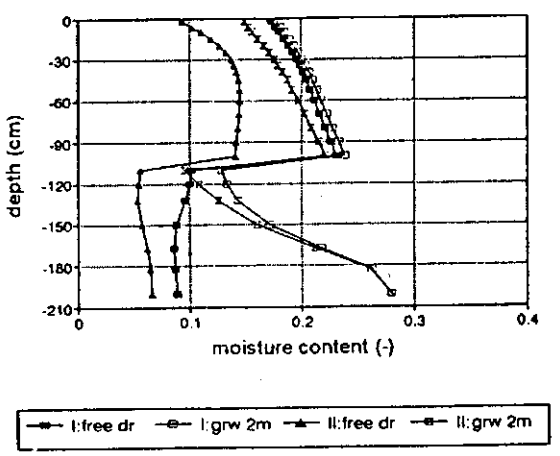

Figure H.24 *Moisture content profile at day 365 at different groundwater depths.*

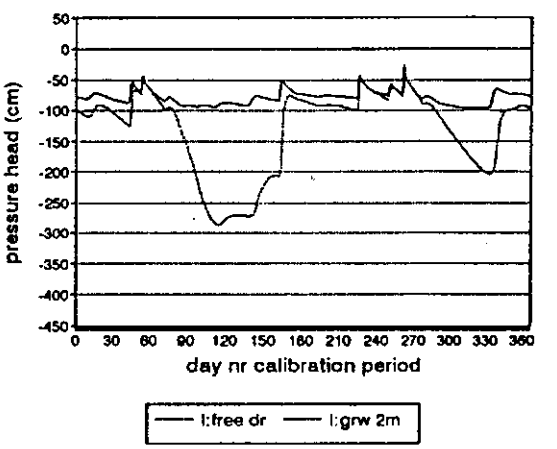

Figure H.25 *Pressure heads at 120 cm at different groundwater table depths.*

ANNEX I RESULTS OF SHORT-TERM ANALYSIS MANAGEMENT VARIABLES

I.1 Quantity of irrigation applications (field 2)

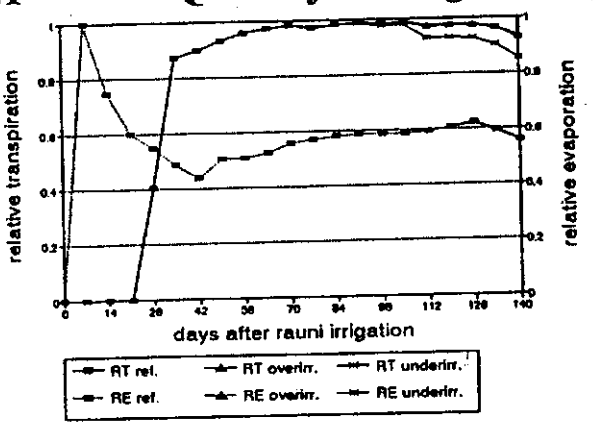

Figure I.1 *Cumulative RT and RE at different irrigation quantities (wheat).*

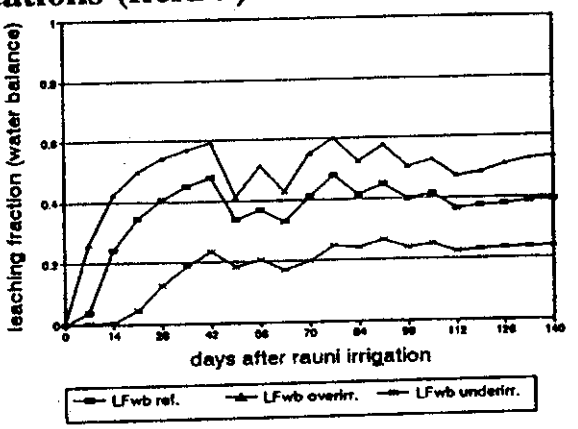

Figure I.2 *Cumulative LF_{wb} at different irrigation quantities (wheat).*

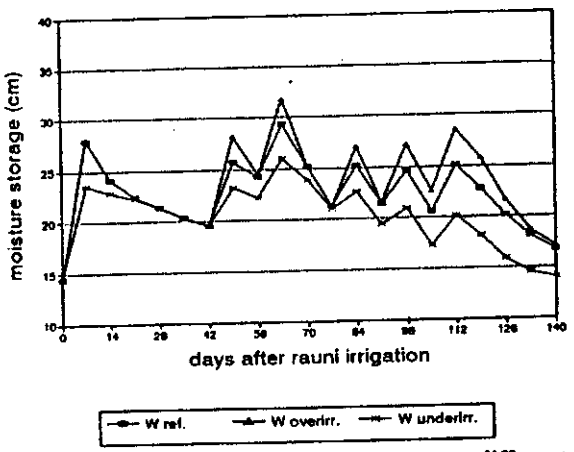

Figure I.3 *Moisture storage at different irrigation quantities (wheat).*

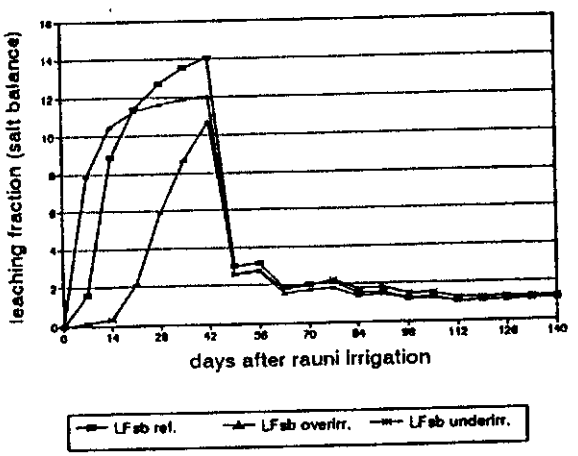

Figure I.4 *Cumulative LF_{sb} at different irrigation quantities (wheat)*

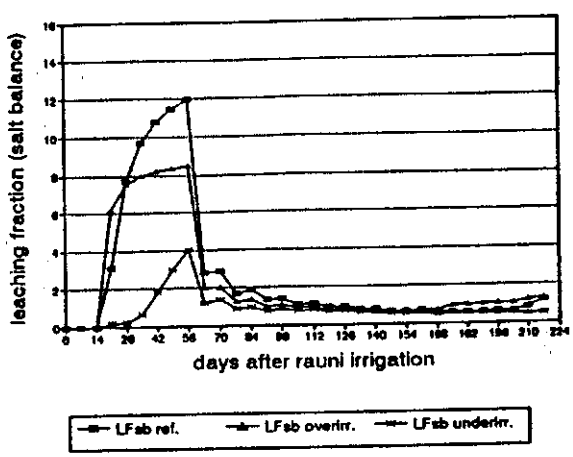

Figure I.5 *Cumulative LF_{sb} at different irrigation quantities (cotton).*

I.2 Frequencies of irrigation applications (field 1)

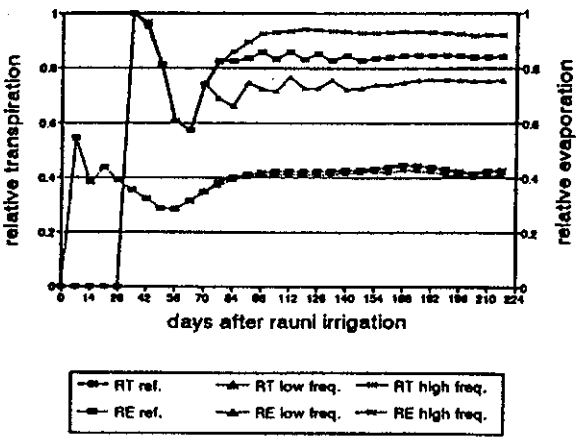

Figure I.6 *Cumulative RT and RE at different irrigation frequencies (cotton).*

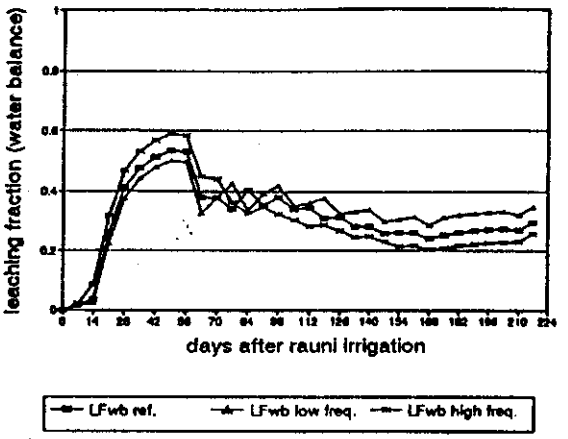

Figure I.7 *Cumulative LF_{wb} at different irrigation frequencies (cotton).*

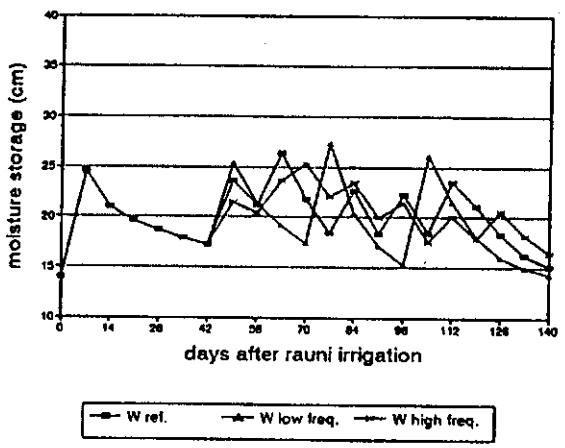

Figure I.8 *Moisture storage at different irrigation frequencies (wheat).*

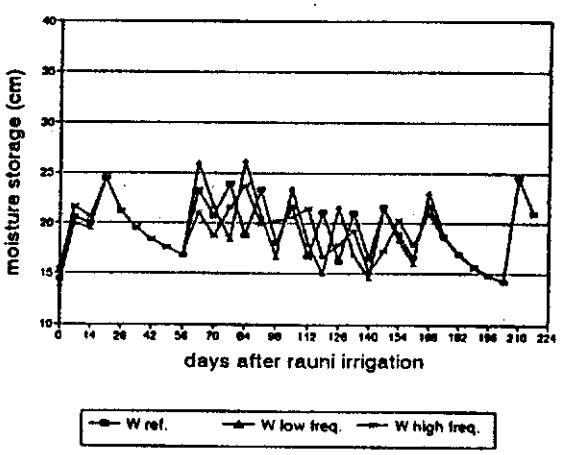

Figure I.9 *Moisture storage at diferent irrigation frequencies (cotton).*

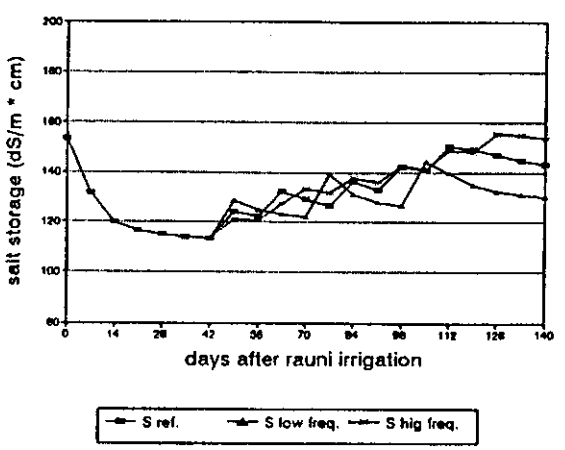

Figure I.10 *Salt storage at different irrigation frequencies (wheat).*

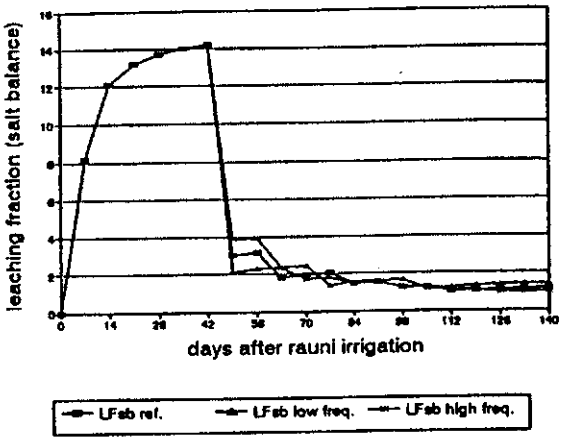

Figure I.11 *Cumulative LF_{sb} at different irrigation frequencies (wheat).*

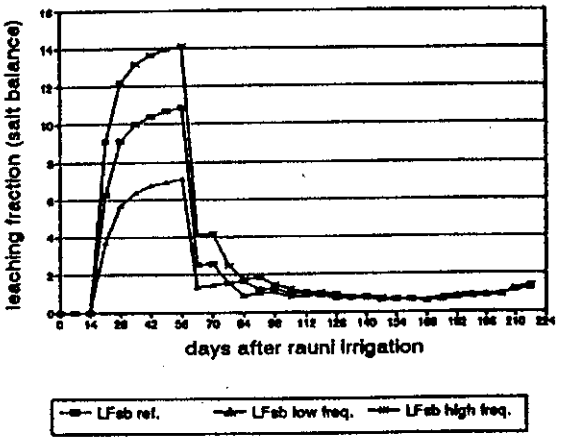

Figure I.12 *Cumulative LF_{sb} at different irrigation frequencies (cotton).*

I.3 Quality of irrigation applications (field 3)

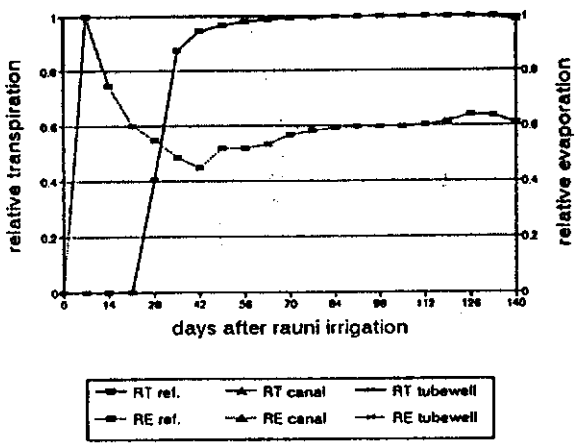

Figure I.13 *Cumulative RT and RE at different irrigation qualities (wheat).*

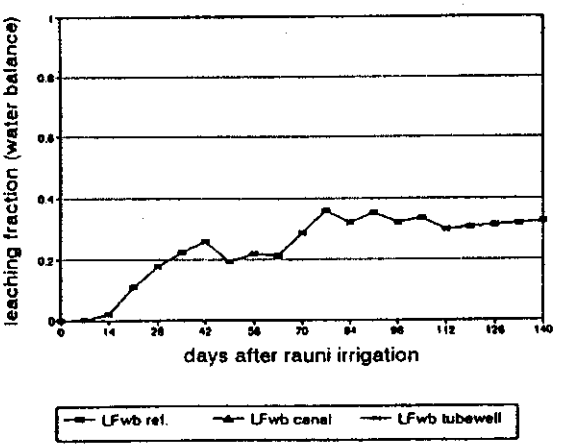

Figure I.14 *Cumulative LF_{wb} at different irrigation qualities (wheat).*

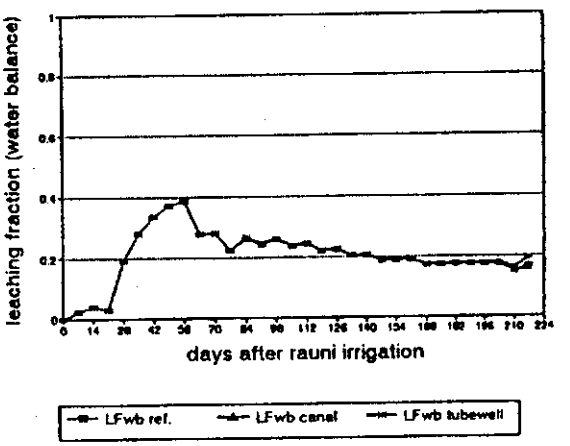

Figure I.15 *Cumulative LF_{wb} at different irrigation qualities (cotton).*

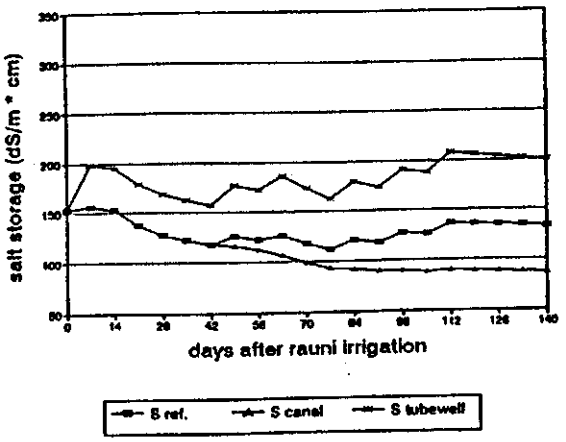

Figure 1.16 *Salt storage at different irrigation qualities (wheat).*

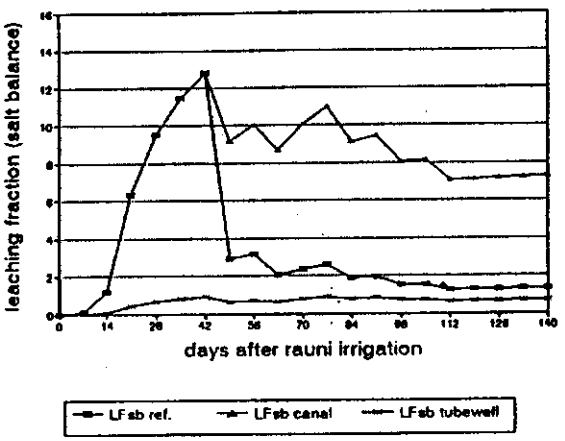

Figure 1.17 *Cumulative LF_{sb} at different irrigation qualities (wheat).*

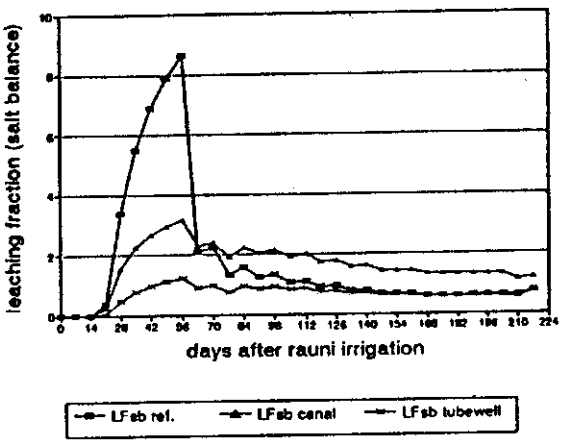

Figure 1.18 *Cumulative LF_{sb} at different irrigation qualities (cotton).*

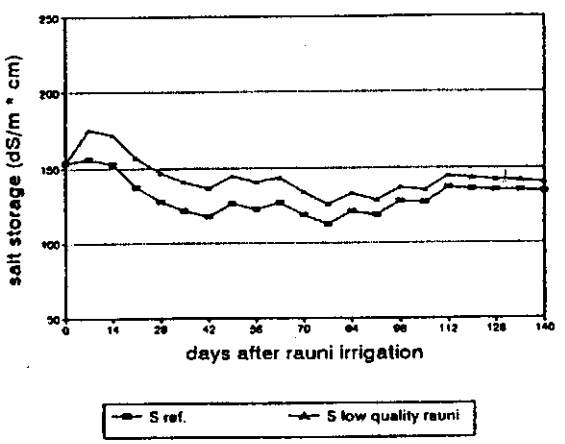

Figure 1.19 *Salt storage at different rauni water qualities (wheat).*

I.4 Initial salinity level (field 4)

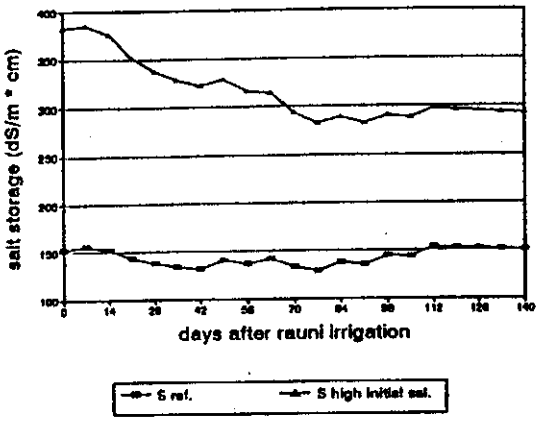

Figure I.20 *Salt storage at different initial salinity levels (wheat).*

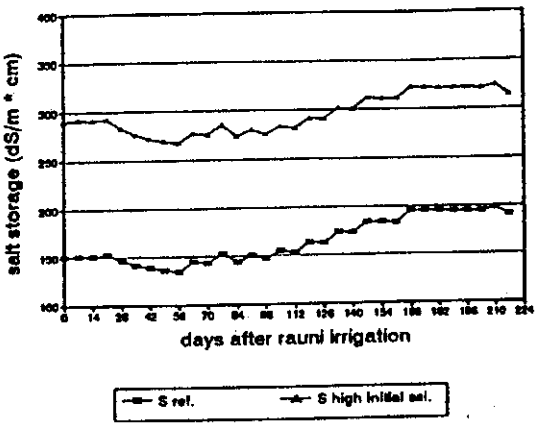

Figure I.21 *Salt storage at different initial salinity levels (cotton).*

I.5 Comparison of results for four sample fields

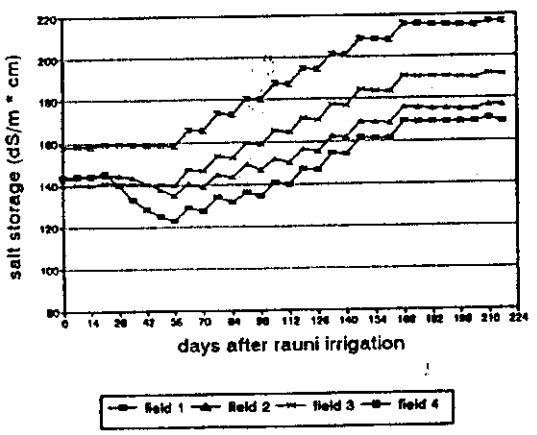

Figure I.22 *Salt storage underirrigation scenario (cotton).*

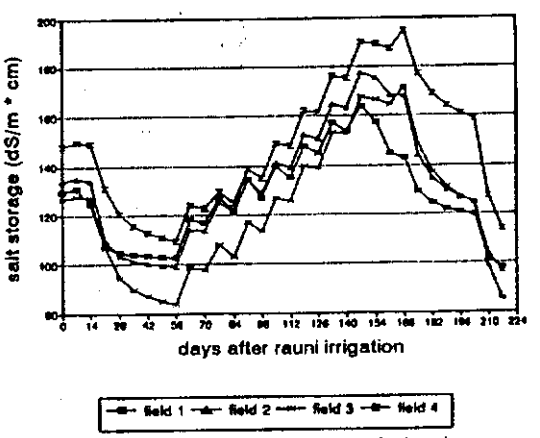

Figure I.23 *Salt storage overirrigation scenario (cotton).*

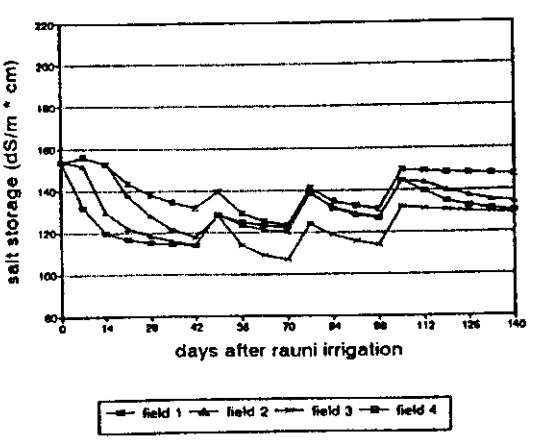

Figure I.24 *Salt storage low frequnecy scenario (wheat).*

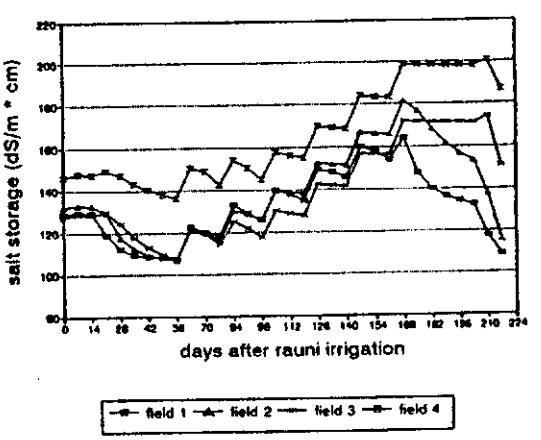

Figure I.25 *Salt storage low frequency scenario (cotton).*

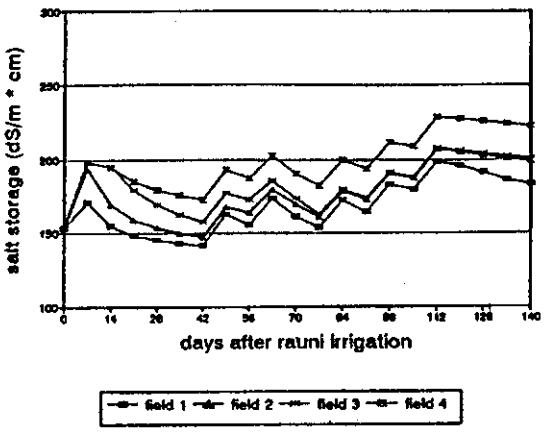

Figure I.26 *Salt storage tubewell water scenario (wheat).*

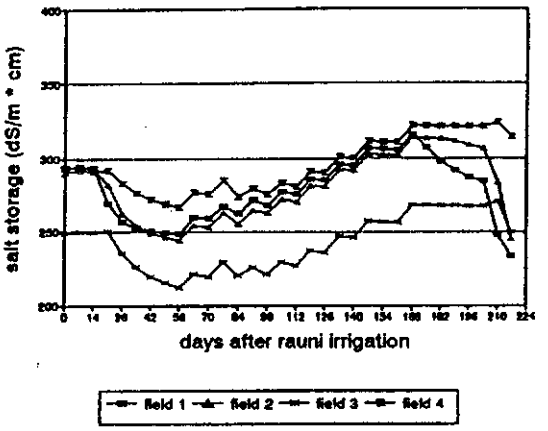

Figure I.27 *Salt storage scenario with high initial salinity level (cotton).*